

SUPPORTING INFORMATION

“Doping” pentacene with sp²-Phosphorus Atoms: Towards High Performance Ambipolar Semiconductors

Guankui Long^{1,2#}, Xuan Yang², Wangqiao Chen¹, Mingtao Zhang^{3*}, Yang Zhao^{1*}, Yongsheng Chen^{2*}, and Qichun Zhang^{1,3*}

¹ School of Materials Science and Engineering, Nanyang Technological University, Singapore, 639798, Singapore

² State Key Laboratory and Institute of Elemento-Organic Chemistry, Synergetic Innovation of Chemical Science and Engineering (Tianjin), Center for Nanoscale Science and Technology, College of Chemistry, Nankai University, Tianjin 300071, China

³ Computational Center for Molecular Science, College of Chemistry, Nankai University, Tianjin, 300071, China

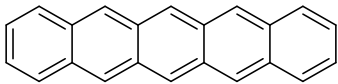
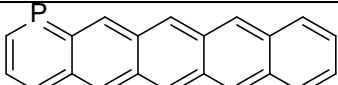
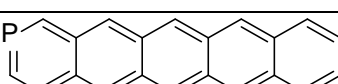
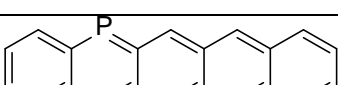
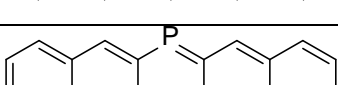
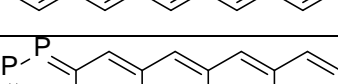
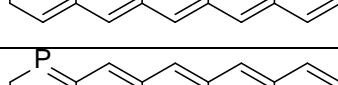
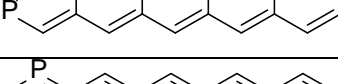
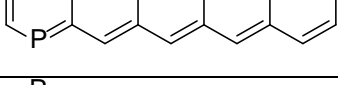
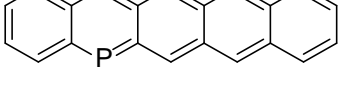
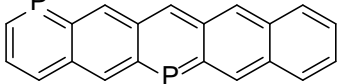
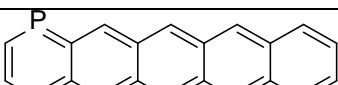
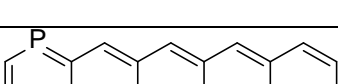
⁴ Division of Chemistry and Biological Chemistry, School of Physical and Mathematical Sciences, Nanyang Technological University, Singapore, 637371, Singapore

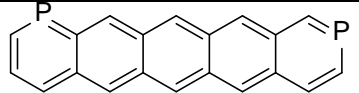
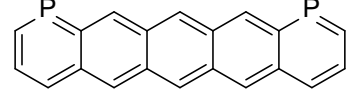
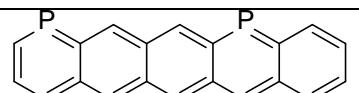
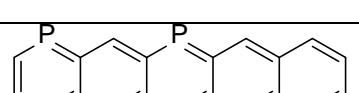
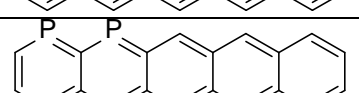
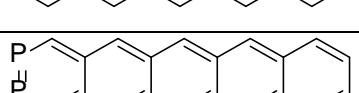
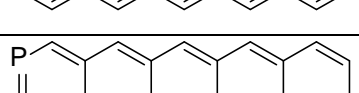
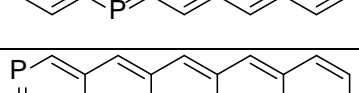
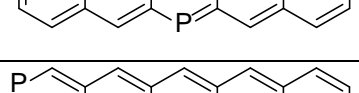
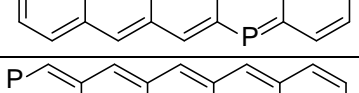
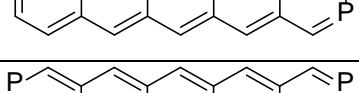
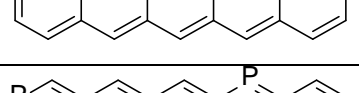
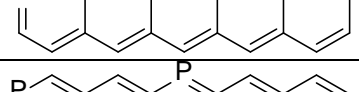
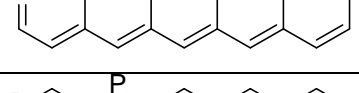
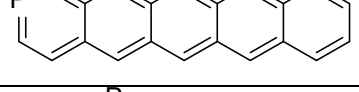
Table S1	Summary of the chemical structures and nomenclatures of the phosphapentacenes studied in this work.
Fig. S1	The optimized structures for pentacene and the phosphapentacene derivatives based on B3LYP/6-311+G** method.
Fig. S2	The optimized cationic structures for pentacene and the phosphapentacene derivatives based on B3LYP/6-311+G** method.
Fig. S3	The optimized anionic structures for pentacene and the phosphapentacene derivatives based on B3LYP/6-311+G** method.
Table S2	Summary of the p_z atomic orbital of the sp^2 -phosphorus in the frontier molecular orbitals and natural bond orbital charge distributions of the phosphapentacenes.
Fig. S4	The contribution of p_z atomic orbital in the HOMO of pentacene.
Fig. S5	Correlations between HOMO energy levels of monophosphapentacene and diphosphapentacene derivatives with the percentage of p_z atomic orbital of the sp^2 -phosphorus in the HOMO of the phosphapentacene derivatives.
Table S3.	Summary of the calculated results for pentacene and the phosphapentacene derivatives based on B3LYP/6-311+G** method.
Fig. S6	Vertical $S_0 \rightarrow S_1$ gaps for pentacene and the phosphapentacene derivatives based on B3LYP/6-311+G** method.
Table S4.	Summary of the calculated hole and electron reorganization energies for the representative pentacene derivatives.
Fig. S7	Evolution of the calculated transfer integrals for hole and electron transfer in the dimer of pentacene and 6,13-diphosphapentacene as a function of the degree of translation of one molecule along the π - π stacking, long axis and short axis intermolecular distance.
Fig. S8	HOMO electron density distributions for pentacene and the phosphapentacene derivatives based on B3LYP/6-311+G** method.
Fig. S9	LUMO electron density distributions for pentacene and the phosphapentacene derivatives based on B3LYP/6-311+G** method.
Table S5.	Comparison of the hole and electron reorganization energies for pentacene and the phosphapentacene derivatives from adiabatic potential energy surface methods and normal mode analysis methods.
Table S6.	Summary of the calculated results for pentacene and the phosphapentacene derivatives based on B3LYP/6-31G* method.
Table S7.	Comparison of the calculated HOMO and LUMO energy levels based on different functional and basis sets.
Fig. S10	Singlet-triplet energy splitting for pentacene and the phosphapentacene derivatives based on B3LYP/6-311+G** method.
Fig. S11	Vertical electron affinities for pentacene and the phosphapentacene derivatives based on B3LYP/6-311+G** method.
Fig. S12	Vertical ionic potentials for pentacene and the phosphapentacene derivatives based on B3LYP/6-311+G** method.
Fig. S13	Electron surface potentials for pentacene and the phosphapentacene derivatives based on B3LYP/6-311+G** method.

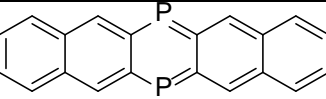
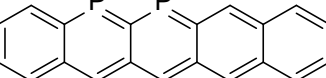
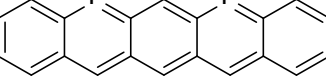
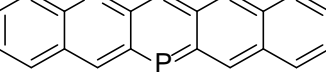
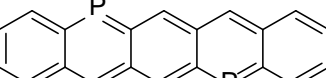
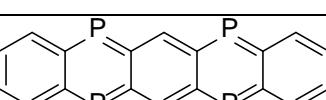
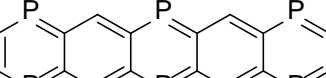
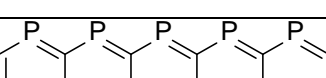
Calculation Method

All the geometries of the ground states, radical cations, radical anions and triplet states were optimized by B3LYP functional and 6-31G* or 6-311+G** basis sets, and the frequency analysis was followed to assure that the optimized structures were stable states. Both basis sets give almost the same calculated reorganization energies and the same trend of HOMO and LUMO energy levels after introducing phosphorus atoms at different positions. In this work, we focused on discussing the calculation results by B3LYP/6-311+G** methods,^[1,2] and the calculated results by B3LYP/6-31G* are summarized in Table S6. TDDFT calculation for the $S_0 \rightarrow S_n$ transitions using B3LYP/6-311+G** were then performed based on the optimized structures at ground states. The lowest 50 singlet roots of the nonhermitian eigenvalue equations were obtained to determine the vertical excitation energies. All the calculations were carried out using Gaussian 09 package.^[3] The normal-mode analysis and the Huang-Rhys factors, as well as the reorganization energies of normal modes for both neutral and charged molecules were obtained through the DUSHIN program developed by Reimers.^[4]

Table S1. Summary of the chemical structures and nomenclatures of the phosphapentacenes studied in this work, and pentacene is also shown for comparison.

Number	Nomenclature	Chemical structure
0	pentacene	
1	1-phosphapentacene	
2	2-phosphapentacene	
3	5-phosphapentacene	
4	6-phosphapentacene	
5	1,2-diphosphapentacene	
6	1,3-diphosphapentacene	
7	1,4-diphosphapentacene	
8	1,5-diphosphapentacene	
9	1,6-diphosphapentacene	
10	1,7-diphosphapentacene	
11	1,8-diphosphapentacene	
12	1,9-diphosphapentacene	

13	1,10-diphosphapentacene	
14	1,11-diphosphapentacene	
15	1,12-diphosphapentacene	
16	1,13-diphosphapentacene	
17	1,14-diphosphapentacene	
18	2,3-diphosphapentacene	
19	2,5-diphosphapentacene	
20	2,6-diphosphapentacene	
21	2,7-diphosphapentacene	
22	2,9-diphosphapentacene	
23	2,10-diphosphapentacene	
24	2,12-diphosphapentacene	
25	2,13-diphosphapentacene	
26	2,14-diphosphapentacene	
27	5,14-diphosphapentacene	

28	6,13-diphosphapentacene	
29	5,6-diphosphapentacene	
30	5,7-diphosphapentacene	
31	5,13-diphosphapentacene	
32	5,12-diphosphapentacene	
33	5,7,12,14-tetraphosphapentacene	
34	1,4,6,8,11,13-hexaphosphapentacene	
35	1,4,5,6,7,8,11,12,13,14-decaphosphapentacene	

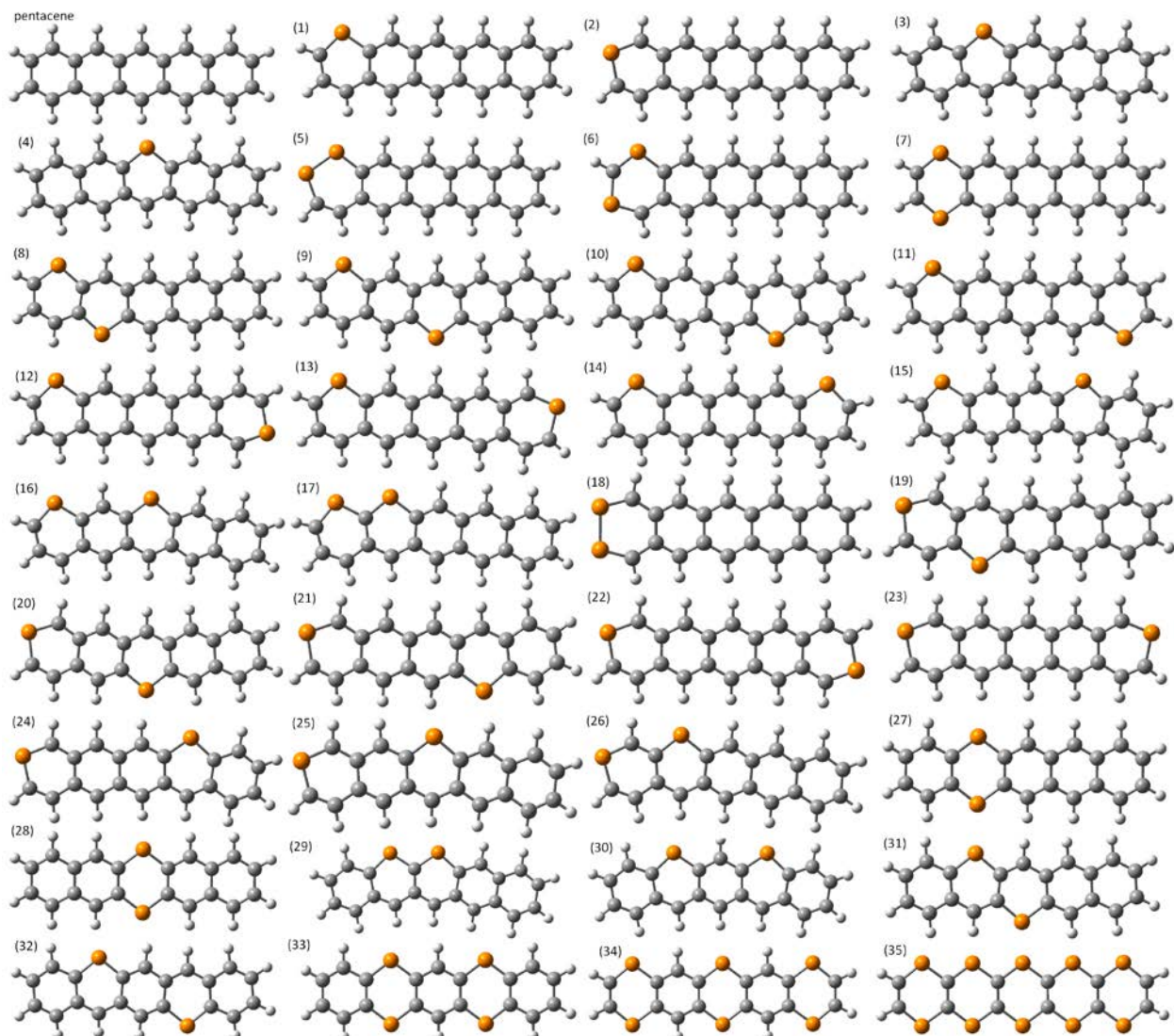


Fig. S1 The optimized structures for pentacene and the phosphapentacene derivatives based on B3LYP/6-311+G** method.



Fig. S2 The optimized cationic structures for pentacene and the phosphapentacene derivatives based on B3LYP/6-311+G** method.

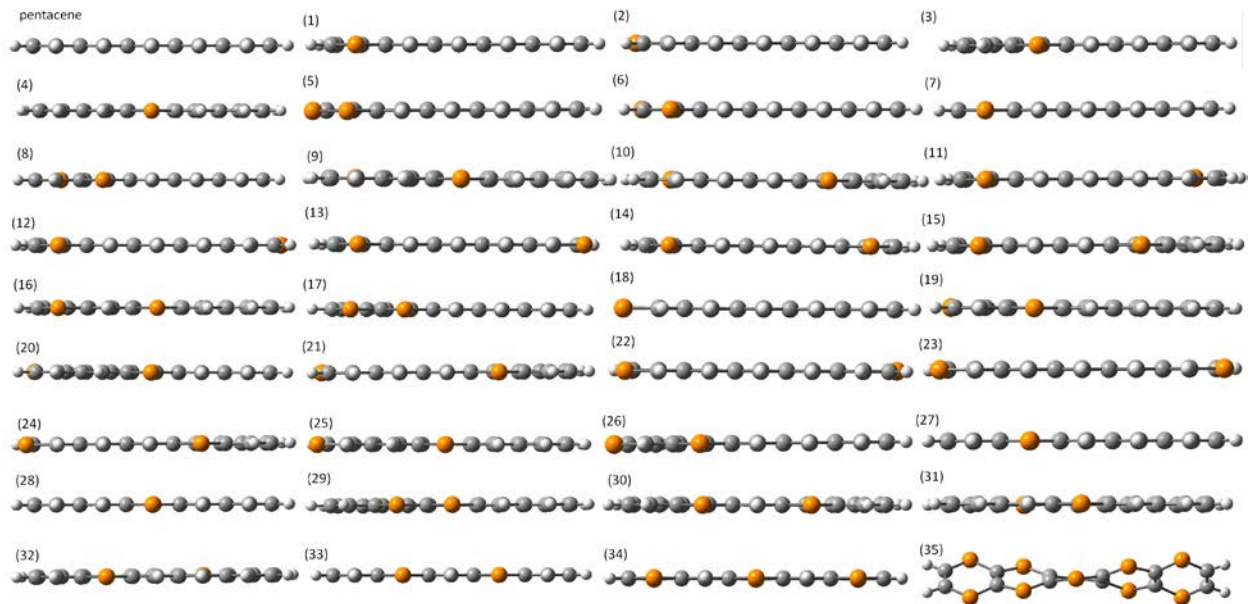
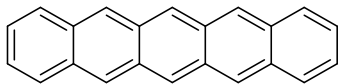
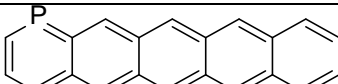
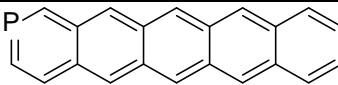
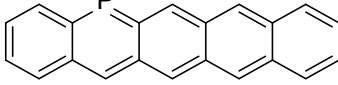
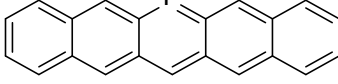
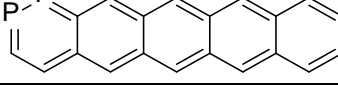
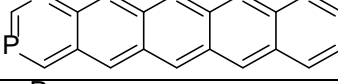
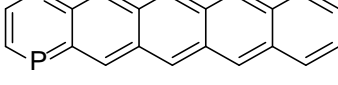
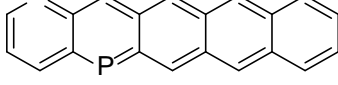
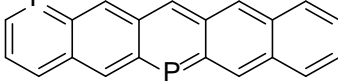
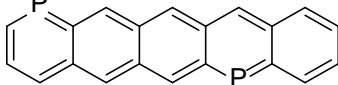
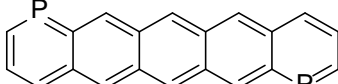
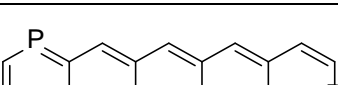
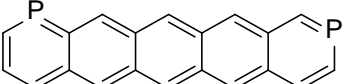
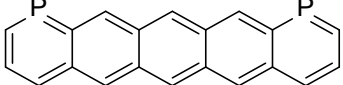
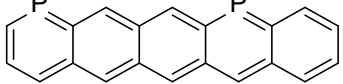
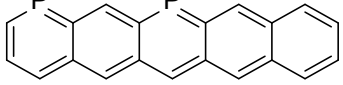
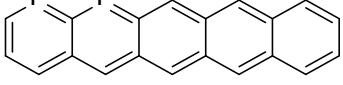
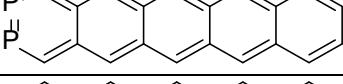
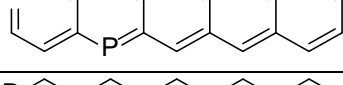
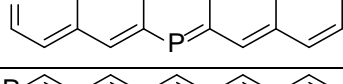
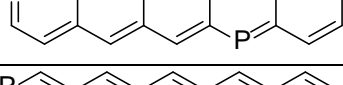
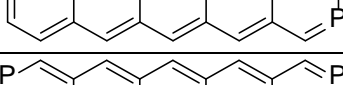
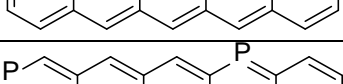
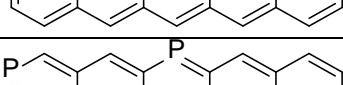
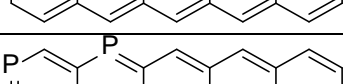
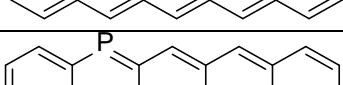
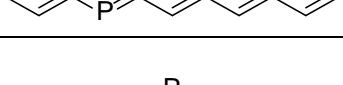
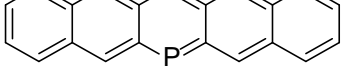


Fig. S3 The optimized anionic structures for pentacene and the phosphapentacene derivatives based on B3LYP/6-311+G** method.

Table S2. Summary of the p_z atomic orbital of the sp^2 -phosphorus in the frontier molecular orbitals (FMO) and natural bond orbital (NBO) charge distributions of the phosphapentacenes, and the calculated results for pentacene is also shown for comparison.

	index	HOMO/%	LUMO/%	Charge
	1	3	3	-0.165
	2	3	3	-0.210
	5	9	9	-0.178
	6	12	12	-0.218
	1	6	10	0.6745
	2	6	9	0.64546
	5	17	19	0.67571
	6	22	23	0.66942
	1	5	15	0.3023
	2	5	13	0.2784
	1	4	12	0.7482
	3	6	8	0.6847
	1	6	15	0.7008
	4	6	15	0.7008
	1	7	9	0.6750
	5	17	19	0.6783
	1	5	8	0.6764
	6	22	21	0.6732
	1	5	8	0.6764
	7	18	17	0.6758
	1	6	8	0.6743
	8	6	8	0.6743
	1	16	5	0.6765
	9	6	8	0.6518

	1	6	8	0.6772
	10	6	8	0.6486
	1	6	8	0.6777
	11	6	8	0.6777
	1	5	7	0.6786
	12	17	17	0.6816
	1	5	6	0.6830
	13	20	21	0.6732
	1	6	6	0.7097
	14	14	19	0.7313
	2	5	7	0.3269
	3	5	7	0.3269
	2	6	6	0.6568
	5	15	19	0.6929
	2	5	6	0.6518
	6	21	21	0.6647
	2	4	7	0.6524
	7	17	16	0.6808
	2	6	8	0.6519
	9	6	8	0.6519
	2	5	7	0.6520
	10	5	7	0.6520
	2	5	8	0.6488
	12	18	17	0.6809
	2	6	9	0.6515
	13	22	22	0.6669
	2	6	11	0.6545
	14	17	21	0.6931
	5	17	25	0.7082
	14	17	25	0.7082
	6	20	27	0.6691
	13	20	27	0.6691

	5	14	13	0.7198
	6	17	19	0.7087
	5	14	15	0.6763
	7	14	15	0.6763
	5	17	17	0.6663
	13	21	21	0.6713
	5	16	16	0.6775
	12	16	16	0.6775
	5	13	16	0.7048
	7	13	16	0.7048
	12	13	16	0.7048
	14	13	16	0.7048
	1	5	5	0.7111
	4	5	5	0.7111
	6	17	23	0.7011
	8	5	5	0.7111
	11	5	5	0.7111
	13	17	23	0.7011
	1	4	3	0.7400
	4	4	3	0.7400
	5	9	11	0.7951
	6	11	16	0.8036
	7	9	11	0.7951
	8	4	3	0.7400
	11	4	3	0.7400
	12	9	11	0.7951
	13	11	16	0.8036
	14	9	11	0.7951

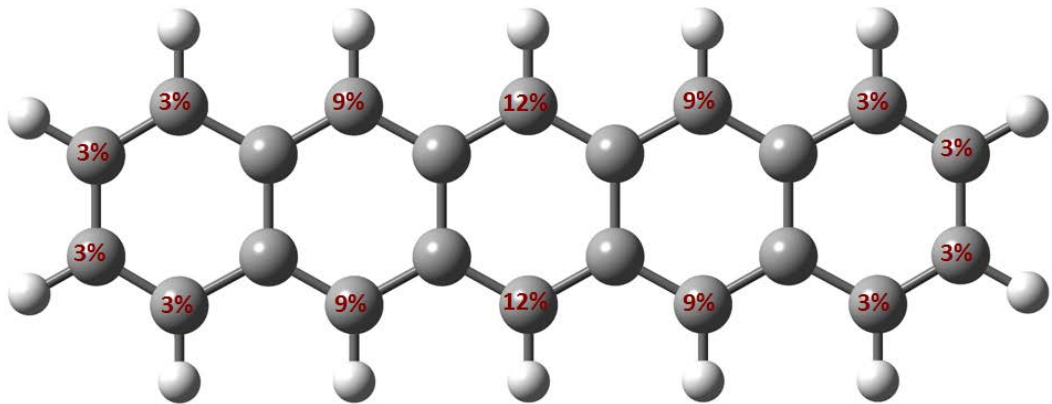


Fig. S4 The contribution of p_z atomic orbital in the HOMO of pentacene.

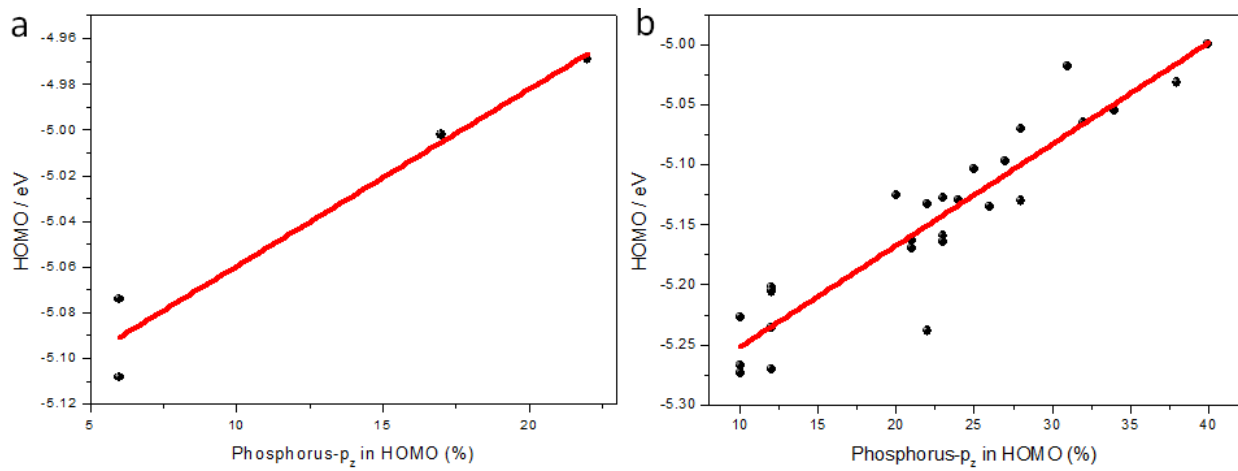


Fig. S5 Correlations between HOMO energy levels of monophosphapentacene (a) and diphosphapentacene derivatives (b) with the percentage of p_z atomic orbital of the sp²-phosphorus in the HOMO of the phosphapentacene derivatives.

Table S3. Summary of the calculated HOMO, LUMO levels, vertical ionic potentials (IPs), electron affinities (EAs), $S_0 \rightarrow S_1$ gaps, singlet-triplet energy splitting (ΔE_{S-T}), hole (λ_h) and electron (λ_e) reorganization energies for pentacene and the phosphapentacene derivatives based on B3LYP/6-311+G** method.

	HOMO/eV	LUMO/eV	IP _v /eV	EA _v /eV	$S_0 \rightarrow S_1$ /eV	ΔE_{S-T} /eV	λ_h /meV	λ_e /meV
pentacene	-4.94	-2.75	6.23	-1.47	1.90	0.78	95.25	134.11
1	-5.07	-2.95	6.34	-1.70	1.82	0.78	95.71	124.89
2	-5.11	-3.00	6.37	-1.75	1.82	0.76	92.59	118.61
3	-5.00	-2.99	6.28	-1.73	1.75	0.64	89.34	126.89
4	-4.97	-3.01	6.25	-1.74	1.73	0.56	83.86	129.98
5	-5.27	-3.20	6.52	-1.97	1.74	0.80	96.15	105.40
6	-5.23	-3.17	6.47	-1.95	1.73	0.76	96.42	114.37
7	-5.21	-3.16	6.46	-1.93	1.71	0.78	95.80	113.35
8	-5.13	-3.17	6.38	-1.93	1.69	0.64	91.35	120.84
9	-5.10	-3.18	6.35	-1.94	1.67	0.56	87.03	123.10
10	-5.13	-3.16	6.38	-1.93	1.70	0.64	90.26	119.38
11	-5.20	-3.13	6.45	-1.90	1.77	0.77	95.49	118.18
12	-5.24	-3.17	6.48	-1.95	1.77	0.76	93.83	112.25
13	-5.24	-3.17	6.48	-1.95	1.77	0.76	92.90	112.96
14	-5.21	-3.12	6.45	-1.90	1.78	0.77	96.44	117.74
15	-5.13	-3.16	6.39	-1.92	1.70	0.65	88.39	117.73
16	-5.10	-3.18	6.36	-1.93	1.68	0.56	83.48	121.49
17	-5.13	-3.14	6.38	-1.90	1.71	0.65	94.25	124.93
18	-5.27	-3.24	6.51	-2.03	1.70	0.71	86.28	114.75
19	-5.17	-3.21	6.42	-1.98	1.69	0.63	87.73	118.06
20	-5.13	-3.22	6.39	-1.98	1.67	0.55	80.44	116.75

21	-5.16	-3.20	6.41	-1.98	1.69	0.63	85.81	112.26
22	-5.27	-3.21	6.51	-2.01	1.76	0.74	90.06	106.85
23	-5.27	-3.21	6.51	-2.01	1.77	0.75	90.93	107.87
24	-5.16	-3.21	6.41	-1.98	1.69	0.63	87.14	114.79
25	-5.13	-3.23	6.38	-2.00	1.67	0.54	83.31	118.30
26	-5.16	-3.23	6.41	-1.99	1.67	0.62	88.62	111.97
27	-5.05	-3.26	6.32	-1.99	1.56	0.43	82.49	120.97
28	-5.00	-3.29	6.27	-2.01	1.53	0.31	69.80	128.20
29	-5.02	-3.16	6.28	-1.90	1.63	0.52	82.47	120.66
30	-5.07	-3.19	6.33	-1.94	1.62	0.58	83.45	114.55
31	-5.03	-3.22	6.29	-1.96	1.61	0.45	76.36	126.75
32	-5.06	-3.21	6.32	-1.96	1.62	0.55	82.85	122.34
33	-5.17	-3.58	6.40	-2.36	1.35	0.39	71.68	95.74
34	-5.47	-3.81	6.66	-2.63	1.42	0.39	75.97	98.37
35	-5.52	-4.05	6.66	-2.89	1.21	0.33	88.72	211.32

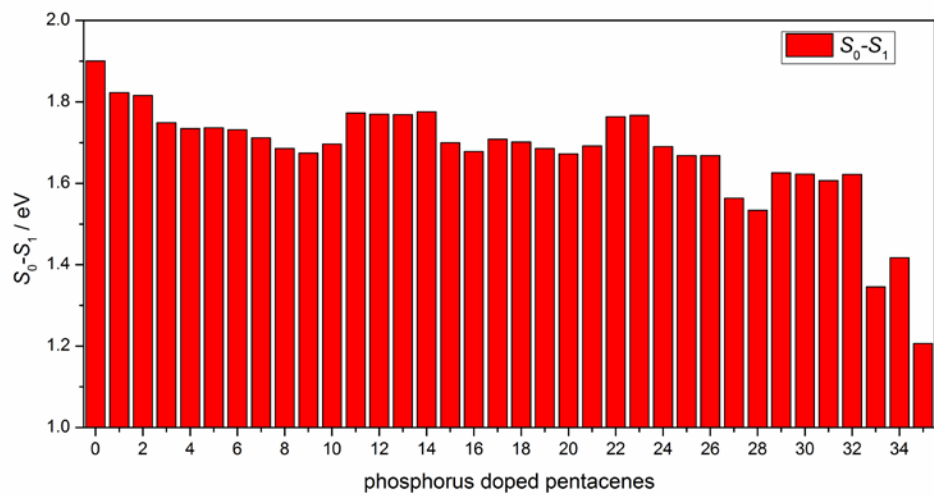
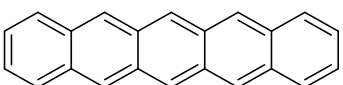
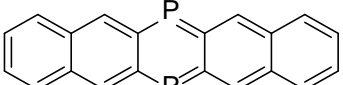
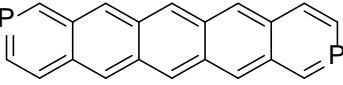
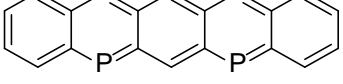
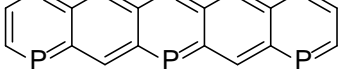
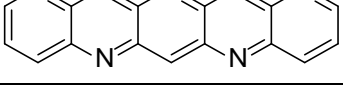
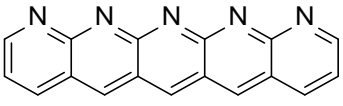
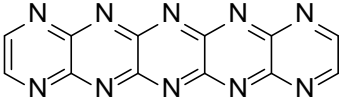
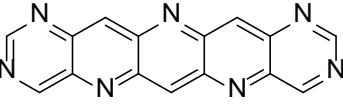
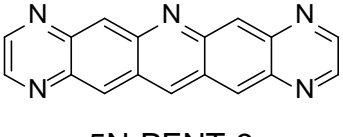
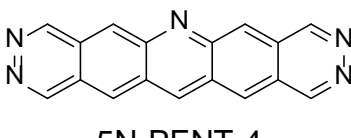
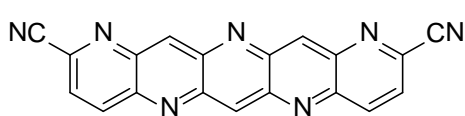
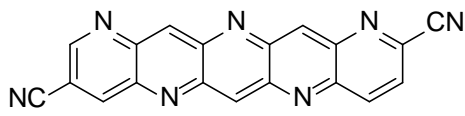
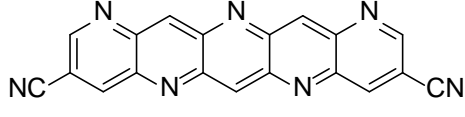
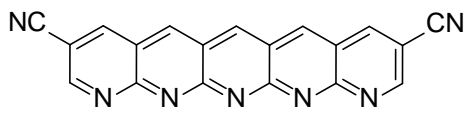
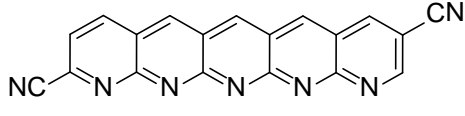
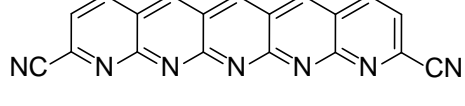


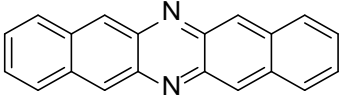
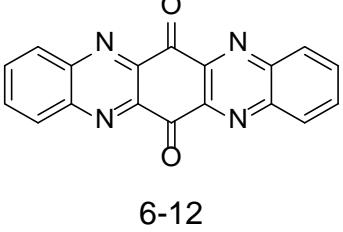
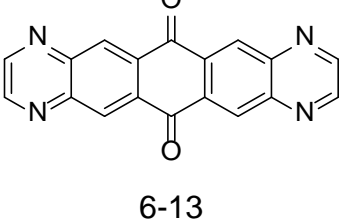
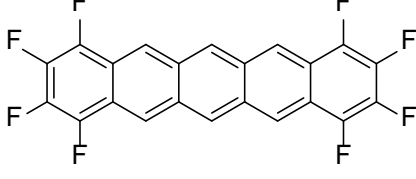
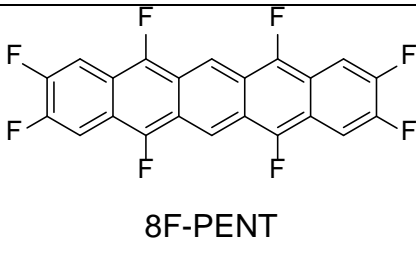
Fig. S6 Vertical $S_0 \rightarrow S_1$ gaps for pentacene and the phosphapentacene derivatives based on B3LYP/6-311+G** method.

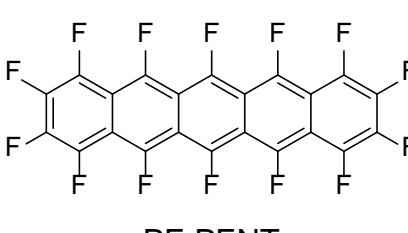
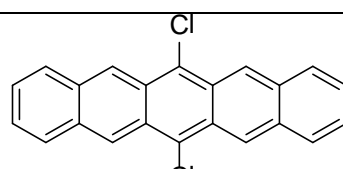
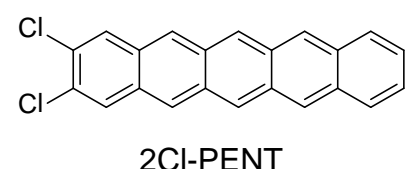
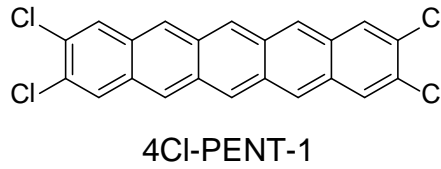
Table S4. Summary of the calculated hole and electron reorganization energies for the representative pentacene derivatives.

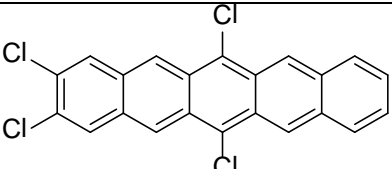
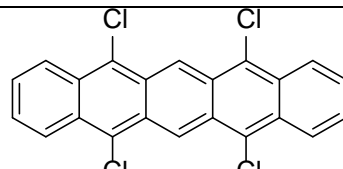
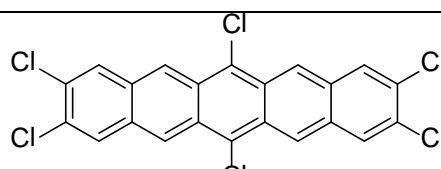
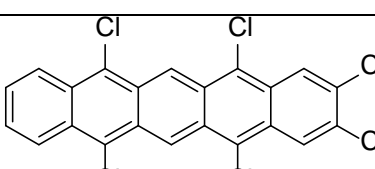
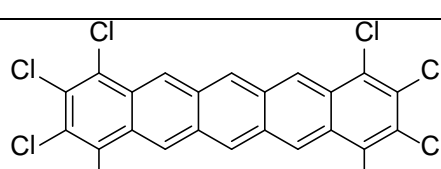
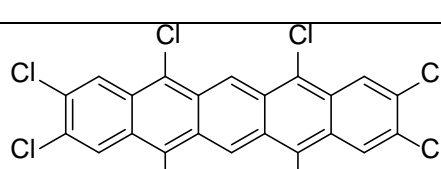
Structure	methods	λ_h/meV	λ_e/meV	Refer
 pentacene	B3LYP/6-311+G**//B3LYP/6-31G*	92	131	Houk, et al. <i>J. Am. Chem. Soc.</i> 2007 , 129, 1805-1815
	B3LYP/6-31G**	94	133	Chao, et al. <i>Chem. Eur. J.</i> 2007 , 13, 4750-4758
	B3LYP/6-31+G(d,p)	108	129	Wang, et al, <i>Comput. Theor. Chem.</i> 2015 , 1057, 67-73
	B3LYP/6-31++G**//B3LYP/6-31G**	95	130	Han, et al. <i>J. Comput. Chem.</i> 2011 , 32, 3218-3225
	B3LYP/6-311+G**	95.25	134.11	This work
	B3LYP/6-311+G**	69.80	128.20	This work
	B3LYP/6-311+G**	90.06	106.85	This work
	B3LYP/6-311+G**	71.68	95.74	This work
	B3LYP/6-311+G**	75.97	98.37	This work
	B3LYP/6-311+G**//	114	150	Houk, et al. <i>J. Am. Chem. Soc.</i>

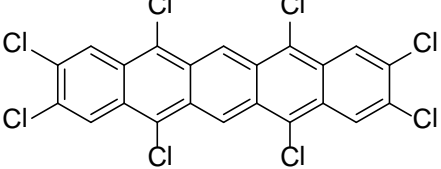
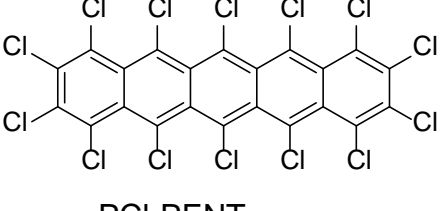
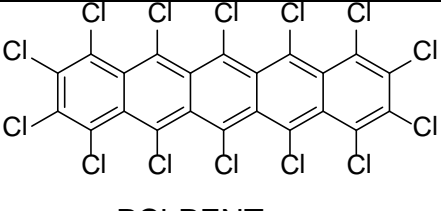
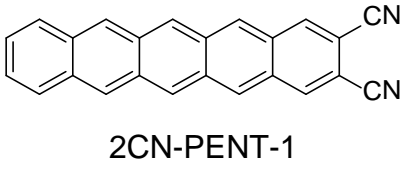
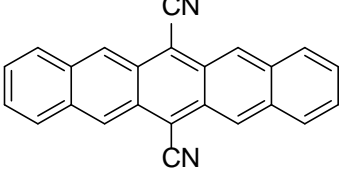
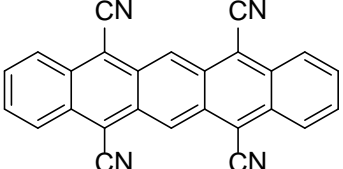
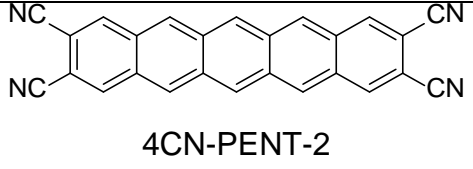
	B3LYP/6-31G*			2007 , 129, 1805-1815
	B3LYP/6-31G**	114	149	Chao, et al., <i>ChemPhysChem</i> 2006 , 7, 2003-2007
	B3LYP/6-311+G**//B3LYP/6-31G*	128	165	Houk, et al. <i>J. Am. Chem. Soc.</i> 2007 , 129, 1805-1815
	B3LYP/6-31G**	126	162	Chao, et al., <i>ChemPhysChem</i> 2006 , 7, 2003-2007
	B3LYP/6-311+G**//B3LYP/6-31G*	340	204	Houk, et al. <i>J. Am. Chem. Soc.</i> 2007 , 129, 1805-1815
	B3LYP/6-31G**	354	201	Chao, et al., <i>ChemPhysChem</i> 2006 , 7, 2003-2007
	B3LYP/6-311+G**//B3LYP/6-31G*	-	178	Houk, et al. <i>J. Am. Chem. Soc.</i> 2007 , 129, 1805-1815
	B3LYP/6-311+G**//B3LYP/6-31G*	-	197	Houk, et al. <i>J. Am. Chem. Soc.</i> 2007 , 129, 1805-1815

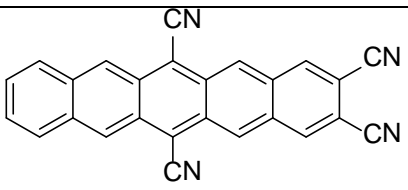
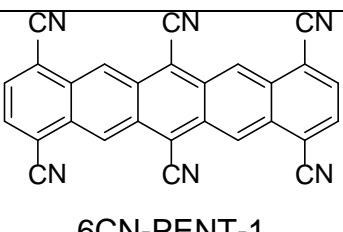
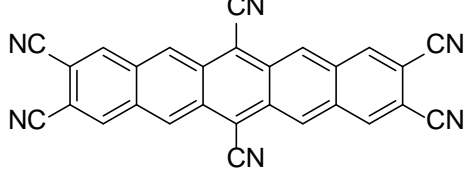
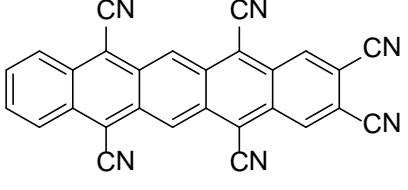
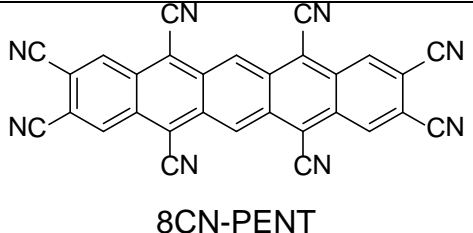
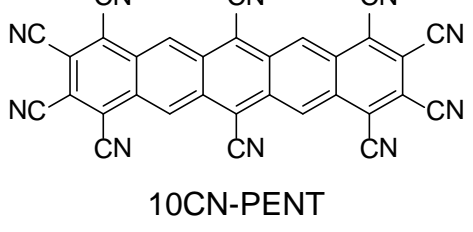
 <p>5N-PENT-3</p>	B3LYP/6-31G**	120	167	Chao, et al., <i>ChemPhysChem</i> 2006 , 7, 2003-2007
 <p>5N-PENT-4</p>	B3LYP/6-31G**	131	157	Chao, et al., <i>ChemPhysChem</i> 2006 , 7, 2003-2007
	B3LYP/6-311+G**//B3LYP/6-31G*	-	132	Houk, et al. <i>J. Am. Chem. Soc.</i> 2007 , 129, 1805-1815
	B3LYP/6-311+G**//B3LYP/6-31G*	-	134	Houk, et al. <i>J. Am. Chem. Soc.</i> 2007 , 129, 1805-1815
	B3LYP/6-311+G**//B3LYP/6-31G*	-	138	Houk, et al. <i>J. Am. Chem. Soc.</i> 2007 , 129, 1805-1815
	B3LYP/6-311+G**//B3LYP/6-31G*	-	135	Houk, et al. <i>J. Am. Chem. Soc.</i> 2007 , 129, 1805-1815
	B3LYP/6-311+G**//B3LYP/6-31G*	-	149	Houk, et al. <i>J. Am. Chem. Soc.</i> 2007 , 129, 1805-1815
	B3LYP/6-311+G**//B3LYP/6-	-	160	Houk, et al. <i>J. Am. Chem. Soc.</i> 2007 , 129,

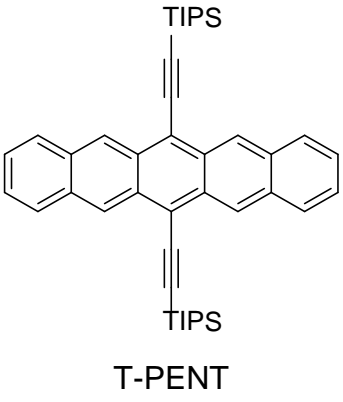
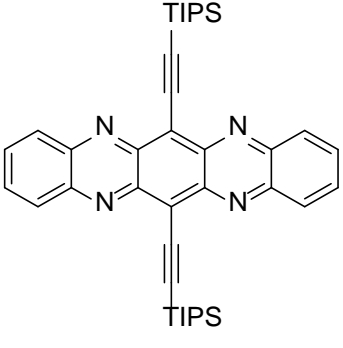
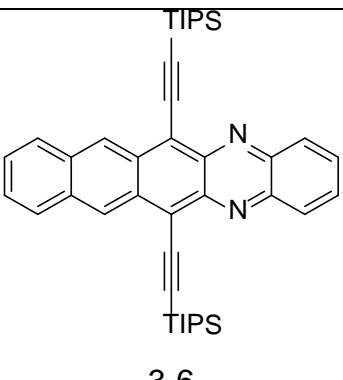
	31G*			1805-1815
	B3LYP/6-31++G**//B3LYP/6-31G**	80	150	Ren, et al. <i>J. Phys. Chem. C</i> 2011 , 115, 21416-21428
 4Cl2N-PENT	B3LYP/6-31G**	113	154	Chao, et al., <i>ChemPhysChem</i> 2006 , 7, 2003-2007
 6-12	B3LYP/6-31++G**//B3LYP/6-31G**	370	130	Ren, et al. <i>J. Phys. Chem. C</i> 2011 , 115, 21416-21428
 6-13	B3LYP/6-31++G**//B3LYP/6-31G**	390	150	Ren, et al. <i>J. Phys. Chem. C</i> 2011 , 115, 21416-21428
 8F-PENT-1	B3LYP/6-31G**	162	188	Chao, et al., <i>ChemPhysChem</i> 2006 , 7, 2003-2007
 8F-PENT	B3LYP/6-31+G(d,p)	195	215	Wang, et al, <i>Comput. Theor. Chem.</i> 2015 , 1057, 67-73
	B3LYP/6-	232	236	Wang, et al,

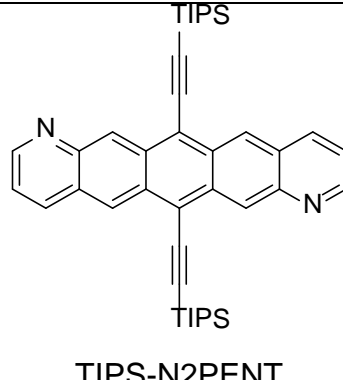
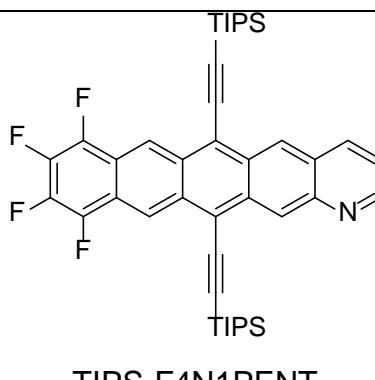
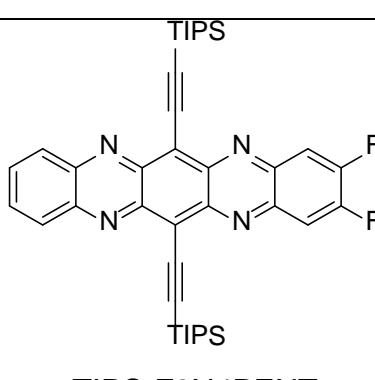
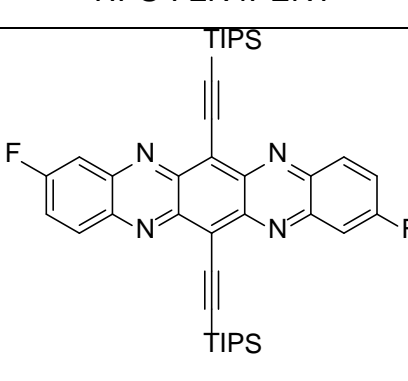
 <p>PF-PENT</p>	31+G(d,p)			<i>Comput. Theor. Chem.</i> 2015 , 1057, 67-73
	B3LYP/6-31G**	222	225	Chao, et al., <i>ChemPhysChem</i> 2006 , 7, 2003-2007
	B3LYP/6-31G**	222	225	Chao, et al. <i>Chem. Eur. J.</i> 2007 , 13, 4750-4758
	B3LYP/6-31++G** //B3LYP/6-31G**	226	229	Han, et al. <i>J. Comput. Chem.</i> 2011 , 32, 3218-3225
 <p>DCP</p>	B3LYP/6-31+G(d,p)	108	141	Wang, et al, <i>Comput. Theor. Chem.</i> 2015 , 1057, 67-73
 <p>2Cl-PENT</p>	B3LYP/6-31+G(d,p)	105	139	Wang, et al, <i>Comput. Theor. Chem.</i> 2015 , 1057, 67-73
 <p>4Cl-PENT-1</p>	B3LYP/6-31+G(d,p)	117	143	Wang, et al, <i>Comput. Theor. Chem.</i> 2015 , 1057, 67-73

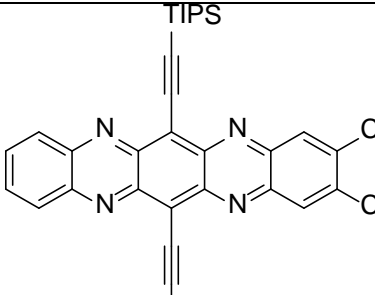
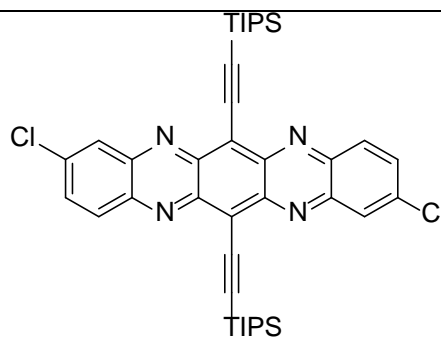
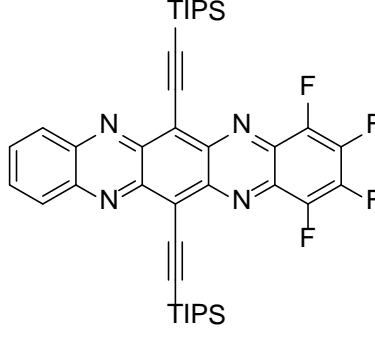
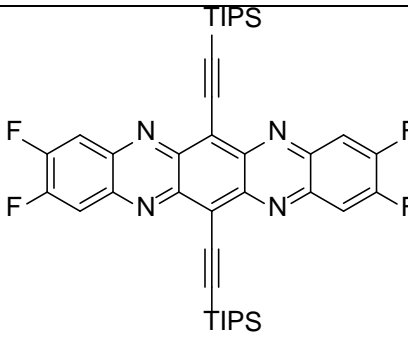
 <p>4Cl-PENT-2</p>	B3LYP/6-31+G(d,p)	119	148	Wang, et al, <i>Comput. Theor. Chem.</i> 2015 , 1057, 67-73
 <p>4Cl-PENT-3</p>	B3LYP/6-31+G(d,p)	124	148	Wang, et al, <i>Comput. Theor. Chem.</i> 2015 , 1057, 67-73
 <p>6Cl-PENT-1</p>	B3LYP/6-31+G(d,p)	130	152	Wang, et al, <i>Comput. Theor. Chem.</i> 2015 , 1057, 67-73
 <p>6Cl-PENT-2</p>	B3LYP/6-31+G(d,p)	132	152	Wang, et al, <i>Comput. Theor. Chem.</i> 2015 , 1057, 67-73
 <p>8Cl-PENT-1</p>	B3LYP/6-31G**	132	151	Chao, et al., <i>ChemPhysChem</i> 2006 , 7, 2003-2007
 <p>8Cl-PENT</p>	B3LYP/6-31+G(d,p)	140	155	Wang, et al, <i>Comput. Theor. Chem.</i> 2015 , 1057, 67-73

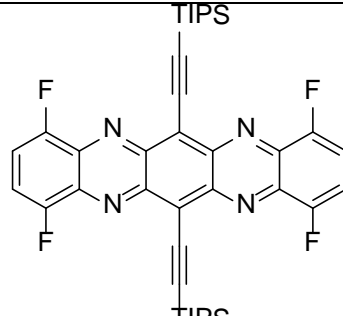
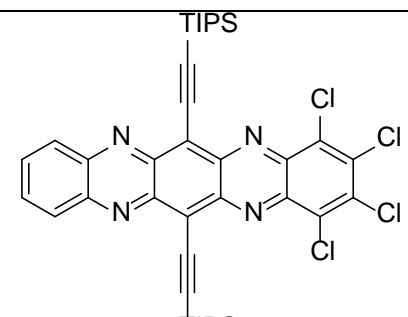
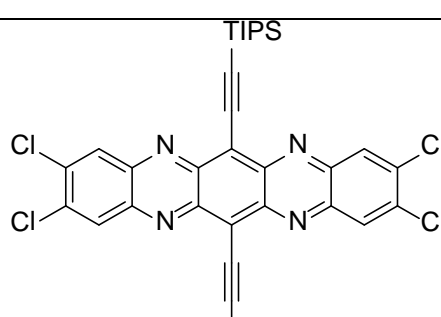
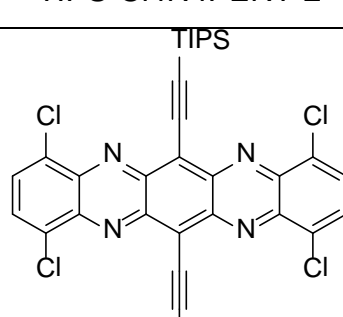
 <p>8Cl-PENT-2</p>	B3LYP/6-31G**	144	159	Chao, et al., <i>ChemPhysChem</i> 2006 , 7, 2003-2007
 <p>PCI-PENT_{nonplanar}</p>	B3LYP/6-31G**	143	160	Chao, et al., <i>ChemPhysChem</i> 2006 , 7, 2003-2007
 <p>PCI-PENT_{planar}</p>	B3LYP/6-31G**	168	154	Chao, et al., <i>ChemPhysChem</i> 2006 , 7, 2003-2007
 <p>2CN-PENT-1</p>	B3LYP/6-31G**	71	135	Chao, et al. <i>Chem. Eur. J.</i> 2007 , 13, 4750-4758
 <p>2CN-PENT-2</p>	B3LYP/6-31G**	93	117	Chao, et al. <i>Chem. Eur. J.</i> 2007 , 13, 4750-4758
 <p>4CN-PENT-1</p>	B3LYP/6-31G**	69	126	Chao, et al. <i>Chem. Eur. J.</i> 2007 , 13, 4750-4758
 <p>4CN-PENT-2</p>	B3LYP/6-31G**	90	103	Chao, et al. <i>Chem. Eur. J.</i> 2007 , 13, 4750-

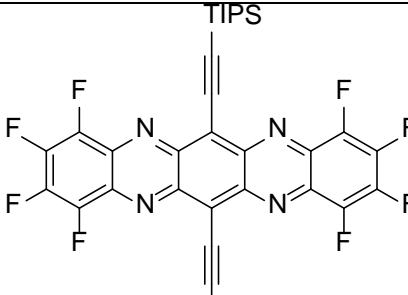
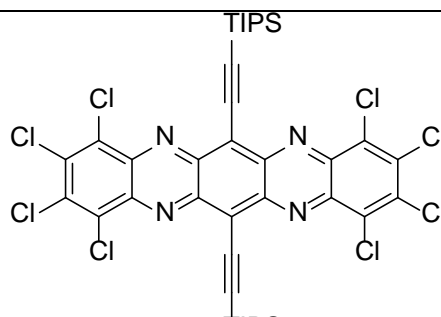
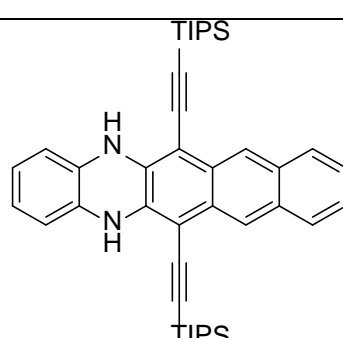
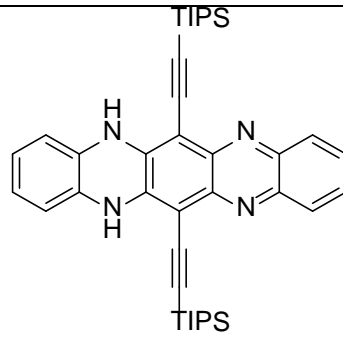
				4758
 4CN-PENT-3	B3LYP/6-31G**	72	119	Chao, et al. <i>Chem. Eur. J.</i> 2007 , 13, 4750-4758
 6CN-PENT-1	B3LYP/6-31G**	78	122	Chao, et al. <i>Chem. Eur. J.</i> 2007 , 13, 4750-4758
 6CN-PENT-2	B3LYP/6-31G**	70	105	Chao, et al. <i>Chem. Eur. J.</i> 2007 , 13, 4750-4758
 6CN-PENT-3	B3LYP/6-31G**	71	109	Chao, et al. <i>Chem. Eur. J.</i> 2007 , 13, 4750-4758
 8CN-PENT	B3LYP/6-31G**	70	95	Chao, et al. <i>Chem. Eur. J.</i> 2007 , 13, 4750-4758
 10CN-PENT	B3LYP/6-31G**	75	87	Chao, et al. <i>Chem. Eur. J.</i> 2007 , 13, 4750-4758
	B3LYP/6-31G**	144	203	Chao, et al. <i>Chem. Eur. J.</i>

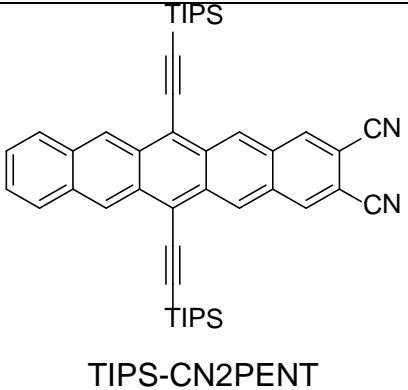
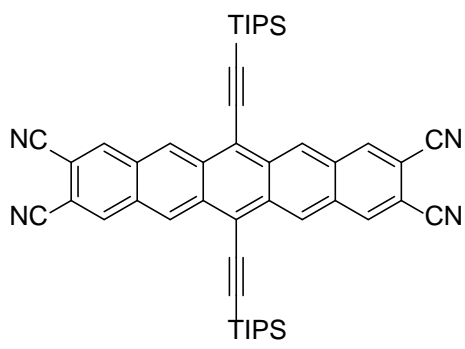
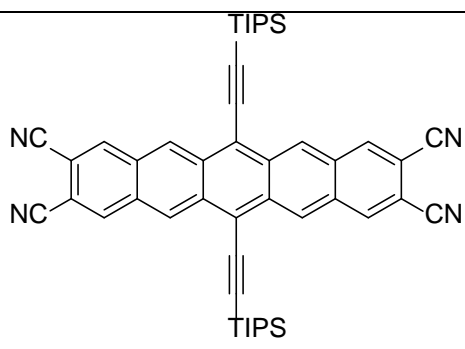
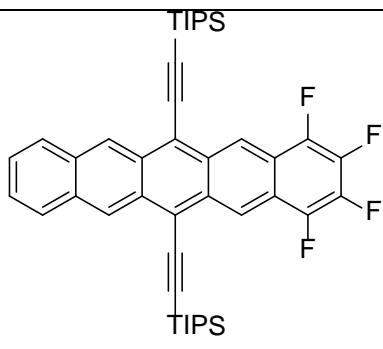
 <p>T-PENT</p>				2007, 13, 4750-4758
	B3LYP/6-31G**	144	203	Kuo, et al, <i>Phys. Chem. Chem. Phys.</i> , 2011 , 13, 11148-11155
	B3LYP/6-31++G**//B3LYP/6-31G**	130	190	Ren, et al. <i>J. Phys. Chem. C</i> 2011 , 115, 21416-21428
 <p>TIPS</p>	B3LYP/6-31++G**//B3LYP/6-31G**	210	210	Ren, et al. <i>J. Phys. Chem. C</i> 2011 , 115, 21416-21428
	B3LYP/6-31G**	211	204	Kuo, et al, <i>Phys. Chem. Chem. Phys.</i> , 2011 , 13, 11148-11155
	B3LYP/6-31+G**	205.9	195.1	Shuai, et al, <i>J. Mater. Chem.</i> , 2012 , 22, 18181
 <p>3-6</p>	B3LYP/6-31++G**//B3LYP/6-31G**	170	200	Ren, et al. <i>J. Phys. Chem. C</i> 2011 , 115, 21416-21428
	B3LYP/6-31+G**	164.4	192.8	Shuai, et al, <i>J. Mater. Chem.</i> , 2012 , 22, 18181

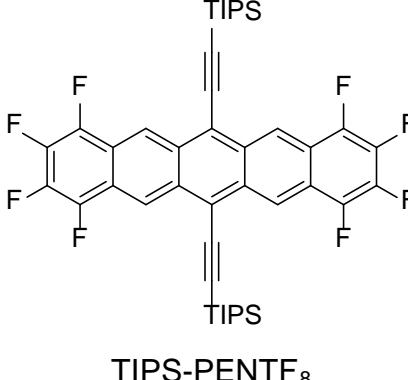
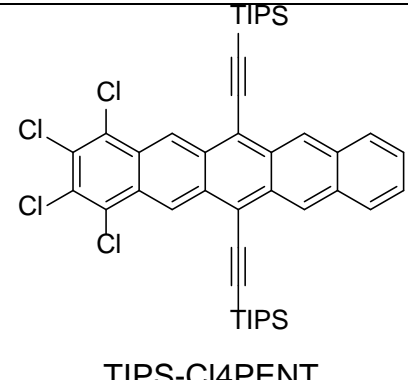
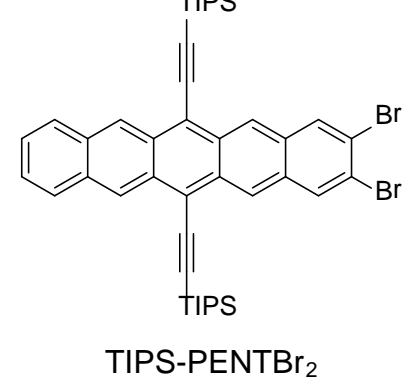
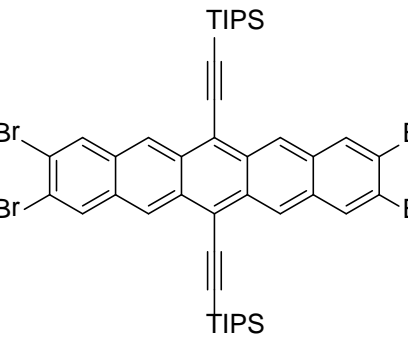
 <p>TIPS-N2PENT</p>	B3LYP/6-31G** 	161	192	Kuo, et al, <i>Phys. Chem. Chem. Phys.</i> , 2011 , 13, 11148-11155
 <p>TIPS-F4N1PENT</p>	B3LYP/6-31G** 	171	204	Kuo, et al, <i>Phys. Chem. Chem. Phys.</i> , 2011 , 13, 11148-11155
 <p>TIPS-F2N4PENT</p>	B3LYP/6-31G** 	227	223	Kuo, et al, <i>Phys. Chem. Chem. Phys.</i> , 2011 , 13, 11148-11155
 <p>TIPS-F2N4PENT-2</p>	B3LYP/6-31G** 	230	223	Kuo, et al, <i>Phys. Chem. Chem. Phys.</i> , 2011 , 13, 11148-11155

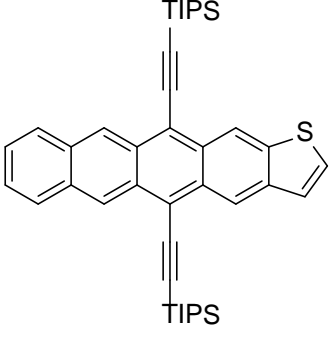
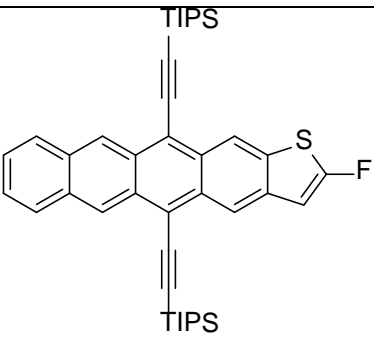
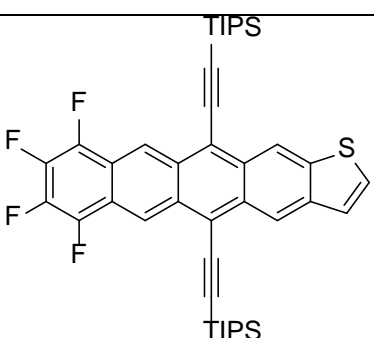
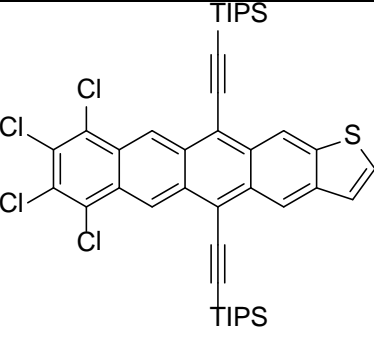
 <p>TIPS-CI2N4PENT</p>	B3LYP/6-31G** 	217	204	Kuo, et al, <i>Phys. Chem. Chem. Phys.</i> , 2011 , 13, 11148-11155
 <p>TIPS-CI2N4PENT-2</p>	B3LYP/6-31G** 	223	211	Kuo, et al, <i>Phys. Chem. Chem. Phys.</i> , 2011 , 13, 11148-11155
 <p>TIPS-F4N4PENT</p>	B3LYP/6-31G** 	225	223	Kuo, et al, <i>Phys. Chem. Chem. Phys.</i> , 2011 , 13, 11148-11155
 <p>TIPS-F4N4PENT-2</p>	B3LYP/6-31G** 	237	239	Kuo, et al, <i>Phys. Chem. Chem. Phys.</i> , 2011 , 13, 11148-11155

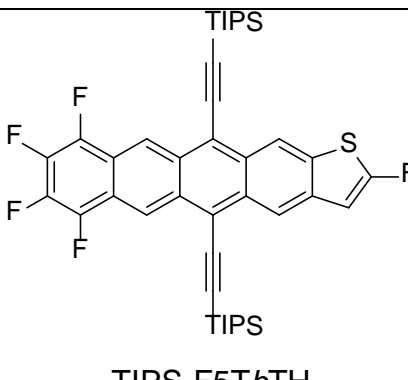
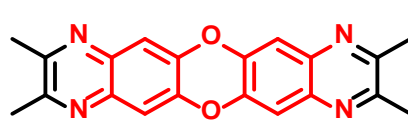
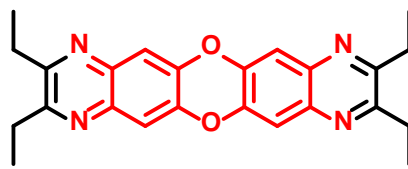
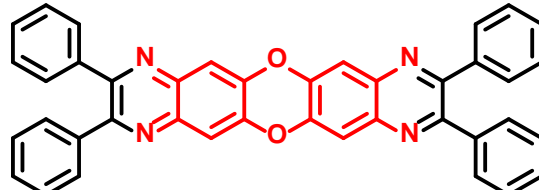
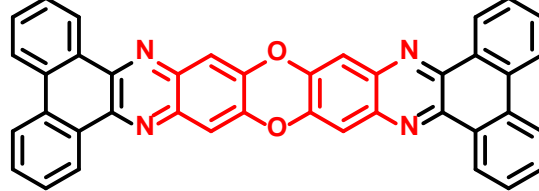
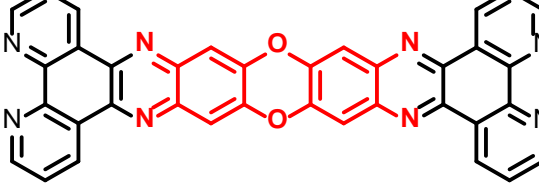
 <p>TIPS-F4N4PENT-3</p>	B3LYP/6-31G**	210	212	Kuo, et al, <i>Phys. Chem. Chem. Phys.</i> , 2011 , 13, 11148-11155
 <p>TIPS-Cl4N4PENT</p>	B3LYP/6-31G**	215	200	Kuo, et al, <i>Phys. Chem. Chem. Phys.</i> , 2011 , 13, 11148-11155
 <p>TIPS-Cl4N4PENT-2</p>	B3LYP/6-31G**	221	201	Kuo, et al, <i>Phys. Chem. Chem. Phys.</i> , 2011 , 13, 11148-11155
 <p>TIPS-Cl4N4PENT-3</p>	B3LYP/6-31G**	208	202	Kuo, et al, <i>Phys. Chem. Chem. Phys.</i> , 2011 , 13, 11148-11155

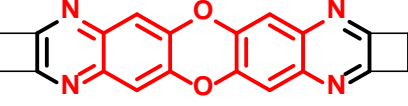
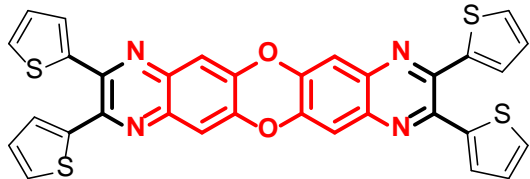
 <p>TIPS-F8N4PENT</p>	B3LYP/6-31G** 	229	235	Kuo, et al, <i>Phys. Chem. Chem. Phys.</i> , 2011 , 13, 11148-11155
 <p>TIPS-Cl8N4PENT</p>	B3LYP/6-31G** 	210	192	Kuo, et al, <i>Phys. Chem. Chem. Phys.</i> , 2011 , 13, 11148-11155
 <p>TIPS-DHDAP-2p</p>	B3LYP/6-31+G** 	198.6	389.6	Shuai, et al, <i>J. Mater. Chem.</i> , 2012 , 22, 18181
 <p>TIPS-DHTAP-2p</p>	B3LYP/6-31+G** 	197.7	330.7	Shuai, et al, <i>J. Mater. Chem.</i> , 2012 , 22, 18181
	B3LYP/6-	139	163	Kuo, et al, <i>Phys.</i>

 <p>TIPS-CN2PENT</p>	31G**			<i>Chem. Chem. Phys.</i> , 2011 , 13, 11148-11155
	B3LYP/6-31G**	139	163	Chao, et al. <i>Chem. Eur. J.</i> 2007 , 13, 4750-4758
	B3LYP/6-31G**	138	139	Chao, et al. <i>Chem. Eur. J.</i> 2007 , 13, 4750-4758
	B3LYP/6-31++G**//B3LYP/6-31G**	136	136	Han, et al. <i>J. Comput. Chem.</i> 2011 , 32, 3218-3225
 <p>TIPS-CN4PENT</p>	B3LYP/6-31G**	138	139	Kuo, et al, <i>Phys. Chem. Chem. Phys.</i> , 2011 , 13, 11148-11155
 <p>TIPS-F4PENT</p>	B3LYP/6-31G**	158	207	Kuo, et al, <i>Phys. Chem. Chem. Phys.</i> , 2011 , 13, 11148-11155

 <p>TIPS-PENTF₈</p>	B3LYP/6-31++G**//B3LYP/6-31G**	178	212	Han, et al. <i>J. Comput. Chem.</i> 2011 , 32, 3218-3225
	B3LYP/6-31G**	178	216	Kuo, et al, <i>Phys. Chem. Chem. Phys.</i> , 2011 , 13, 11148-11155
 <p>TIPS-Cl₄PENT</p>	B3LYP/6-31G**	148	184	Kuo, et al, <i>Phys. Chem. Chem. Phys.</i> , 2011 , 13, 11148-11155
	B3LYP/6-31++G**//B3LYP/6-31G**	136	182	Han, et al. <i>J. Comput. Chem.</i> 2011 , 32, 3218-3225
 <p>TIPS-PENTBr₂</p>	B3LYP/6-31G**	139	186	Kuo, et al, <i>Phys. Chem. Chem. Phys.</i> , 2011 , 13, 11148-11155
	B3LYP/6-31++G**//B3LYP/6-31G**	138	173	Han, et al. <i>J. Comput. Chem.</i> 2011 , 32, 3218-3225
 <p>TIPS-PENTBr₄</p>	B3LYP/6-31G**	140	175	Kuo, et al, <i>Phys. Chem. Chem. Phys.</i> , 2011 , 13,
	B3LYP/6-31++G**//B3LYP/6-31G**			

TIPS-PENTBr ₄				11148-11155
 TIPS-TbTH	B3LYP/6-31G**	143	217	Kuo, et al, <i>Phys. Chem. Chem. Phys.</i> , 2011 , 13, 11148-11155
 TIPS-F1TbTH	B3LYP/6-31G**	154	226	Kuo, et al, <i>Phys. Chem. Chem. Phys.</i> , 2011 , 13, 11148-11155
 TIPS-F4TbTH	B3LYP/6-31G**	161	225	Kuo, et al, <i>Phys. Chem. Chem. Phys.</i> , 2011 , 13, 11148-11155
 TIPS-TCBT	B3LYP/6-31++G**//B3LYP/6-31G**	147	195	Han, et al. <i>J. Comput. Chem.</i> 2011 , 32, 3218-3225
	B3LYP/6-31G**	152	198	Kuo, et al, <i>Phys. Chem. Chem. Phys.</i>

				<i>Phys.</i> , 2011 , <i>13</i> , 11148-11155
 <p>TIPS-F5TbTH</p>	B3LYP/6-31G**	176	234	Kuo, et al, <i>Phys. Chem. Chem. Phys.</i> , 2011 , <i>13</i> , 11148-11155
	B3LYP/6-31G(d)	168	214	Zhang, et al, <i>Asian J. Org. Chem.</i> 2013 , <i>2</i> , 852-856
	B3LYP/6-31G(d)	170	221	Zhang, et al, <i>Asian J. Org. Chem.</i> 2013 , <i>2</i> , 852-856
	B3LYP/6-31G(d)	173	170	Zhang, et al, <i>Asian J. Org. Chem.</i> 2013 , <i>2</i> , 852-856
	B3LYP/6-31G(d)	102	117	Zhang, et al, <i>Asian J. Org. Chem.</i> 2013 , <i>2</i> , 852-856
	B3LYP/6-31G(d)	123	121	Zhang, et al, <i>Asian J. Org. Chem.</i> 2013 , <i>2</i> , 852-856

	B3LYP/6-31G(d)	169	195	Zhang, et al, <i>Asian J. Org. Chem.</i> 2013 , 2, 852-856
	B3LYP/6-31G(d)	197	191	Zhang, et al, <i>Asian J. Org. Chem.</i> 2013 , 2, 852-856

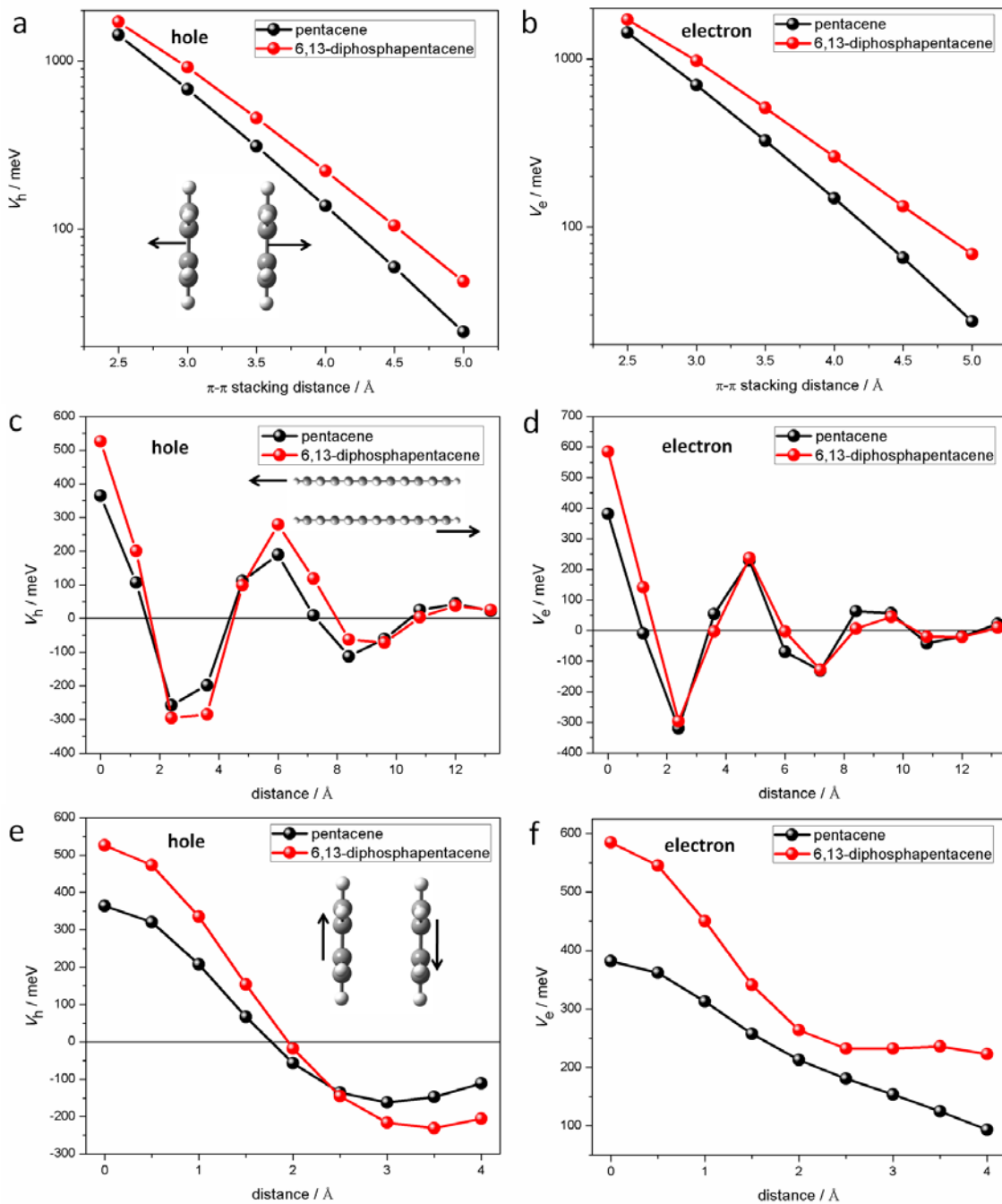


Fig. S7 Evolution of the calculated transfer integrals for hole (a, c, e) and electron transfer (b, d, f) in the dimer of pentacene and 6,13-diphosphapentacene as a function of the degree of translation of one molecule along the $\pi\text{-}\pi$ stacking (a, b), long axis (c, d) and short axis (e, f) intermolecular distance. The inset in (a) shows the $\pi\text{-}\pi$ stacking direction, the long axis (c) and short axis direction (e) is fixed with $\pi\text{-}\pi$ stacking distance of 3.4 Å during calculating the transfer integrals.

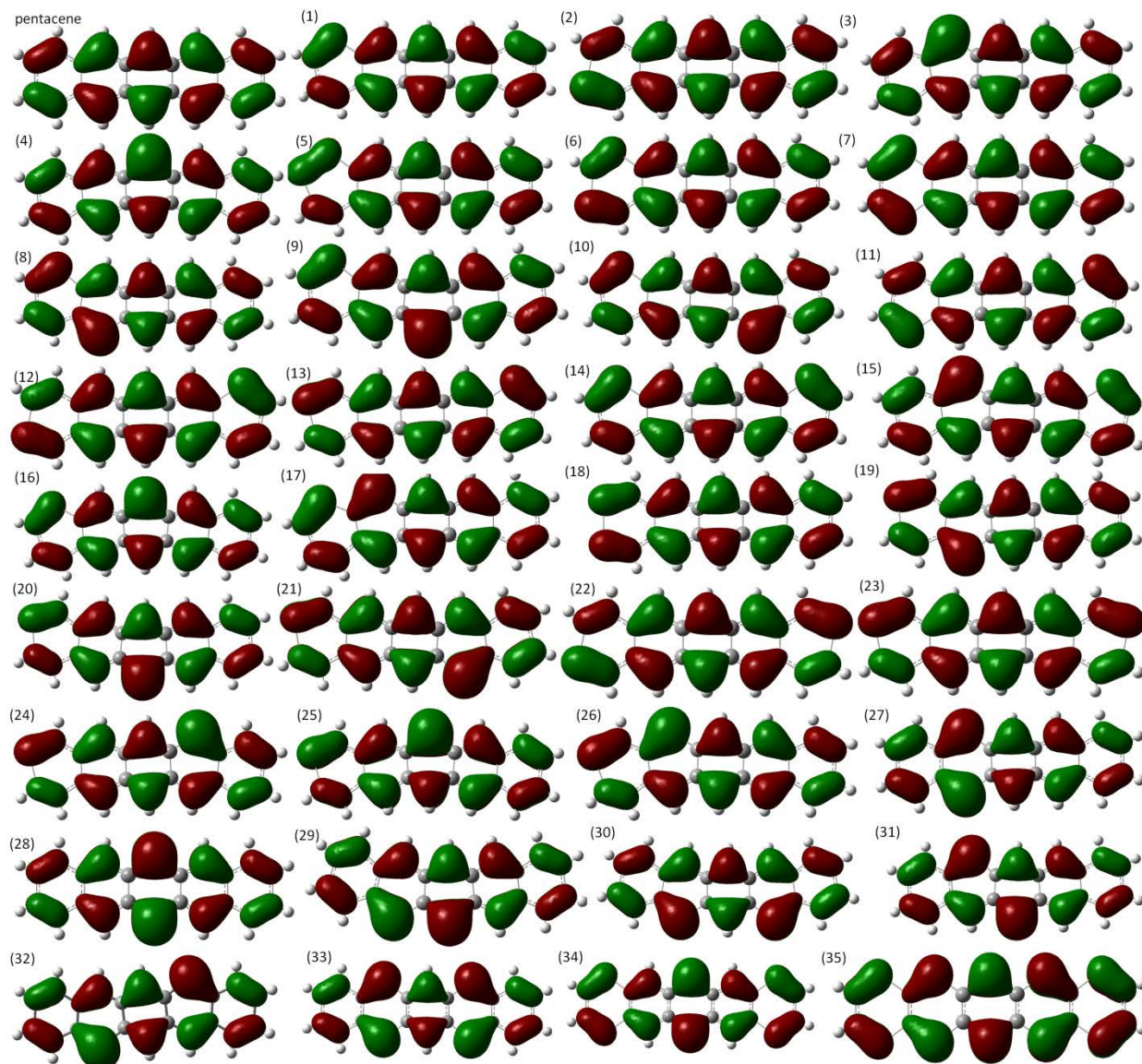


Fig. S8 HOMO electron density distributions for pentacene and the phosphapentacene derivatives based on B3LYP/6-311+G** method. Red and green surfaces represent positive and negative phase, drawn as isosurface of 0.02 au, respectively.

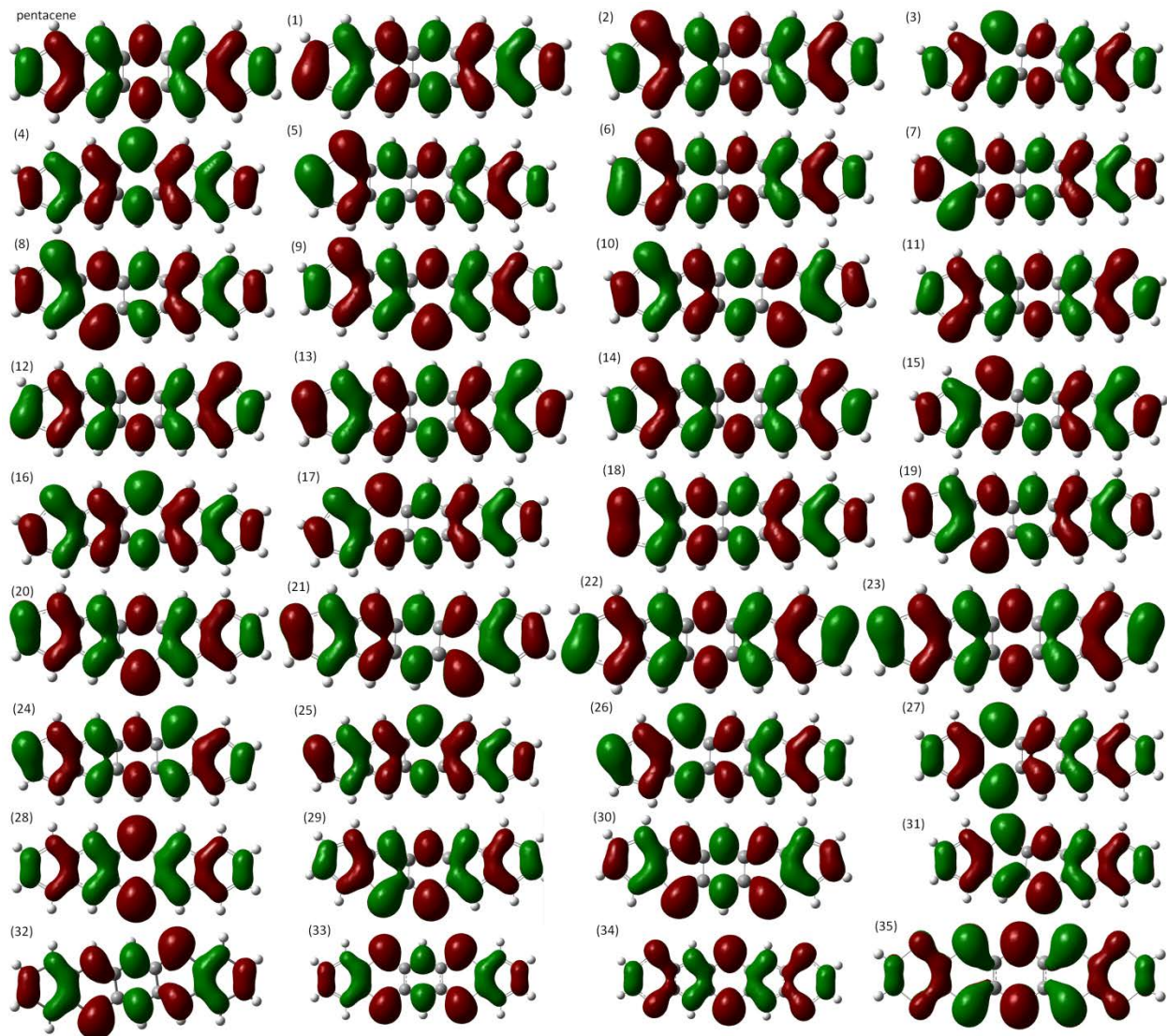


Fig. S9 LUMO electron density distributions for pentacene and the phosphapentacene derivatives based on B3LYP/6-311+G** method. Red and green surfaces represent positive and negative phase, drawn as isosurface of 0.02 au, respectively.

Table S5. Comparison of the hole (λ_h) and electron (λ_e) reorganization energies for pentacene and the phosphapentacene derivatives from adiabatic potential (AP) energy surface methods and normal mode (NM) analysis methods (B3LYP/6-311+G**).

	AP		NM	
	λ_h/meV	λ_e/meV	λ_h/meV	λ_e/meV
pentacene	95.25	134.11	94.97	133.77
1	95.71	124.89	95.34	124.60
2	92.59	118.61	92.24	118.40
3	89.34	126.89	89.02	126.83
4	83.86	129.98	83.56	129.81
5	96.15	105.40	95.59	105.01
6	96.42	114.37	96.21	114.43
7	95.80	113.35	95.34	112.95
8	91.35	120.84	90.75	120.51
9	87.03	123.10	86.54	122.86
10	90.26	119.38	89.89	119.14
11	95.49	118.18	95.09	117.91
12	93.83	112.25	93.36	111.83
13	92.90	112.96	92.49	112.82
14	96.44	117.74	96.08	117.53
15	88.39	117.73	87.90	117.53
16	83.48	121.49	83.07	121.13
17	94.25	124.93	93.36	124.72
18	86.28	114.75	86.17	114.43
19	87.73	118.06	87.28	117.91

20	80.44	116.75	79.97	116.42
21	85.81	112.26	85.42	111.95
22	90.06	106.85	89.64	106.50
23	90.93	107.87	90.51	107.61
24	87.14	114.79	86.66	114.56
25	83.31	118.30	82.82	118.03
26	88.62	111.97	88.15	111.83
27	82.49	120.97	81.83	120.63
28	69.80	128.20	69.18	127.95
29	82.47	120.66	81.95	120.26
30	83.45	114.55	83.07	114.31
31	76.36	126.75	75.75	126.58
32	82.85	122.34	82.32	122.12
33	71.68	95.74	70.67	95.34
34	75.97	98.37	75.26	97.94
35	88.72	211.32	89.64	257.63

Table S6. Summary of the calculated HOMO, LUMO levels, vertical ionic potentials (IPs), electron affinities (EAs), $S_0 \rightarrow S_1$ gaps, singlet-triplet energy splitting (ΔE_{S-T}), hole (λ_h) and electron (λ_e) reorganization energies for pentacene and the phosphapentacene derivatives based on B3LYP/6-31G* method.

	HOMO/eV	LUMO/eV	IP _v /eV	EA _v /eV	$S_0 \rightarrow S_1$ /eV ^a	ΔE_{S-T} /eV	λ_h /meV	λ_e /meV
pentacene	-4.60	-2.39	5.93	-1.06	2.31	0.78	91.71	131.30
1	-4.89	-2.81	6.06	-1.32	2.24	0.77	92.92	122.48
2	-4.80	-2.67	6.10	-1.38	2.24	0.76	90.63	117.65
3	-4.69	-2.67	6.01	-1.35	2.11	0.64	86.97	126.60
4	-4.66	-2.69	5.98	-1.36	2.06	0.56	81.63	129.18
5	-4.97	-2.91	6.26	-1.63	2.19	0.79	94.60	101.83
6	-4.89	-2.87	6.21	-1.60	2.17	0.75	93.34	114.66
7	-4.83	-2.87	6.18	-1.58	2.14	0.76	92.63	111.64
8	-4.81	-2.89	6.13	-1.58	2.05	0.63	87.40	119.57
9	-4.83	-2.86	6.10	-1.59	2.02	0.55	83.48	121.76
10	-4.94	-2.86	6.12	-1.58	2.08	0.64	86.58	118.18
11	-4.89	-2.81	6.18	-1.54	2.20	0.76	91.68	115.63
12	-4.94	-2.86	6.22	-1.60	2.20	0.75	90.61	111.10
13	-4.90	-2.81	6.22	-1.60	2.20	0.75	89.70	111.53
14	-4.81	-2.88	6.18	-1.54	2.21	0.76	93.06	115.49
15	-4.84	-2.86	6.13	-1.57	2.09	0.64	84.32	116.75
16	-4.83	-2.84	6.11	-1.59	2.03	0.56	80.12	120.22
17	-4.99	-2.95	6.12	-1.54	2.08	0.64	90.85	123.69
18	-4.93	-2.87	6.26	-1.68	2.13	0.71	85.27	112.40
19	-4.88	-2.92	6.17	-1.63	2.06	0.62	84.53	118.30
20	-4.86	-2.93	6.15	-1.64	2.02	0.55	77.54	116.53

21	-4.88	-2.90	6.17	-1.63	2.08	0.63	82.65	112.56
22	-4.99	-2.92	6.26	-1.66	2.19	0.74	87.34	105.76
23	-4.99	-2.91	6.26	-1.66	2.20	0.74	88.05	107.29
24	-4.88	-2.91	6.16	-1.64	2.07	0.63	83.70	114.50
25	-4.85	-2.94	6.14	-1.66	2.01	0.54	80.16	117.71
26	-4.88	-2.94	6.16	-1.66	2.04	0.61	85.90	111.15
27	-4.77	-2.98	6.07	-1.66	1.86	0.42	79.74	122.75
28	-4.72	-3.02	6.03	-1.68	1.77	0.30	67.43	129.69
29	-4.74	-2.87	6.04	-1.56	1.94	0.52	79.57	120.72
30	-4.78	-2.89	6.08	-1.60	1.98	0.58	80.23	145.31
31	-4.75	-2.93	6.05	-1.62	1.90	0.46	72.74	126.36
32	-4.78	-2.91	6.07	-1.61	1.97	0.55	78.90	122.14
33	-4.92	-3.35	6.19	-2.08	1.65	0.37	67.30	95.13
34	-5.23	-3.59	6.46	-2.37	1.75	0.36	71.23	96.08
35	-5.33	-3.87	6.50	-2.69	1.50	0.32	79.13	176.23

^a Time-dependent DFT (TDDFT) calculation for the S₀→S_n transitions using CAM-B3LYP/6-31G* were performed based on the optimized structures at ground states (B3LYP/6-31G*). The lowest 50 singlet roots of the nonhermitian eigenvalue equations were obtained to determine the vertical excitation energies.

Table S7. Comparison of the calculated HOMO and LUMO energy levels based on different functional and basis sets.

Pentacene	HOMO/eV	Relative error/%	LUMO/eV	Relative error/%	E _g /eV	Relative error/%
Experiment ^a	-4.91		-3.00		1.91	
B3LYP/6-31G*	-4.60	-6.31	-2.39	-20.33	2.21	15.71
B3LYP/6-311+G**	-4.94	0.65	-2.75	-8.33	2.19	14.66
CAM-B3LYP/6-311+G*	-6.04	22.85	-1.70	-43.19	4.33	126.94
M06-2X/6-311+G**	-5.96	17.44	-2.04	-32.08	3.93	105.54
wB97XD/6-311+G**	-6.57	27.89	-1.14	-62.02	5.43	184.51

^a The experimental data for pentacene is adapted from Seongil Im *et al.* (*Adv. Funct. Mater.* **2014**, *24*, 1109-1116).

Singlet-triplet energy splitting for phosphapentacene derivatives

In order to investigate the stabilities of these phosphapentacene derivatives, the singlet-triplet energy splitting (ΔE_{S-T}) are then calculated (Fig. S9). The ΔE_{S-T} decreases significantly from 0.78 eV for pentacene to 0.39 eV for 5,7,12,14-tetraphosphapentacene (**33**) and 1,4,6,8,11,13-hexaphosphapentacene (**34**), and even 0.31 eV for 6,13-diphosphapentacene (**28**). While 1,4-diphosphapentacene (**7**) shows a slightly increased ΔE_{S-T} of 0.80 eV, and others mainly exhibit decreased value for ΔE_{S-T} . Although the values of ΔE_{S-T} are decreased with different numbers and positions of phosphorus atoms, however, these values are still higher than the benchmark for the open-shell singlet diradicals,^[5] further indicating that these phosphapentacenes still exhibit the close-shell singlet ground states.

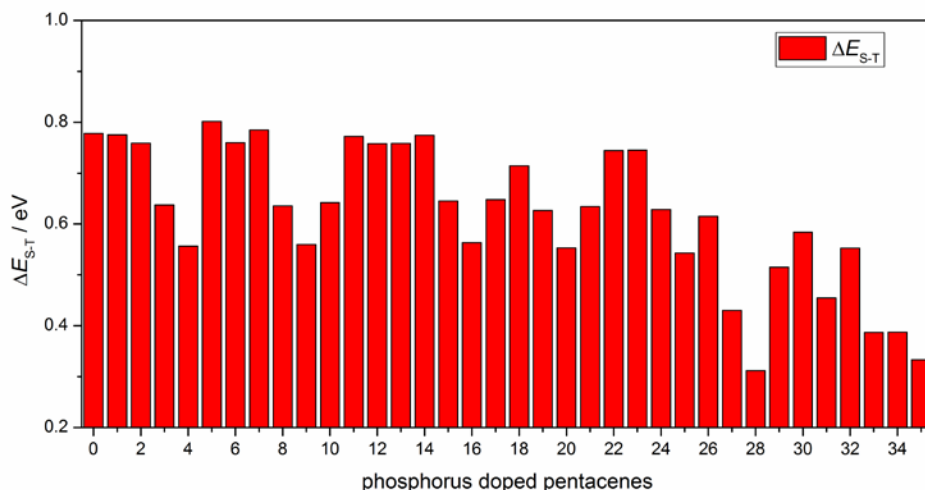


Fig. S10 Singlet-triplet energy splitting (ΔE_{S-T}) for pentacene and the phosphapentacene derivatives based on B3LYP/6-311+G** method.

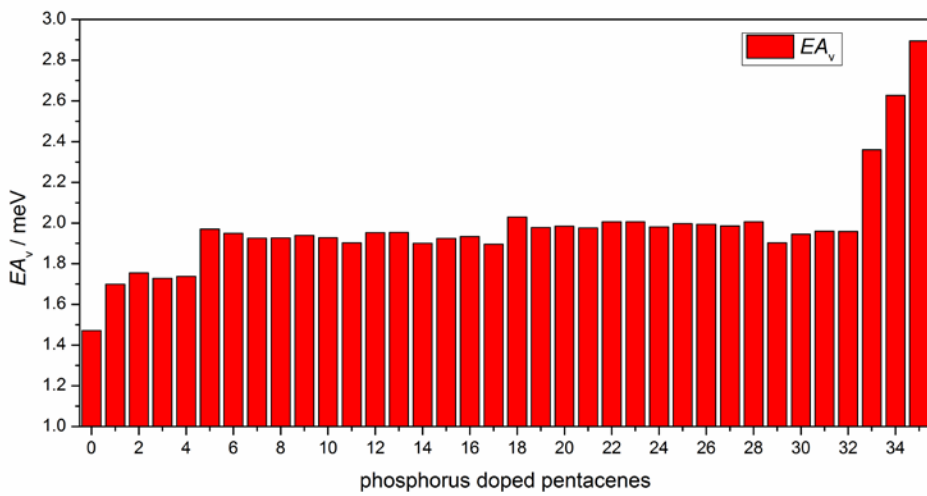


Fig. S11 Vertical electron affinities (EAs) for pentacene and the phosphapentacene derivatives based on B3LYP/6-311+G** method.

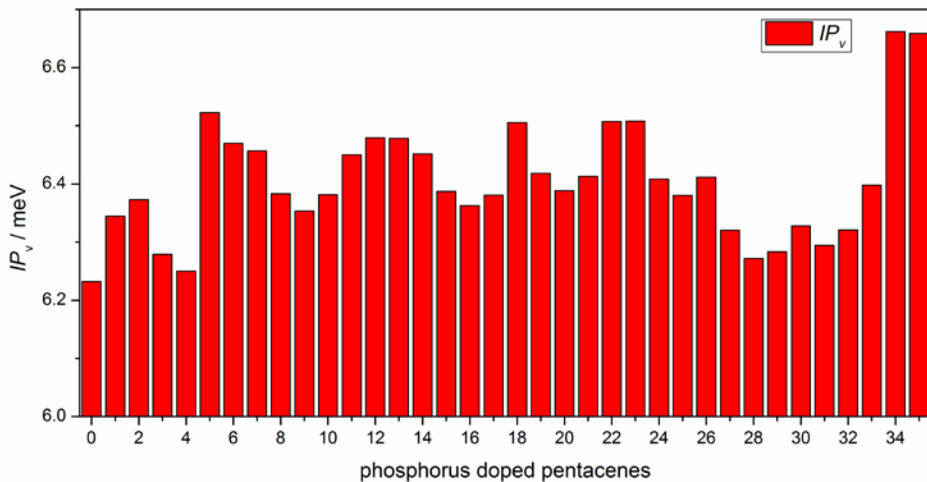
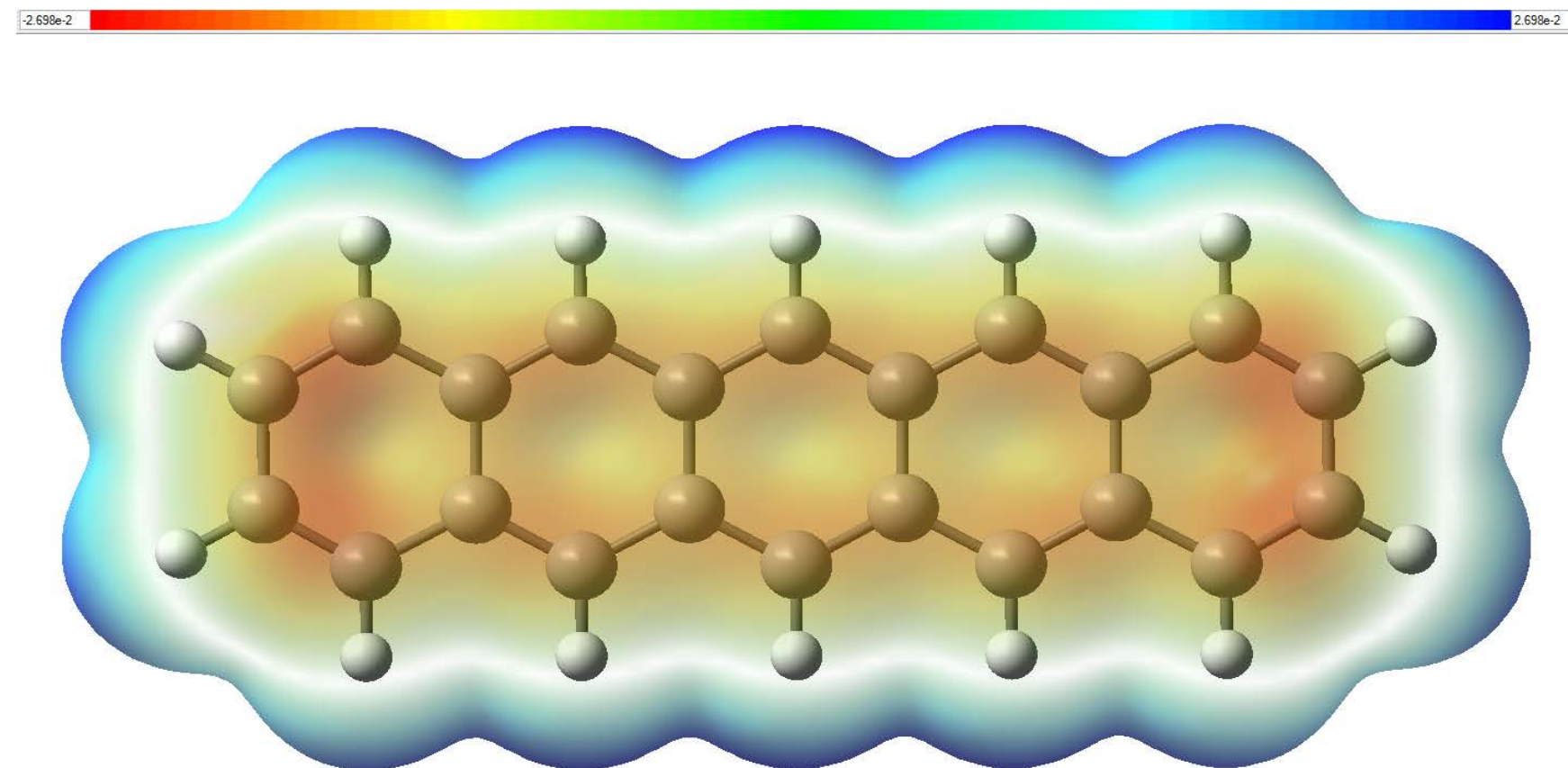


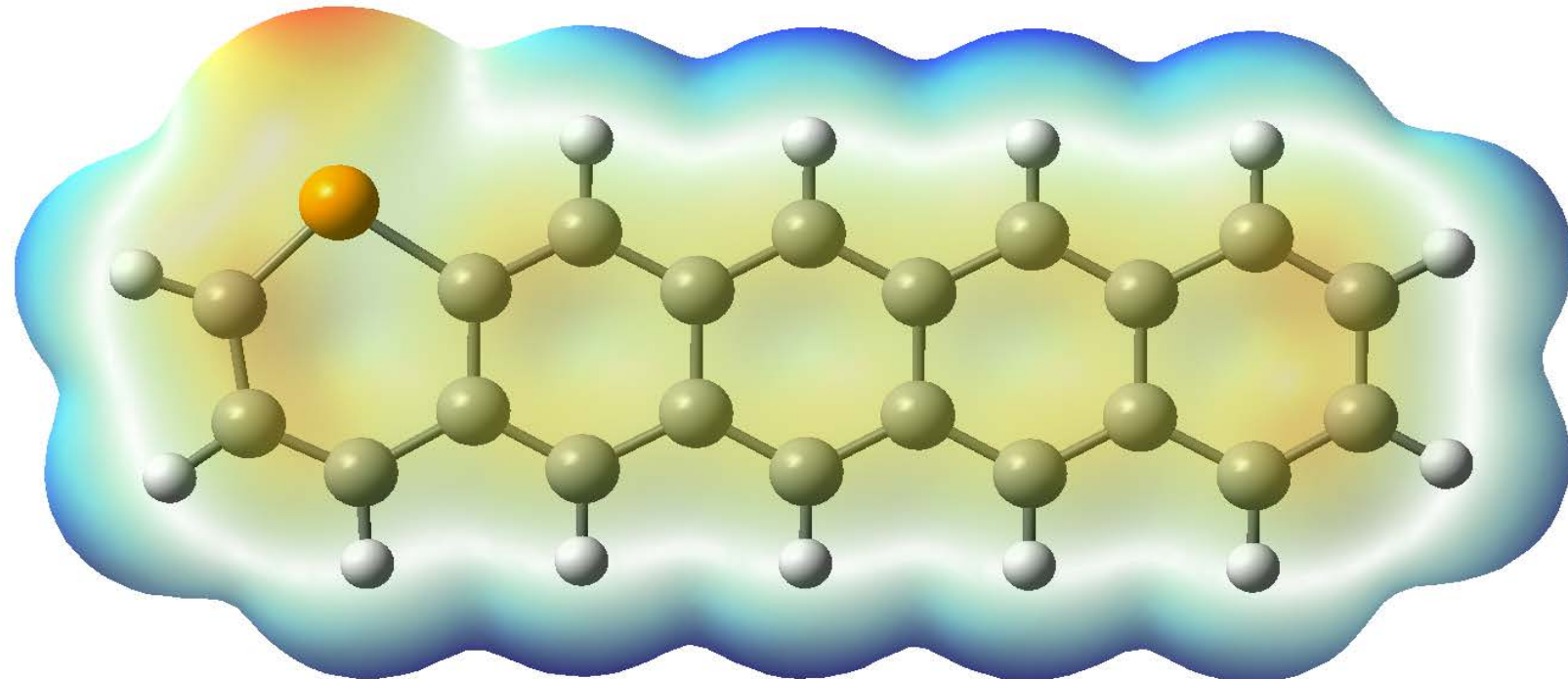
Fig. S12 Vertical ionic potentials (IPs) for pentacene and the phosphapentacene derivatives based on B3LYP/6-311+G** method.

Fig. S13 Electron surface potentials (ESPs) for pentacene and the phosphapentacene derivatives based on B3LYP/6-311+G** method.

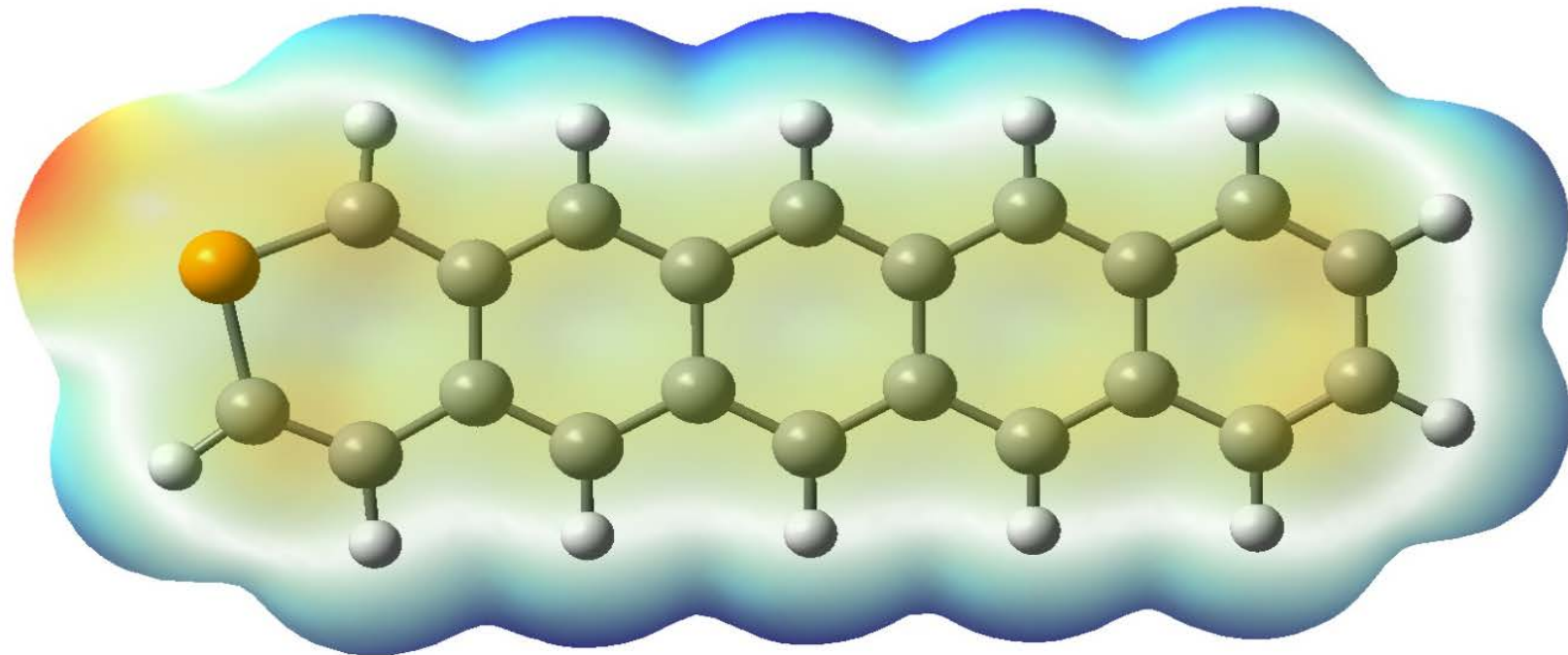
Pentacene



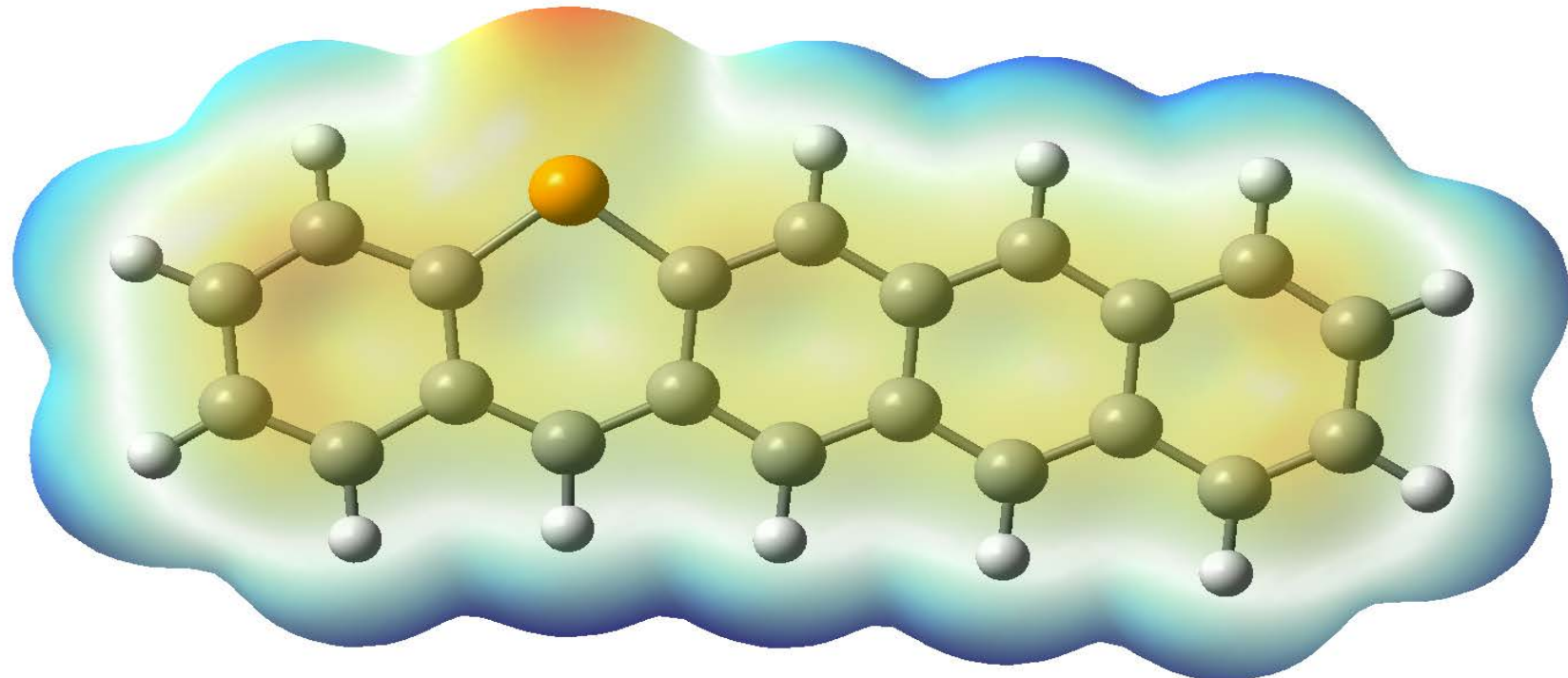
1-phosphapentacene



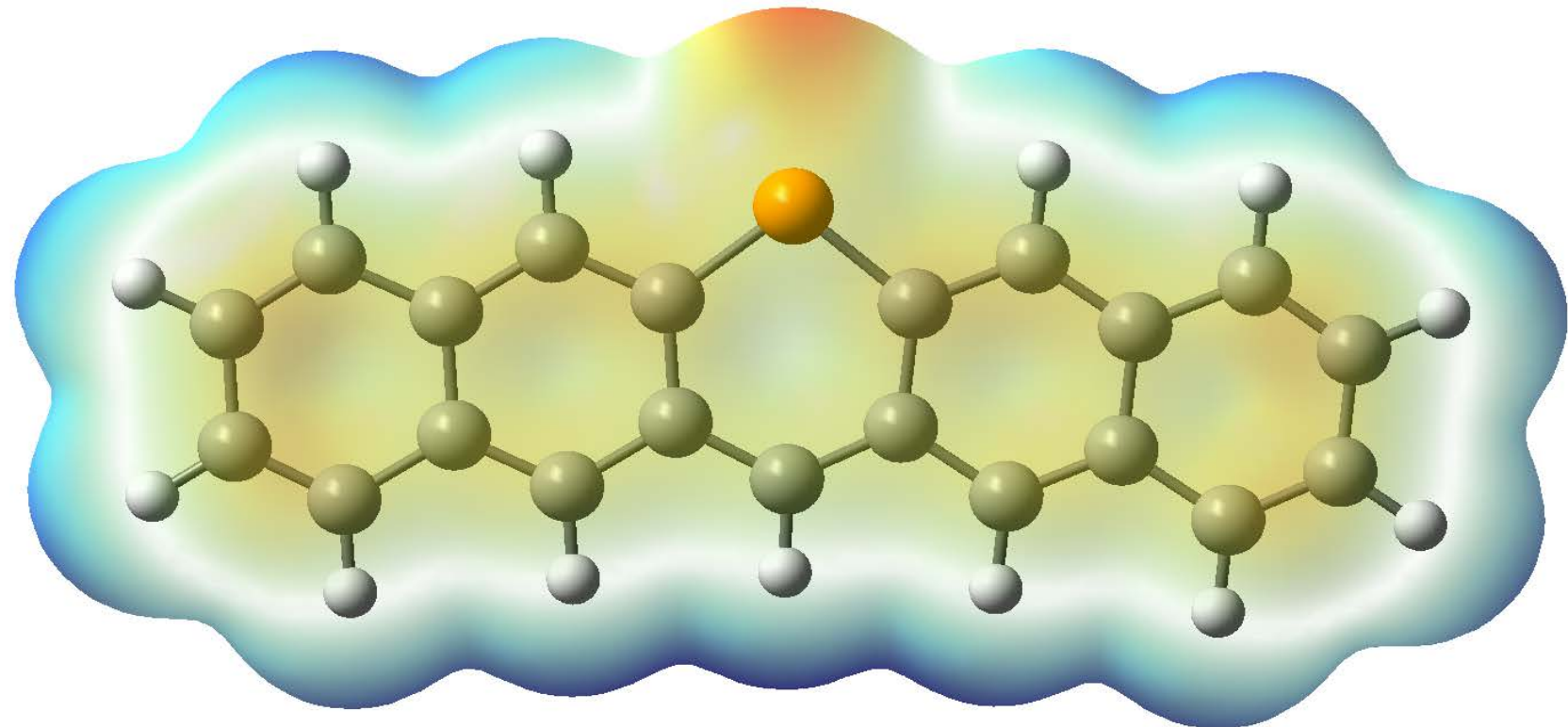
2-phosphapentacene



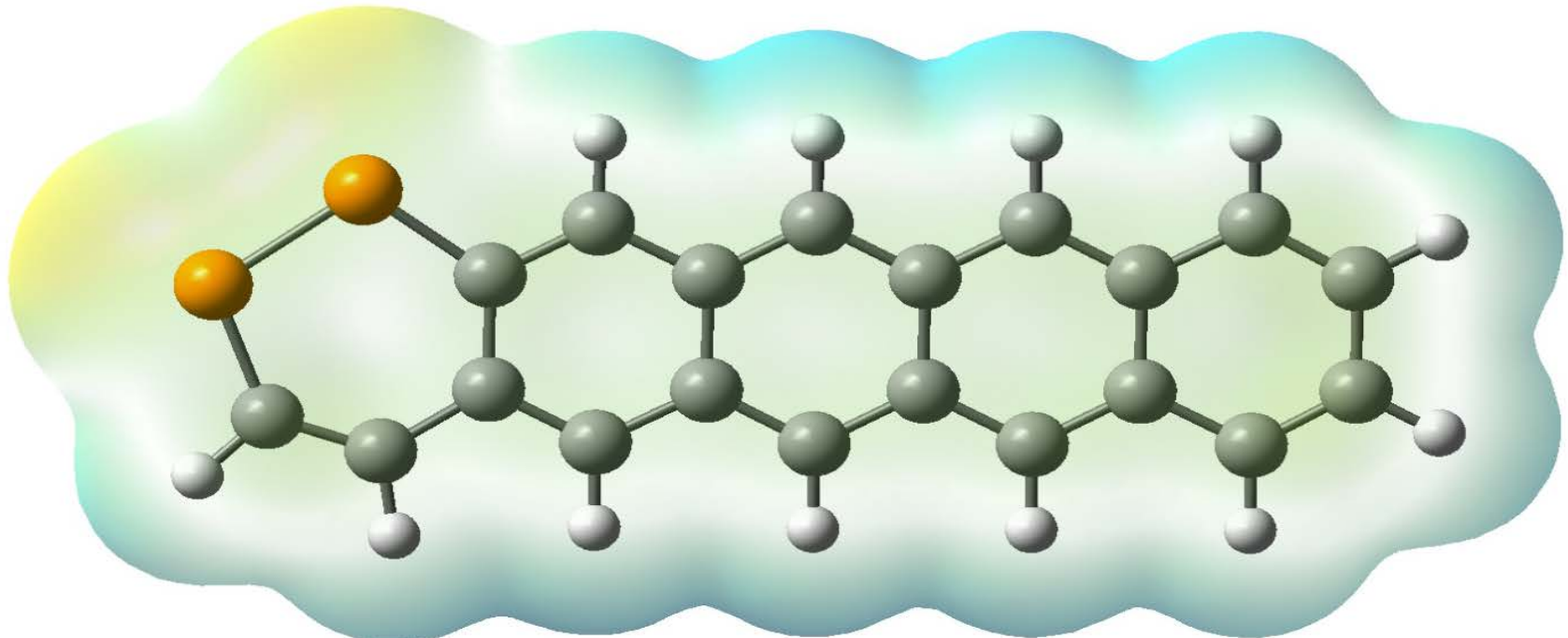
5-phosphapentacene



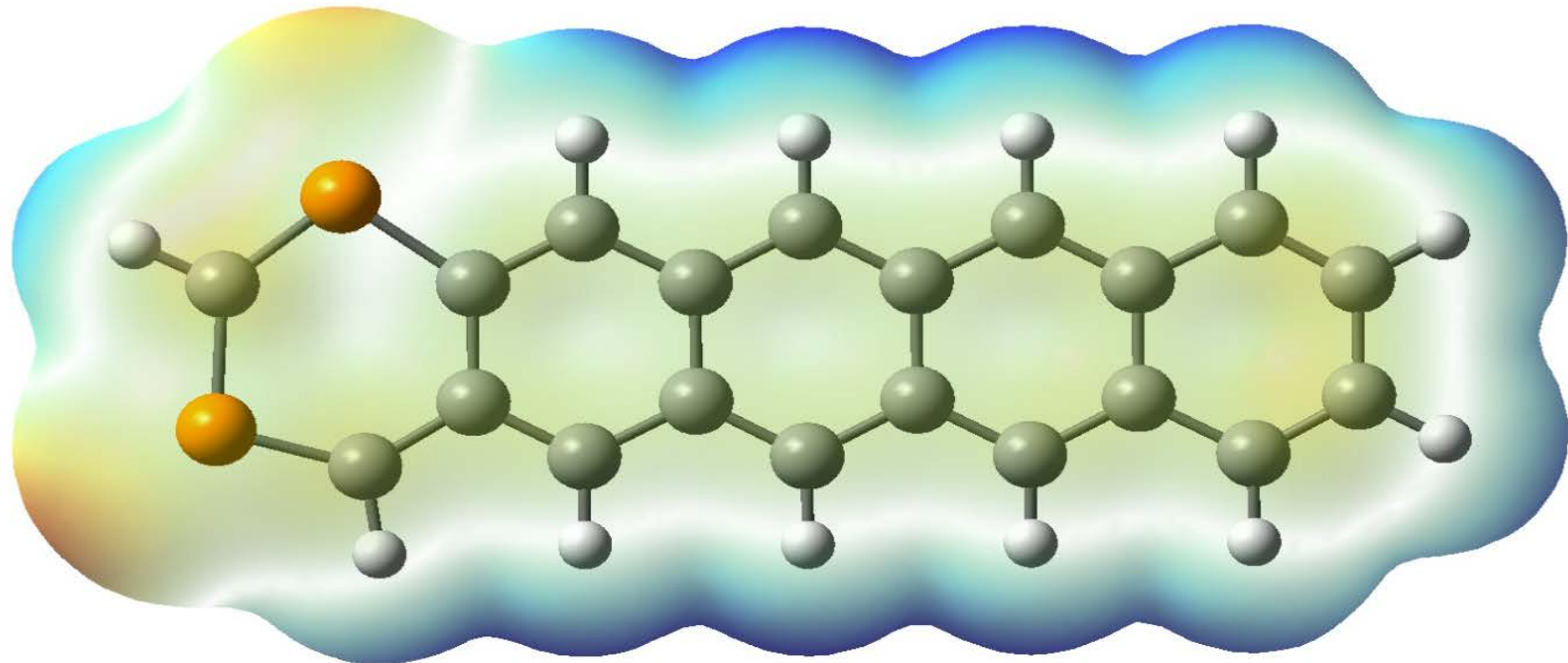
6-phosphapentacene



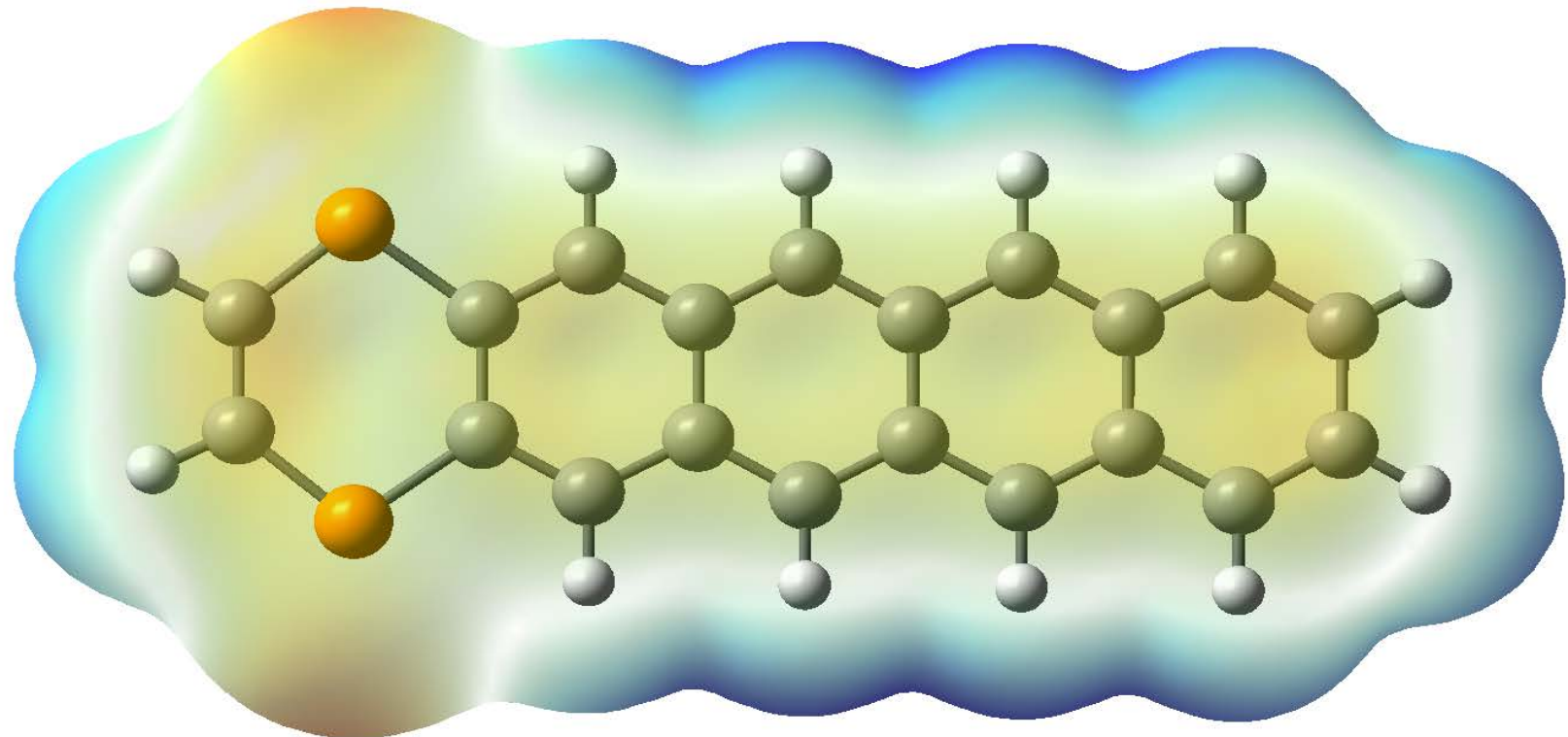
1,2-diphosphapentacene



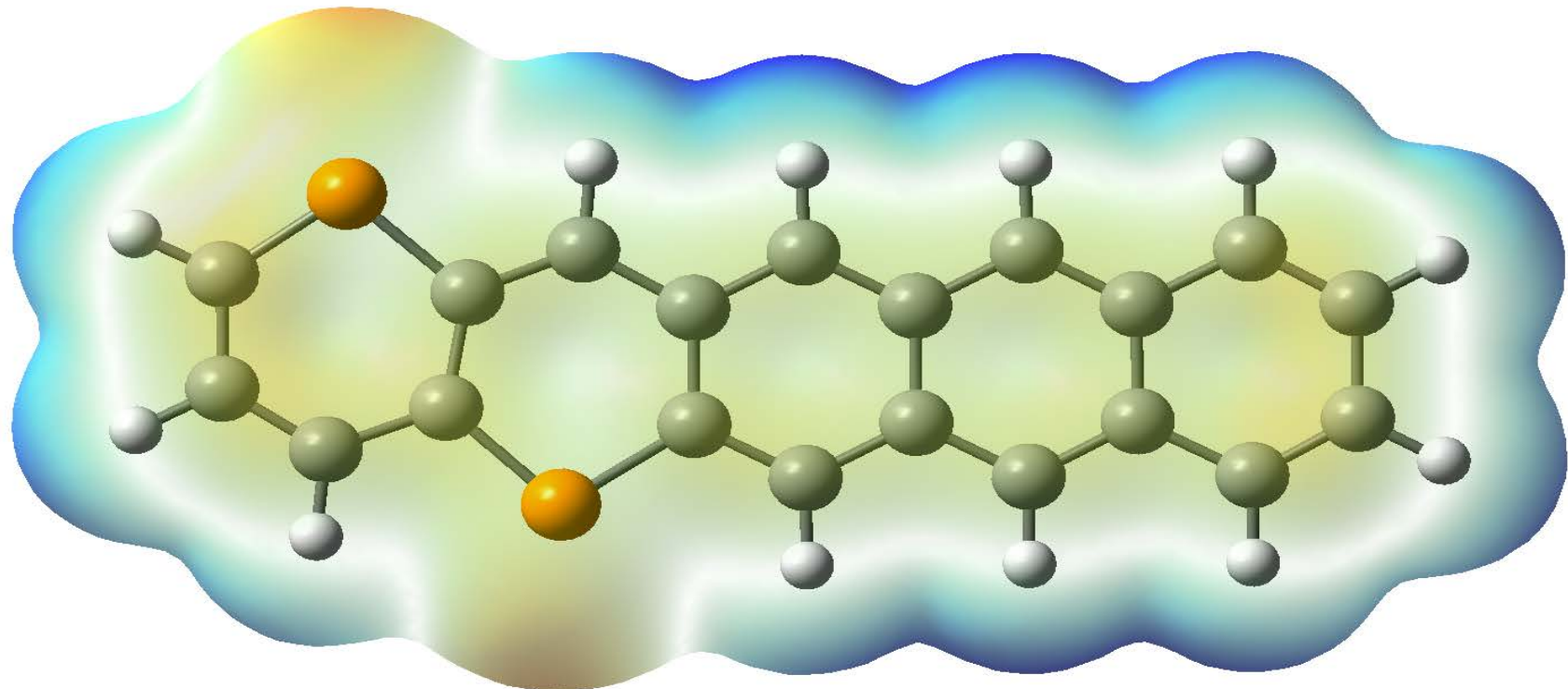
1,3-diphosphapentacene



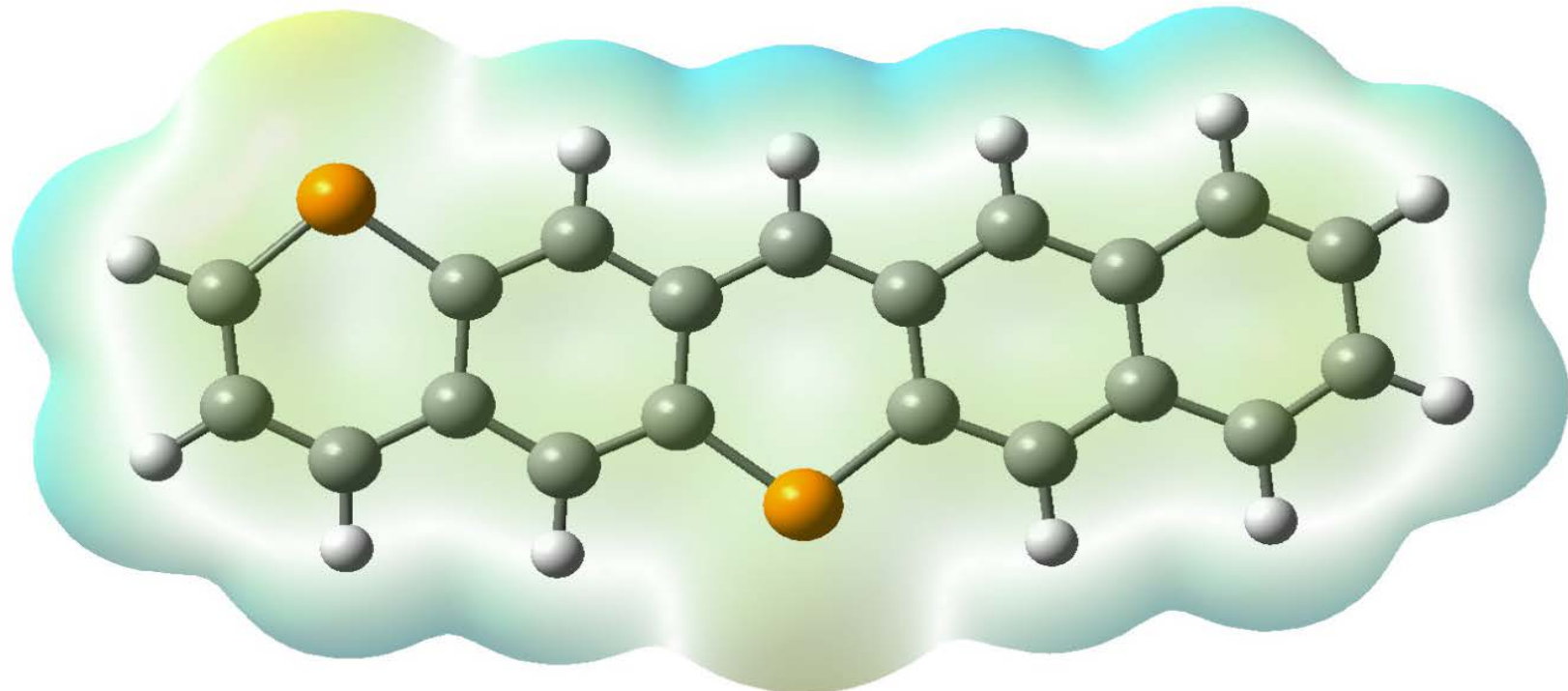
1,4-diphosphapentacene



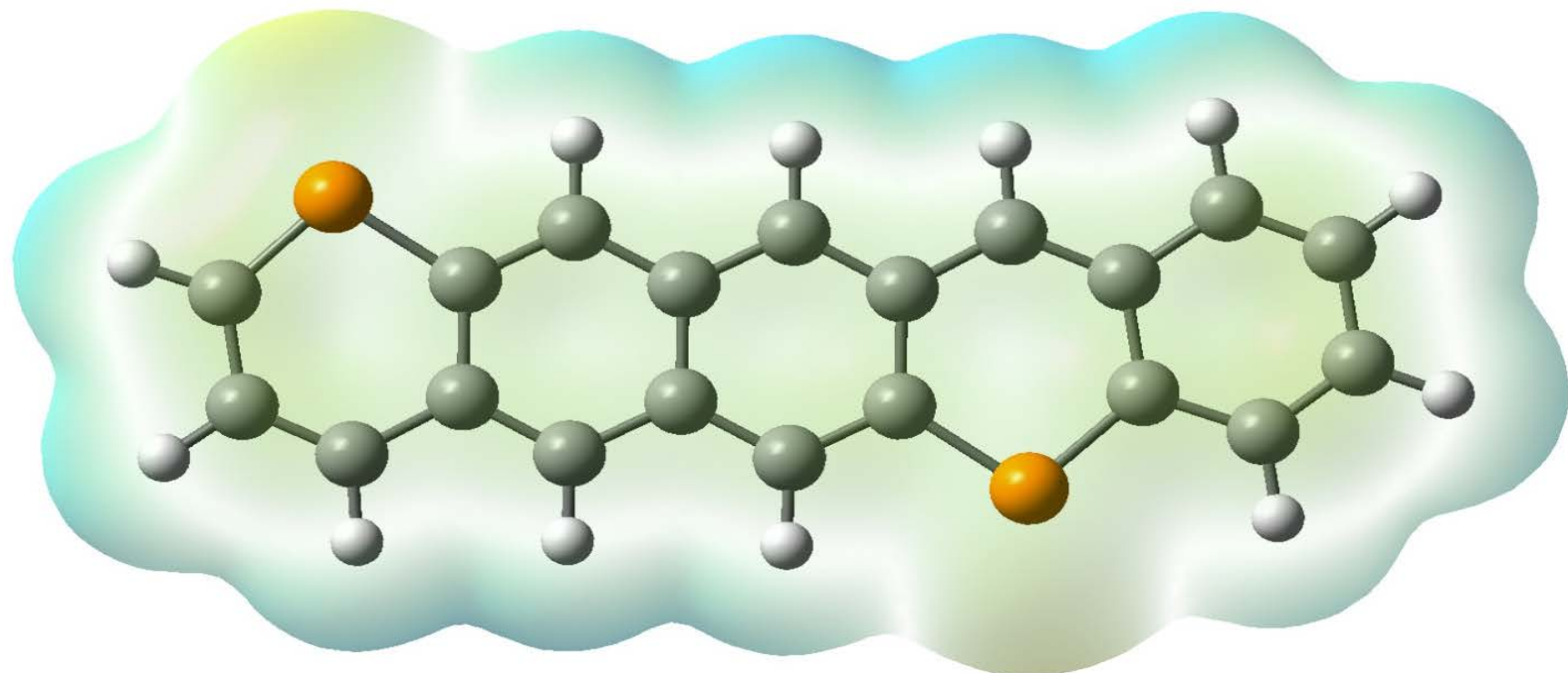
1,5-diphosphapentacene



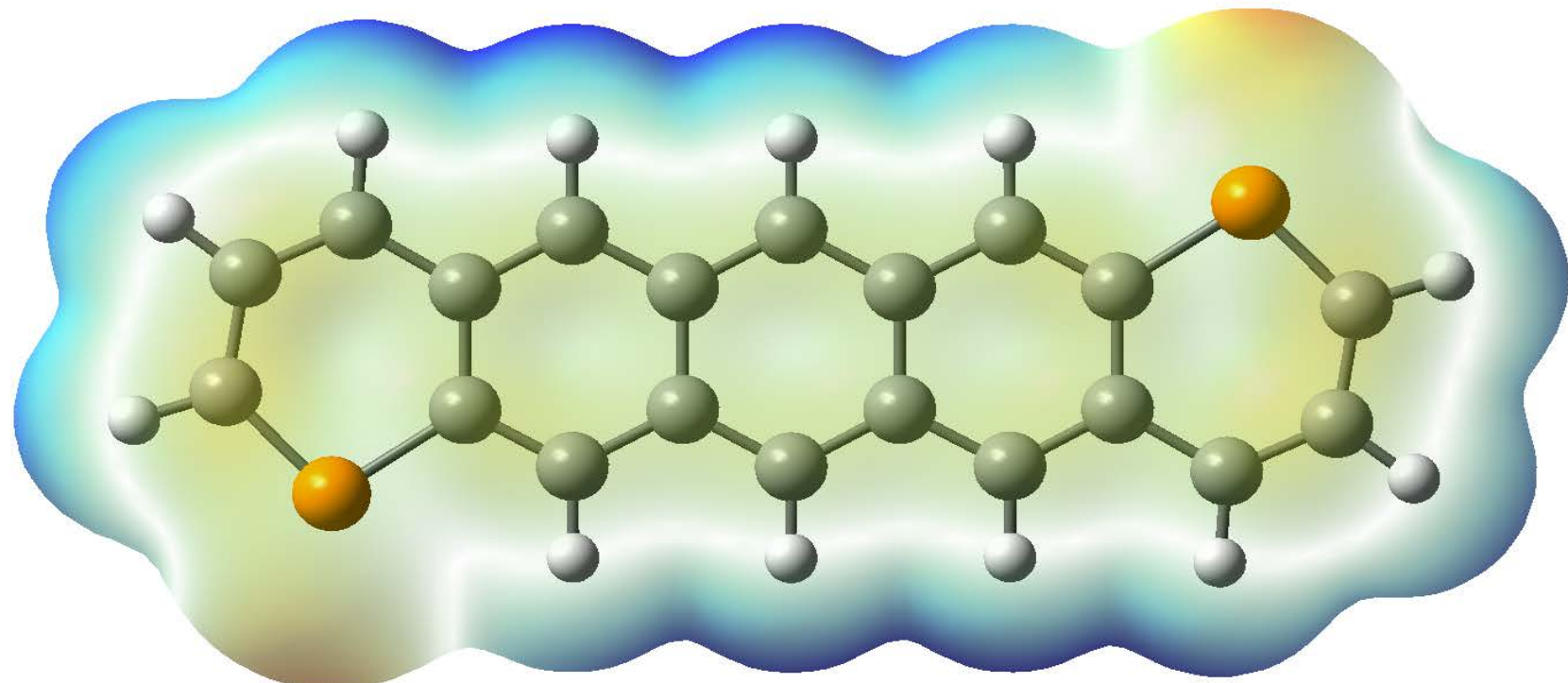
1,6-diphosphapentacene



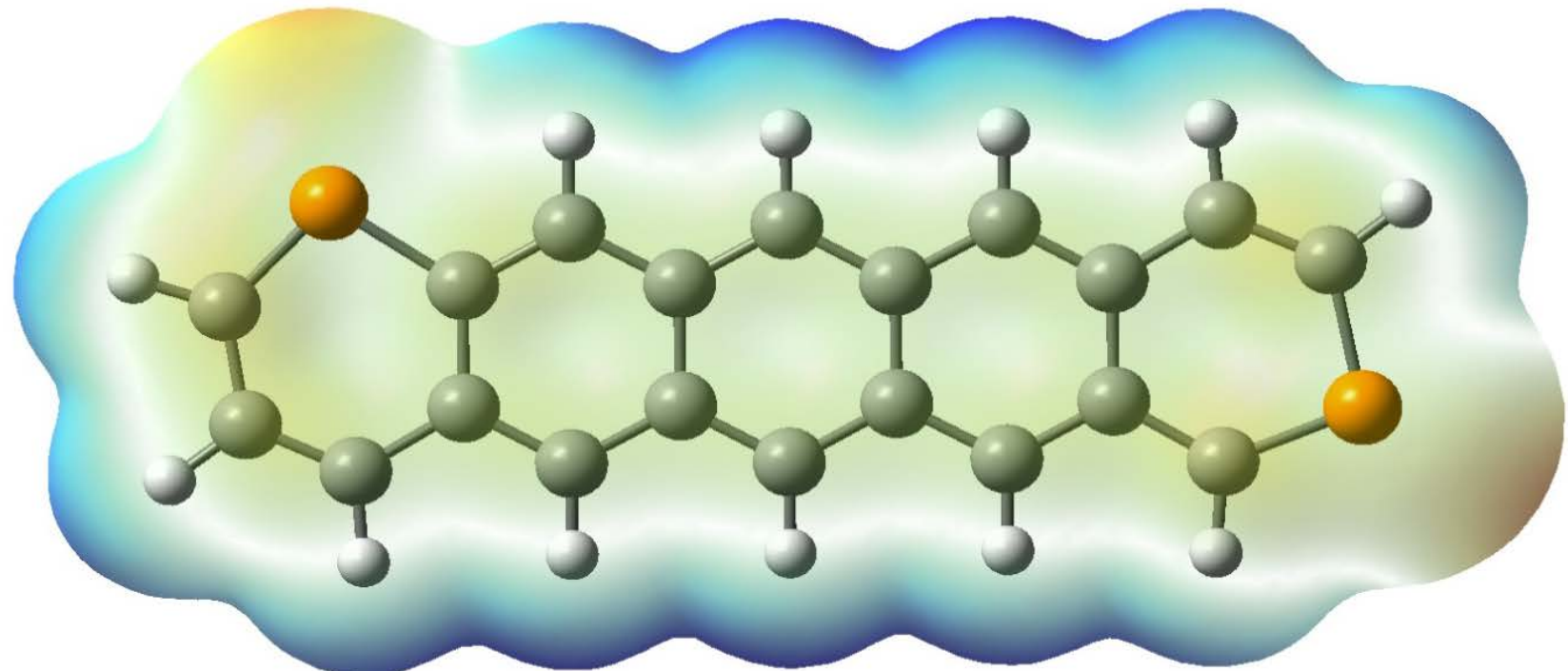
1,7-diphosphapentacene



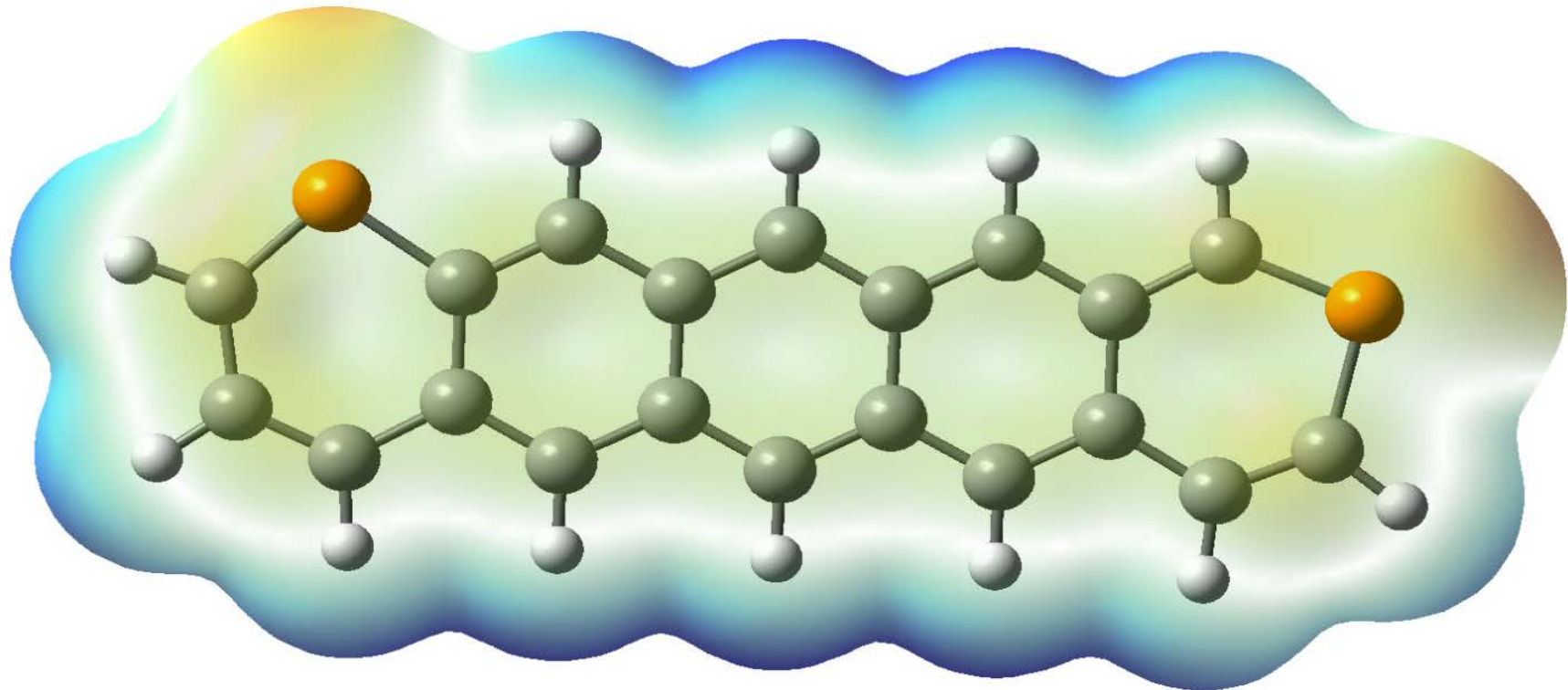
1,8-diphosphapentacene



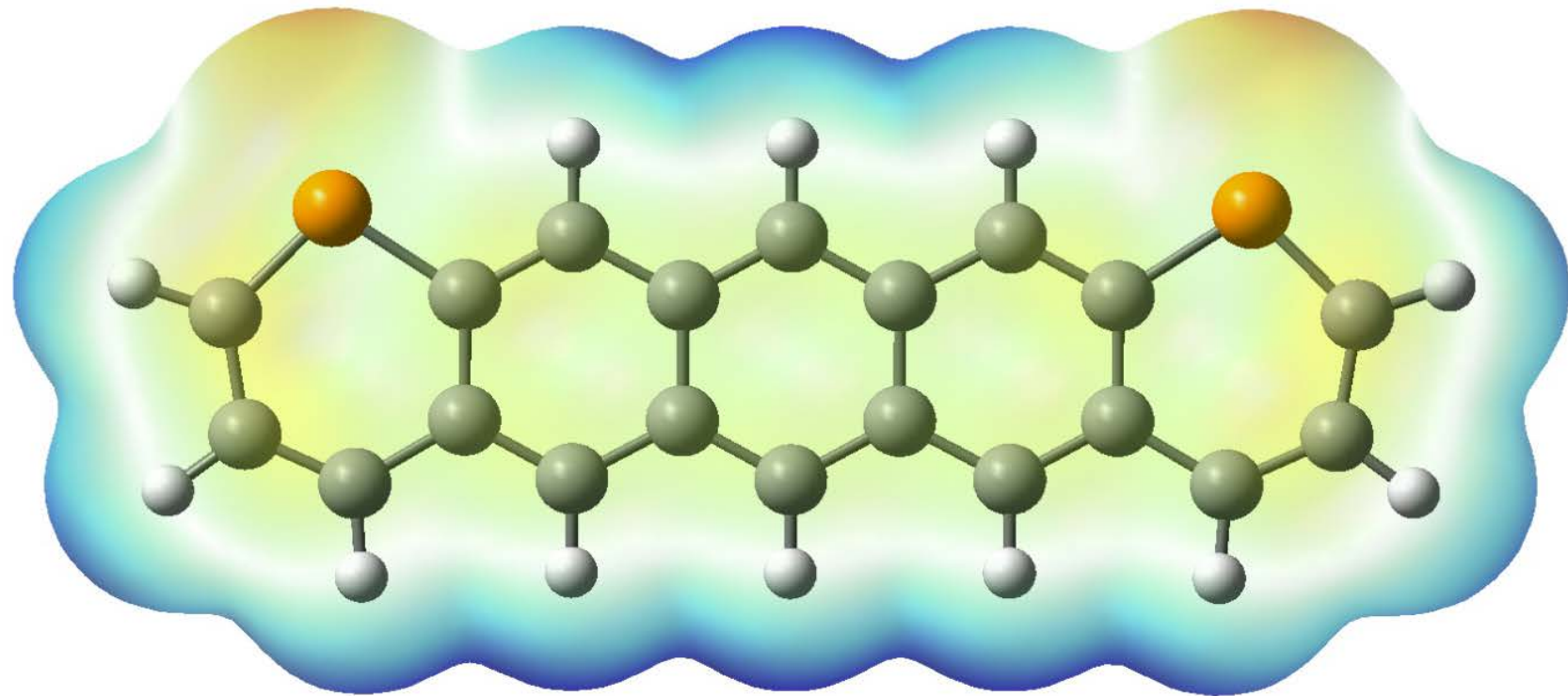
1,9-diphosphapentacene



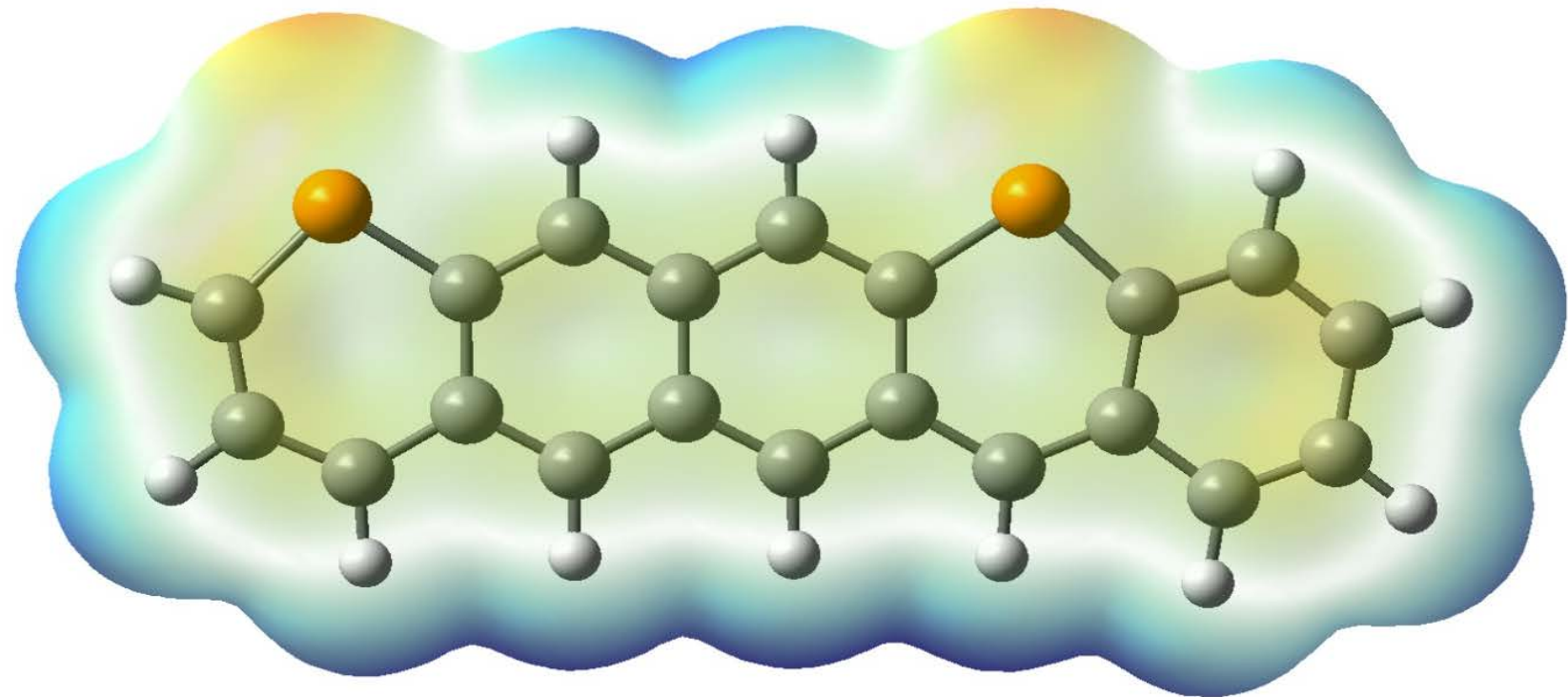
1,10-diphosphapentacene



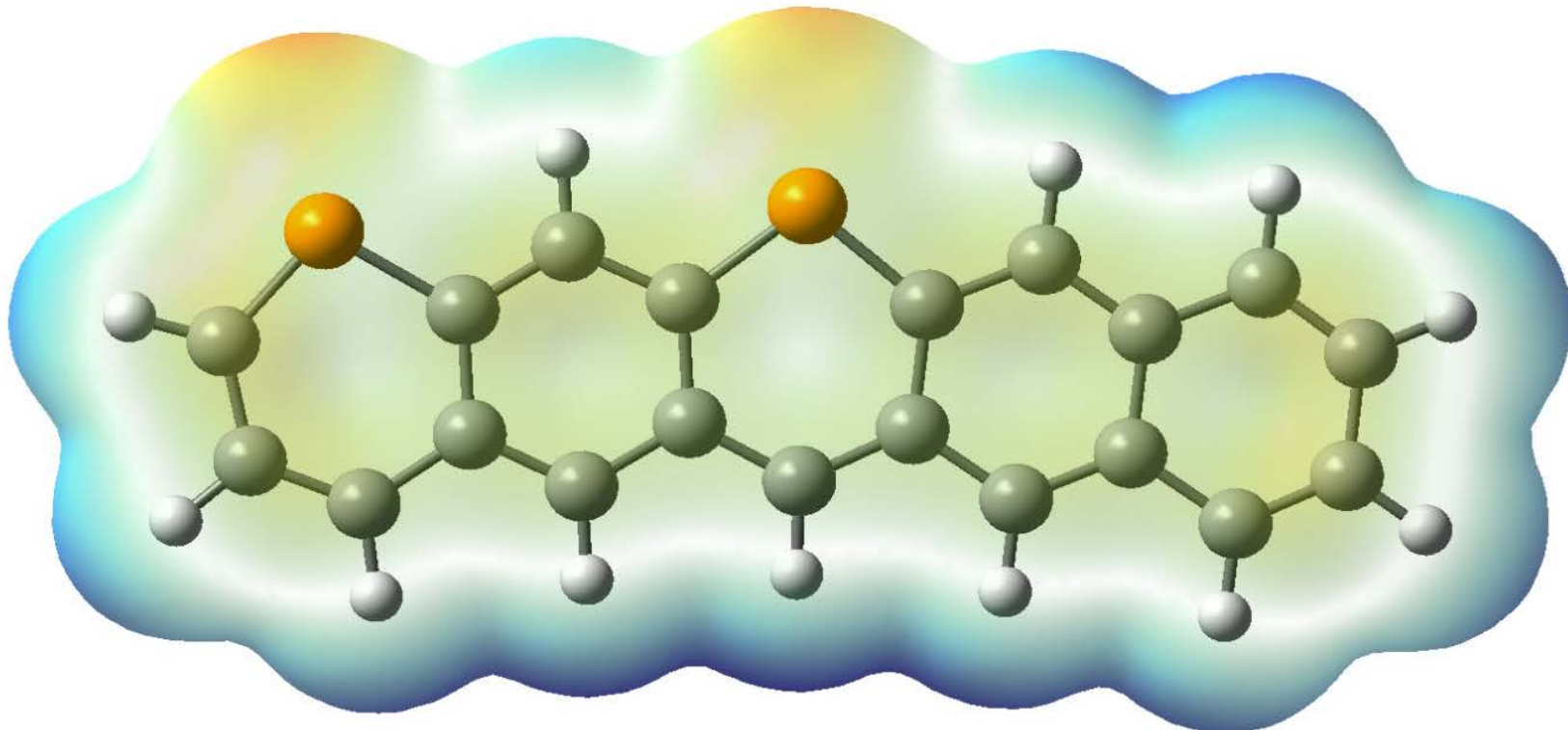
1,11-diphosphapentacene



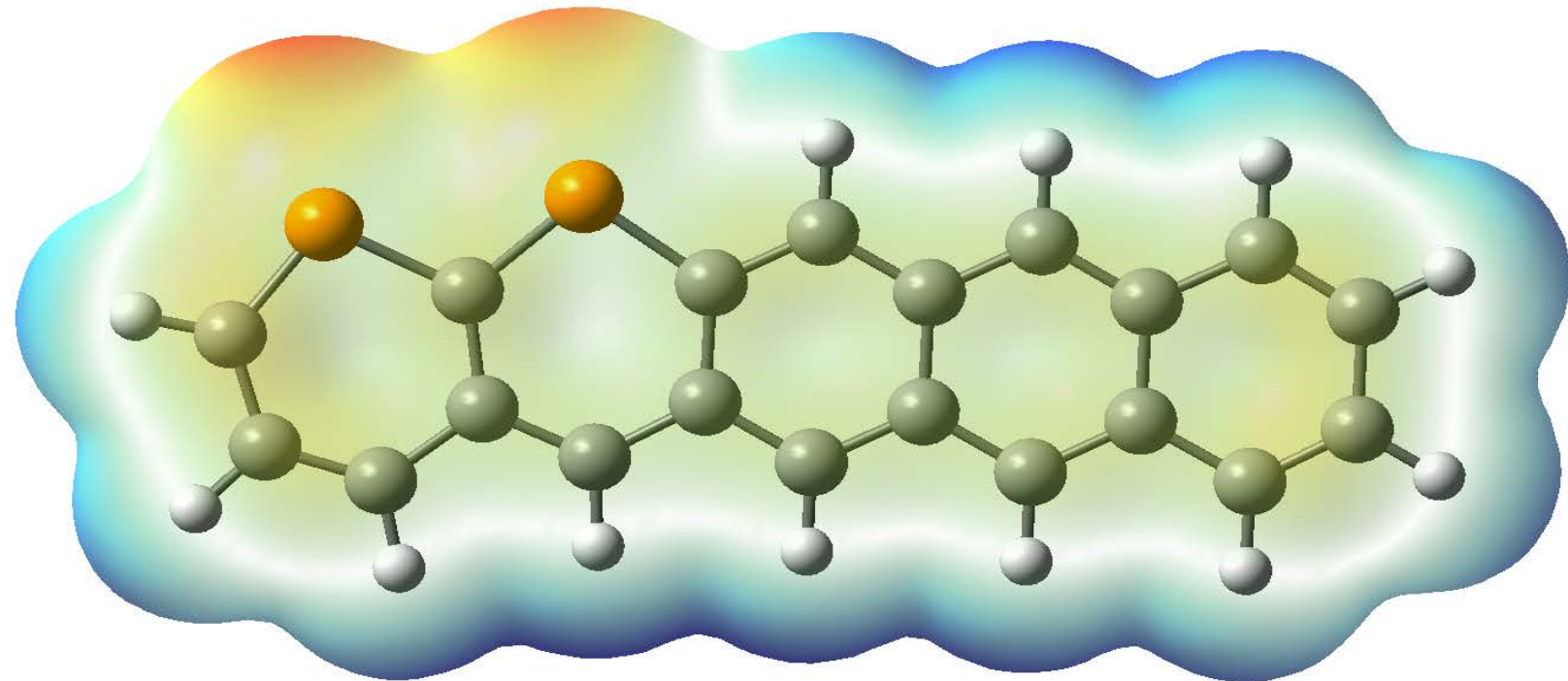
1,12-diphosphapentacene



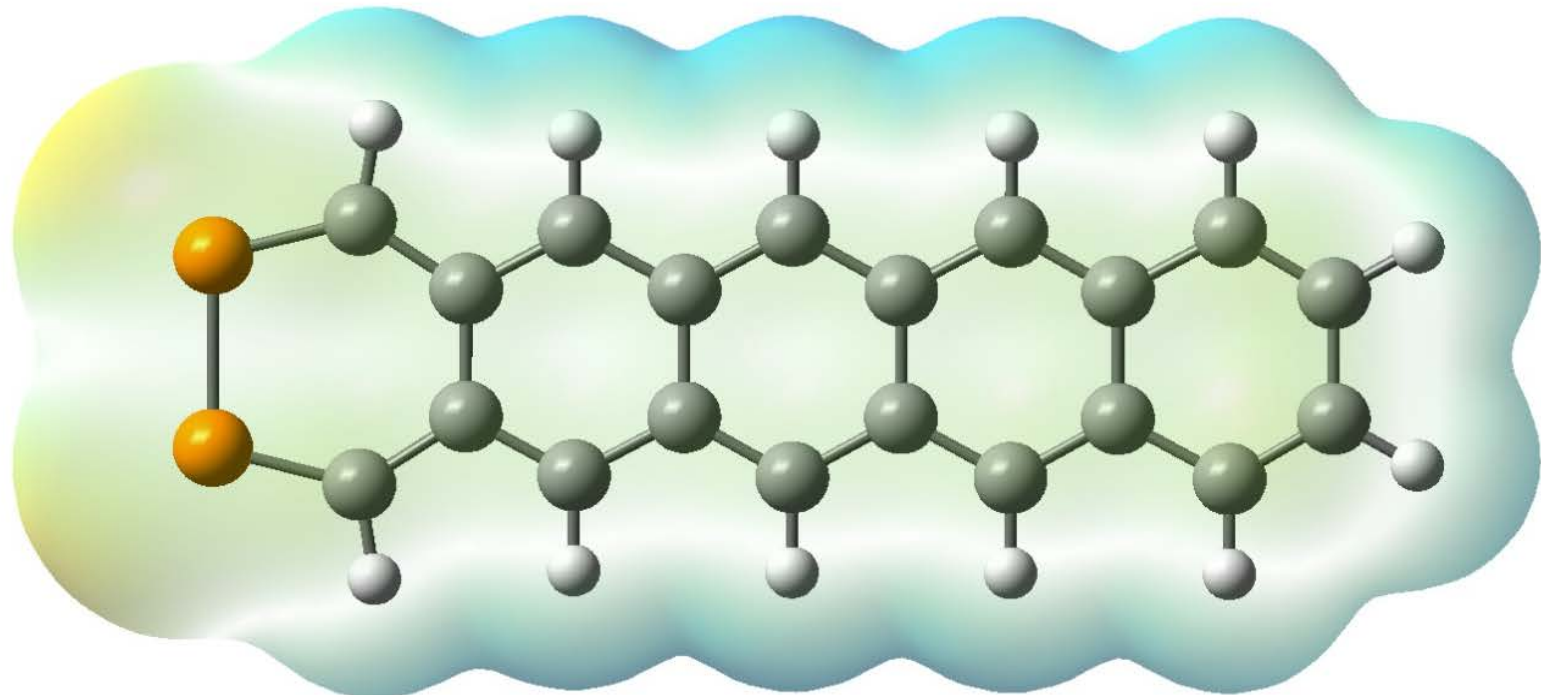
1,13-diphosphapentacene



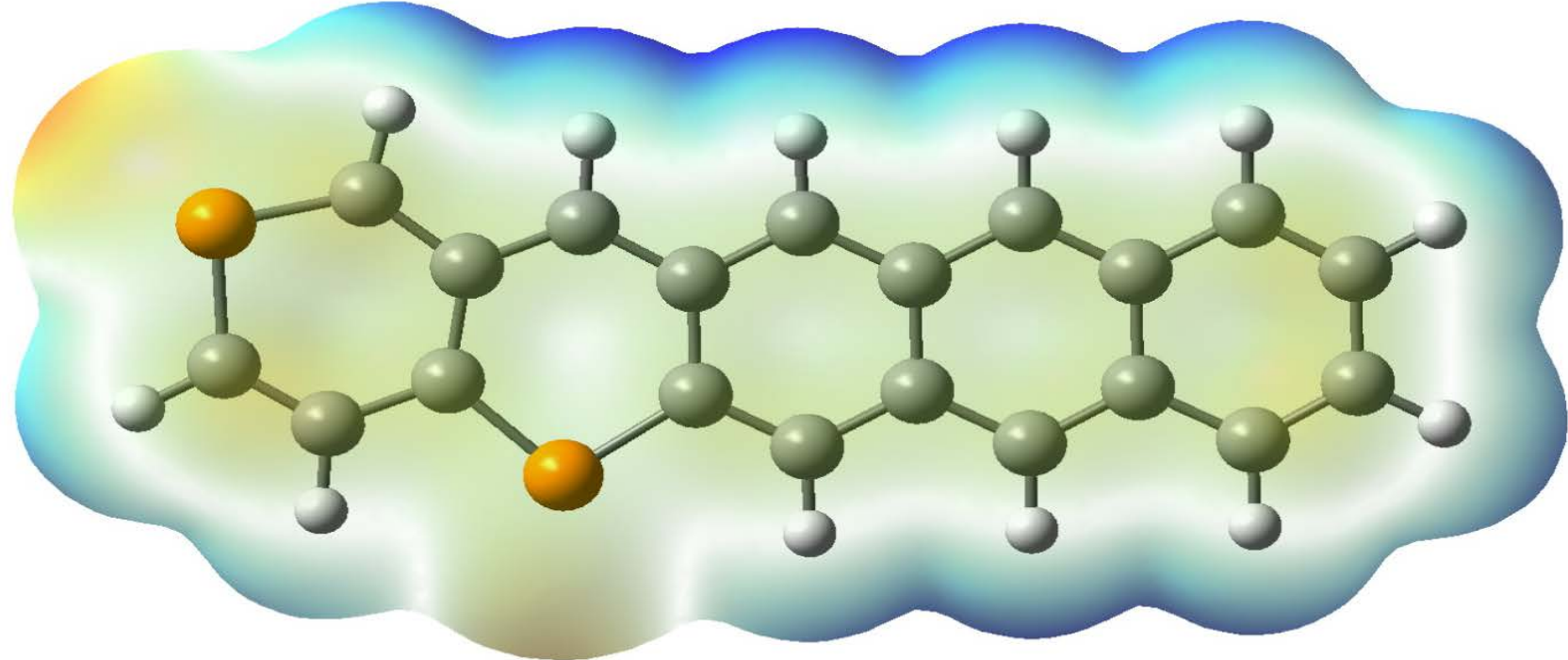
1,14-diphosphapentacene



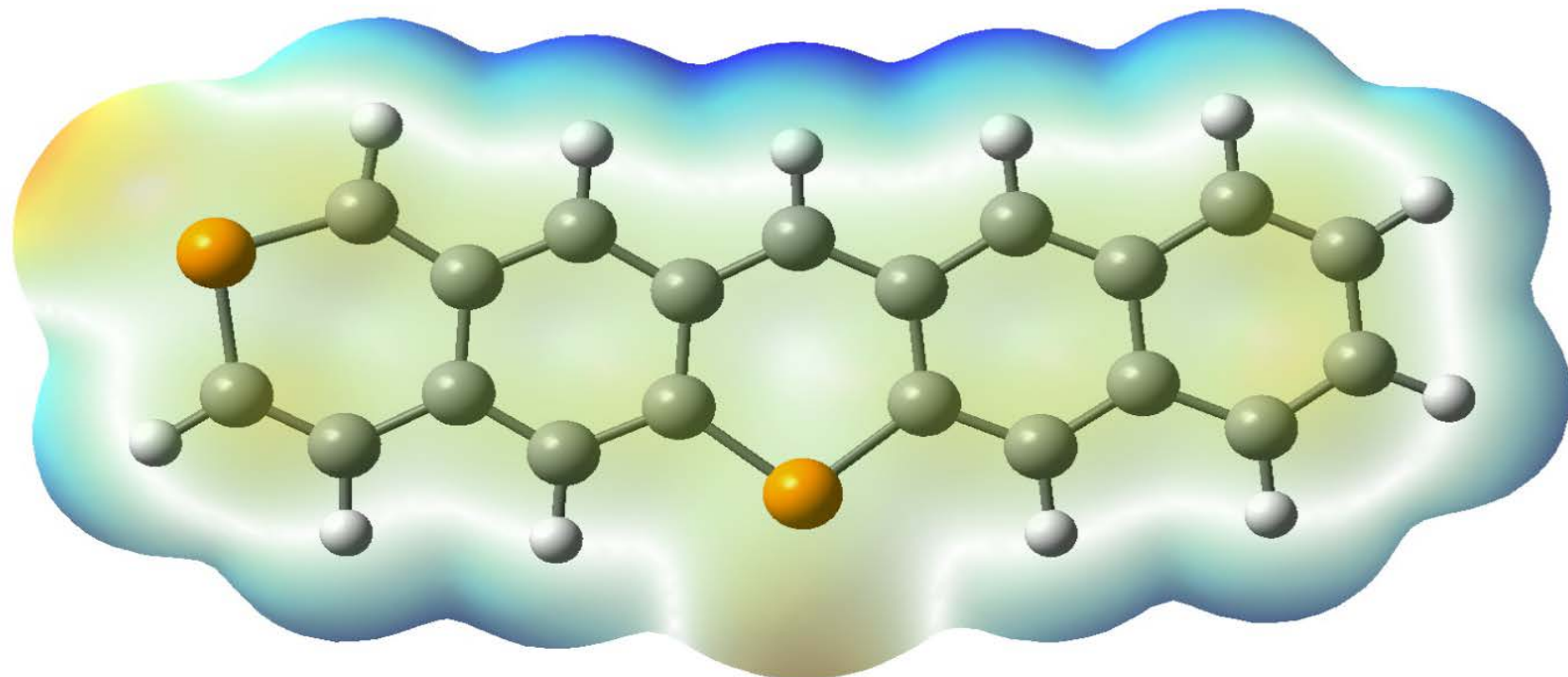
2,3-diphosphapentacene



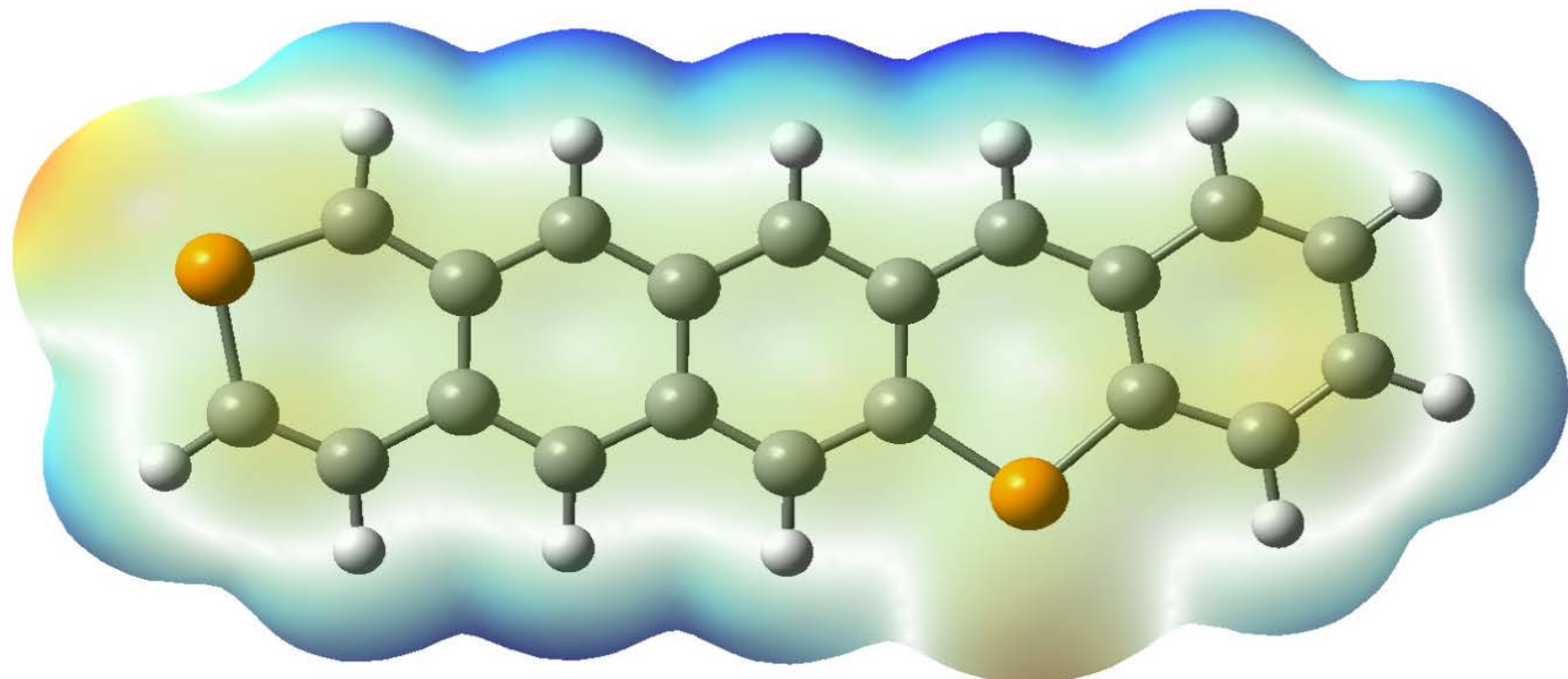
2,5-diphosphapentacene



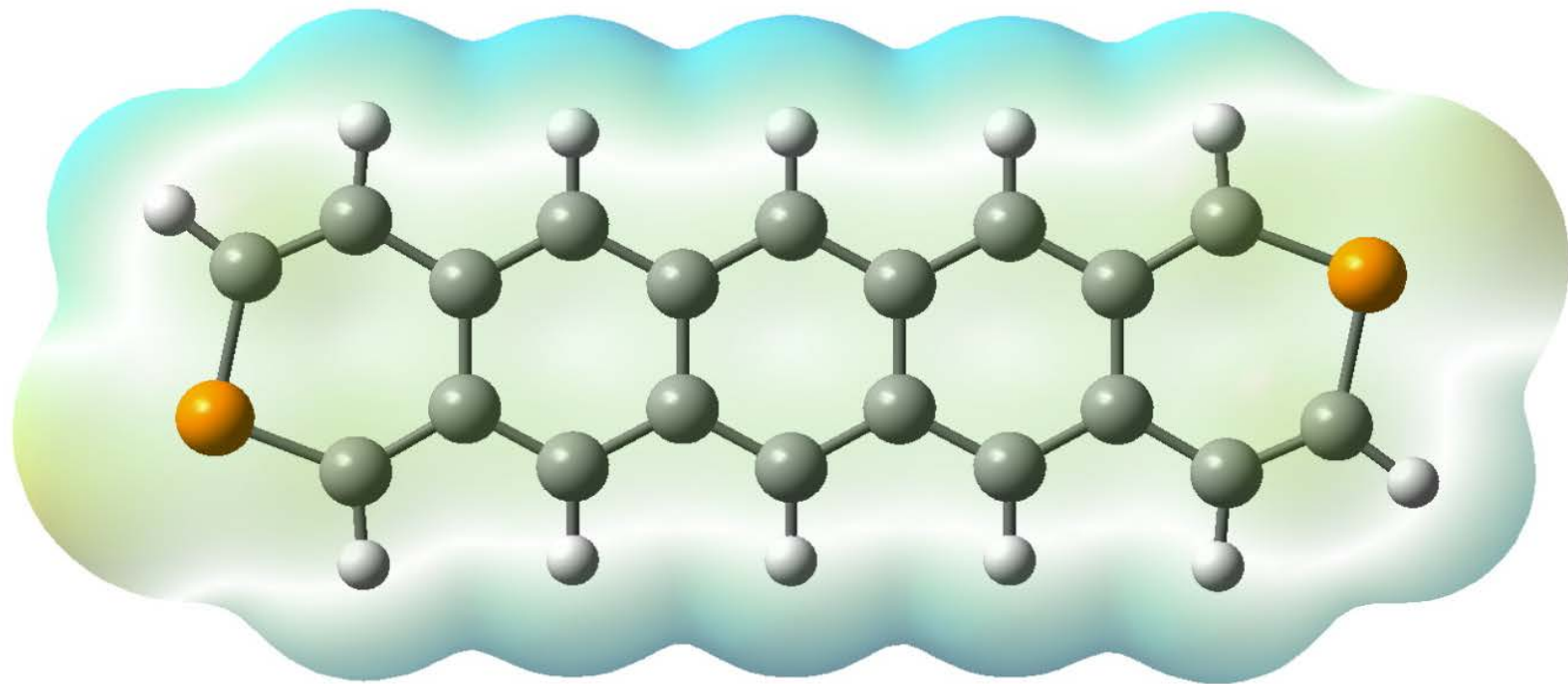
2,6-diphosphapentacene



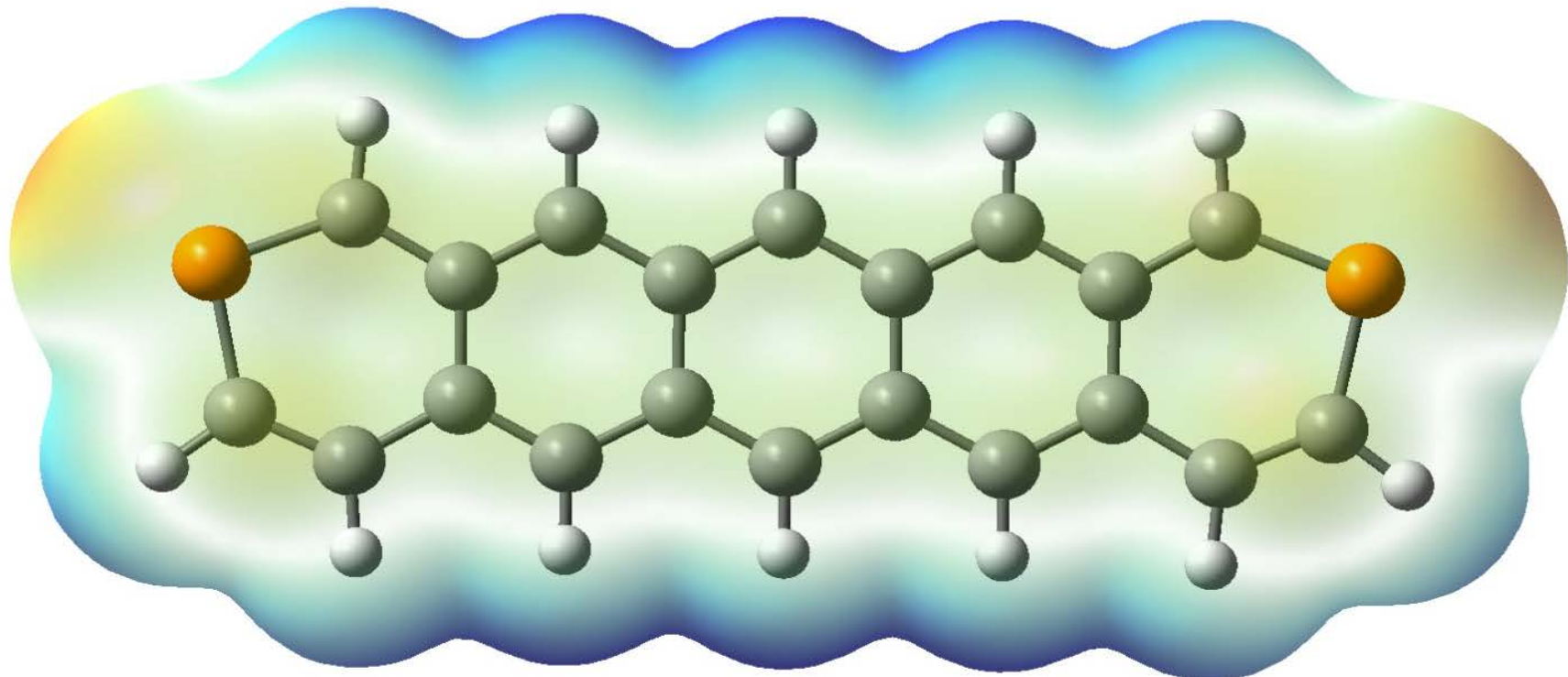
2,7-diphosphapentacene



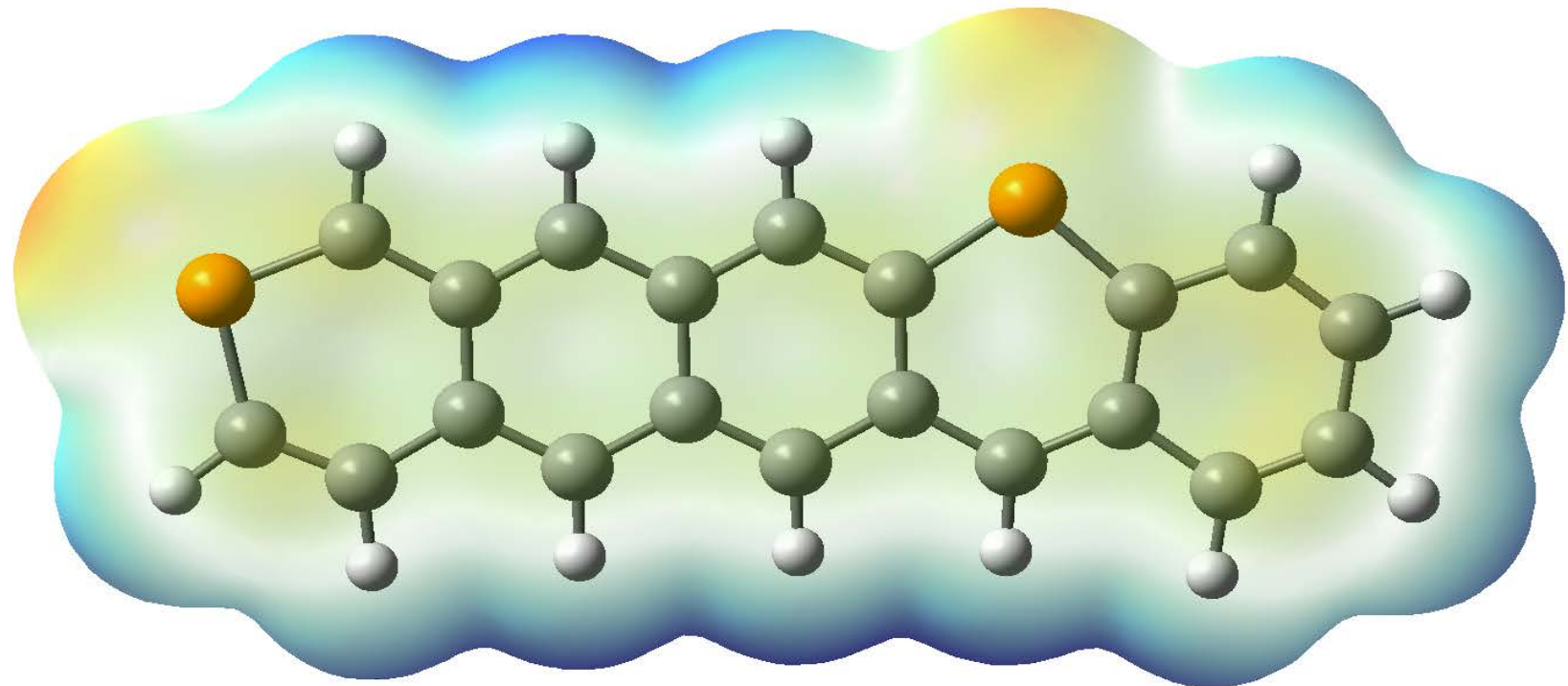
2,9-diphosphapentacene



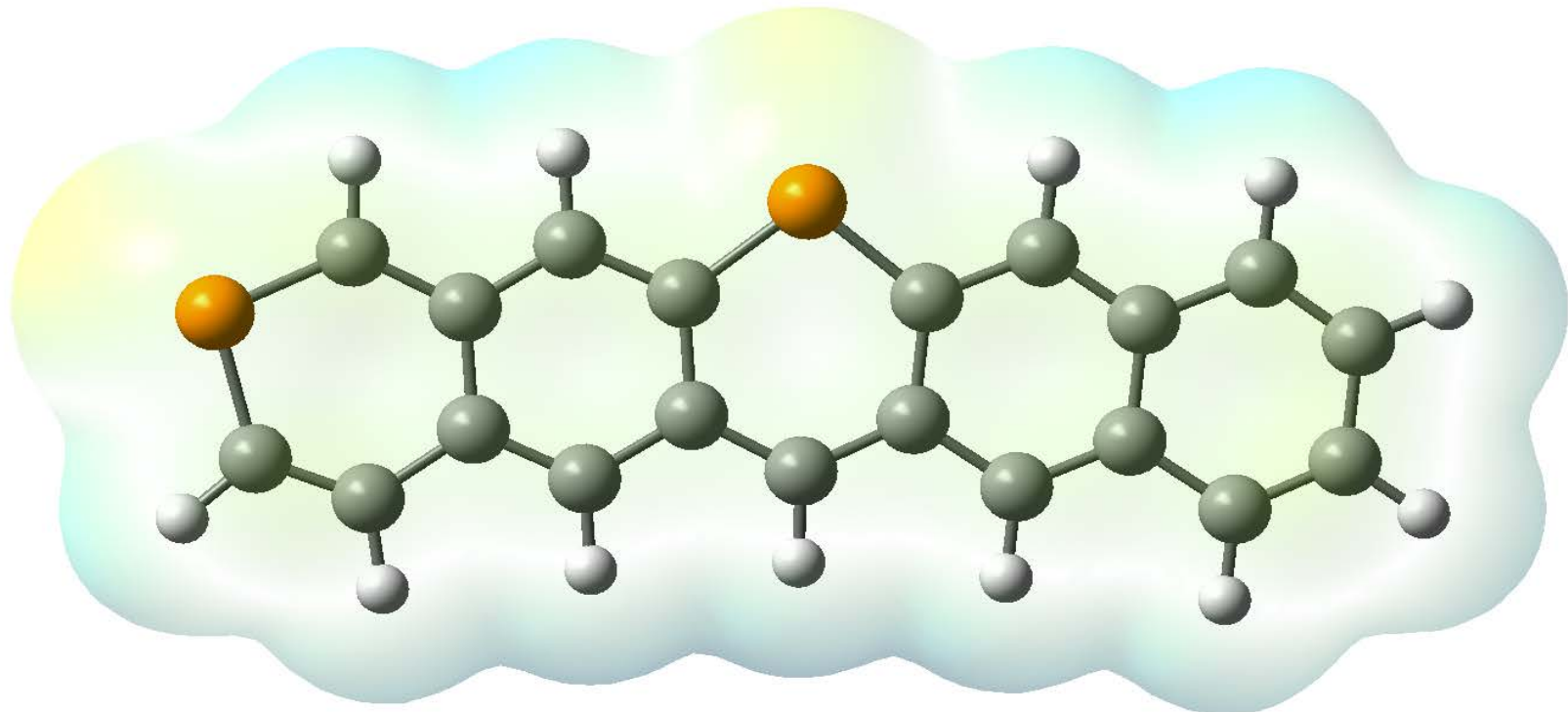
2,10-diphosphapentacene



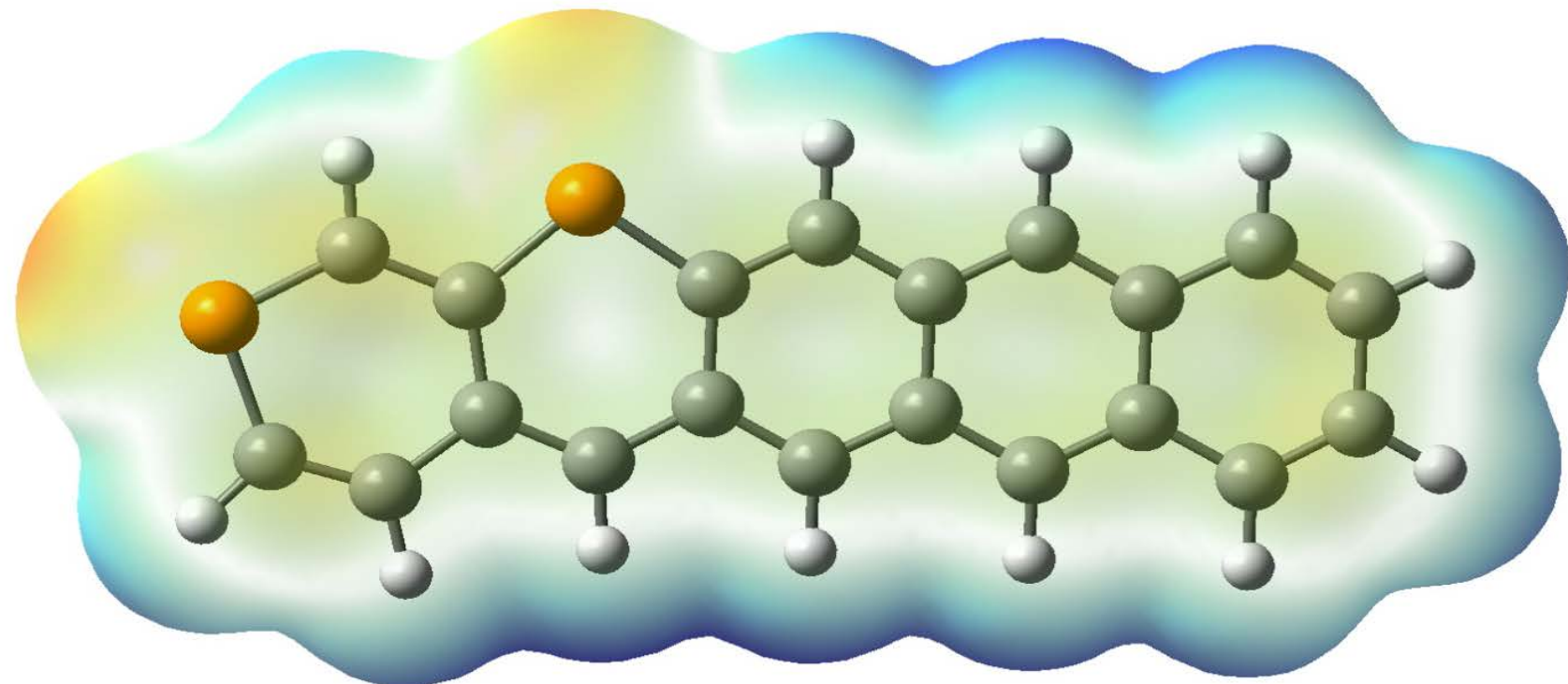
2,12-diphosphapentacene



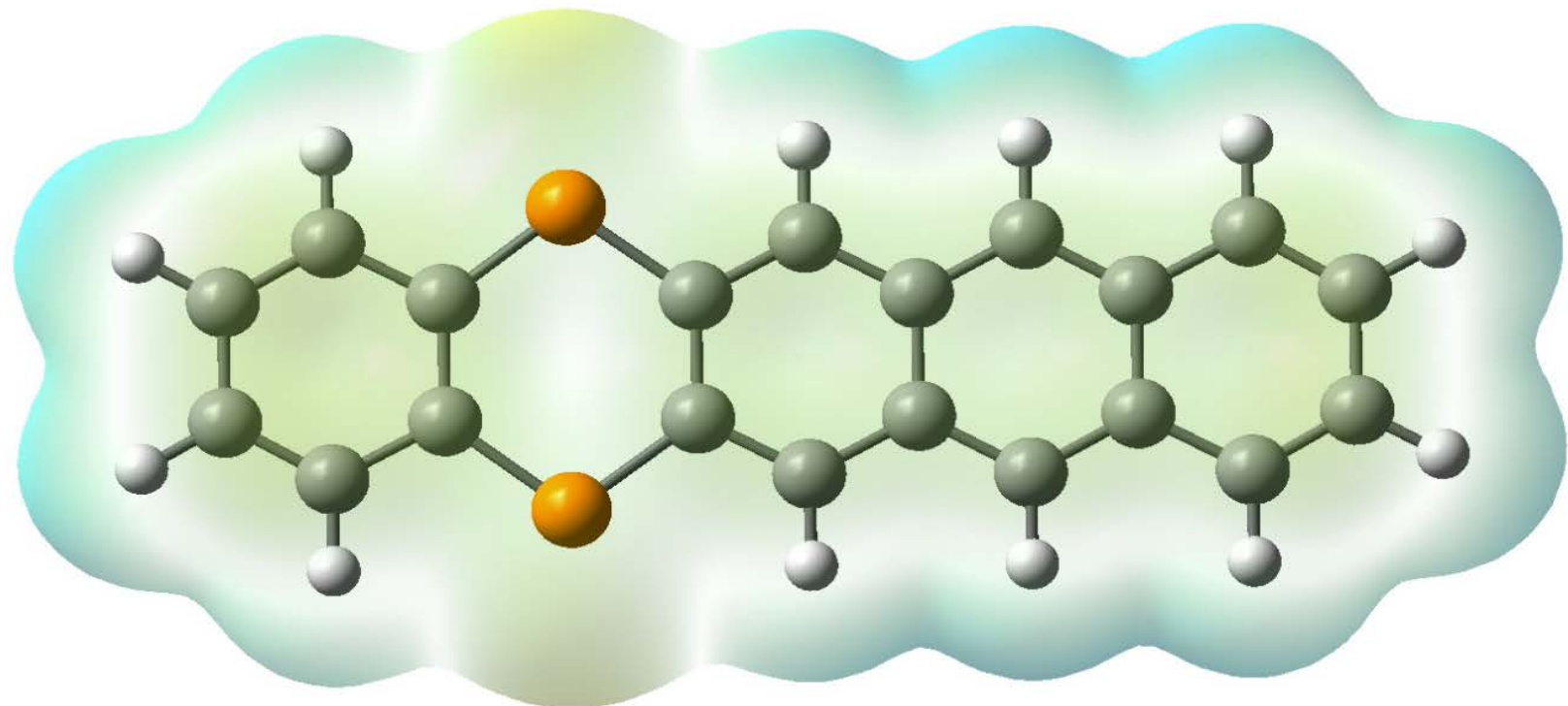
2,13-diphosphapentacene



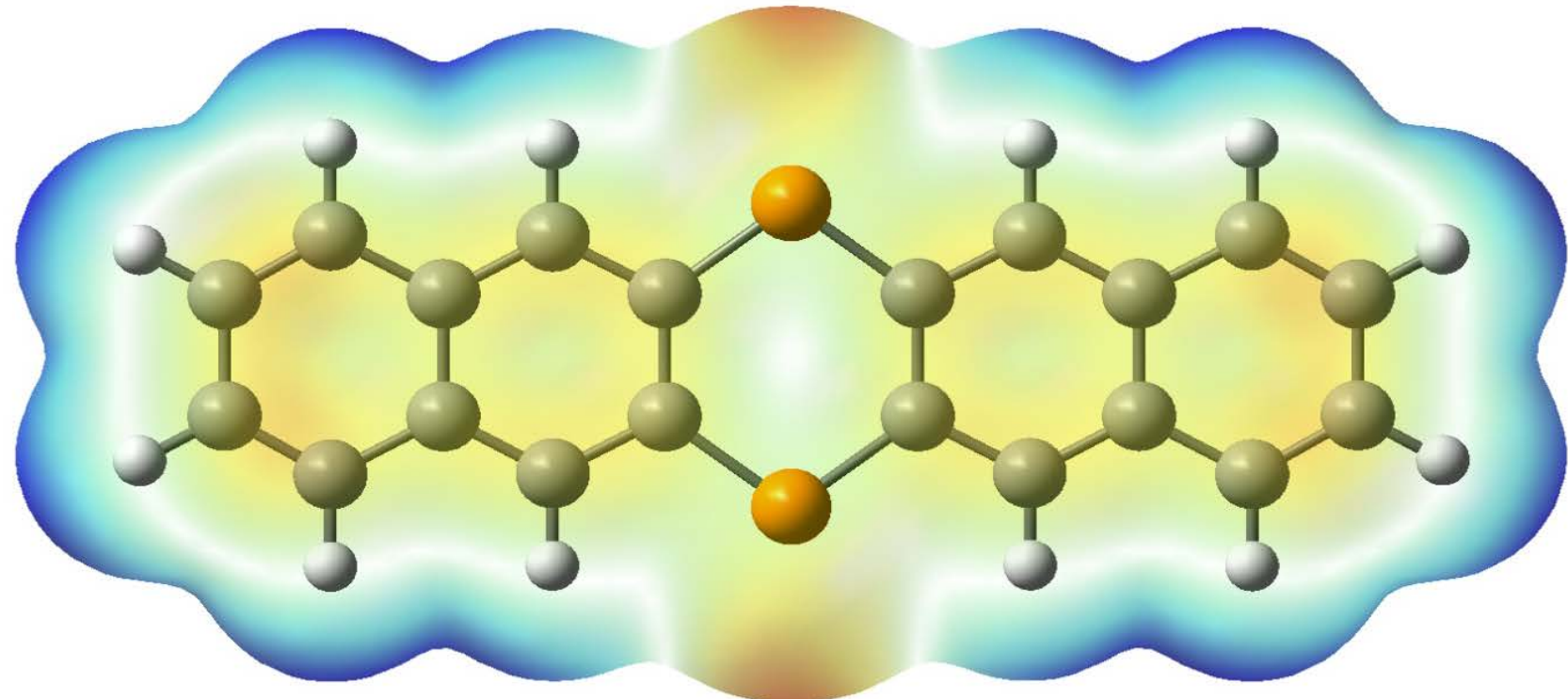
2,14-diphosphapentacene



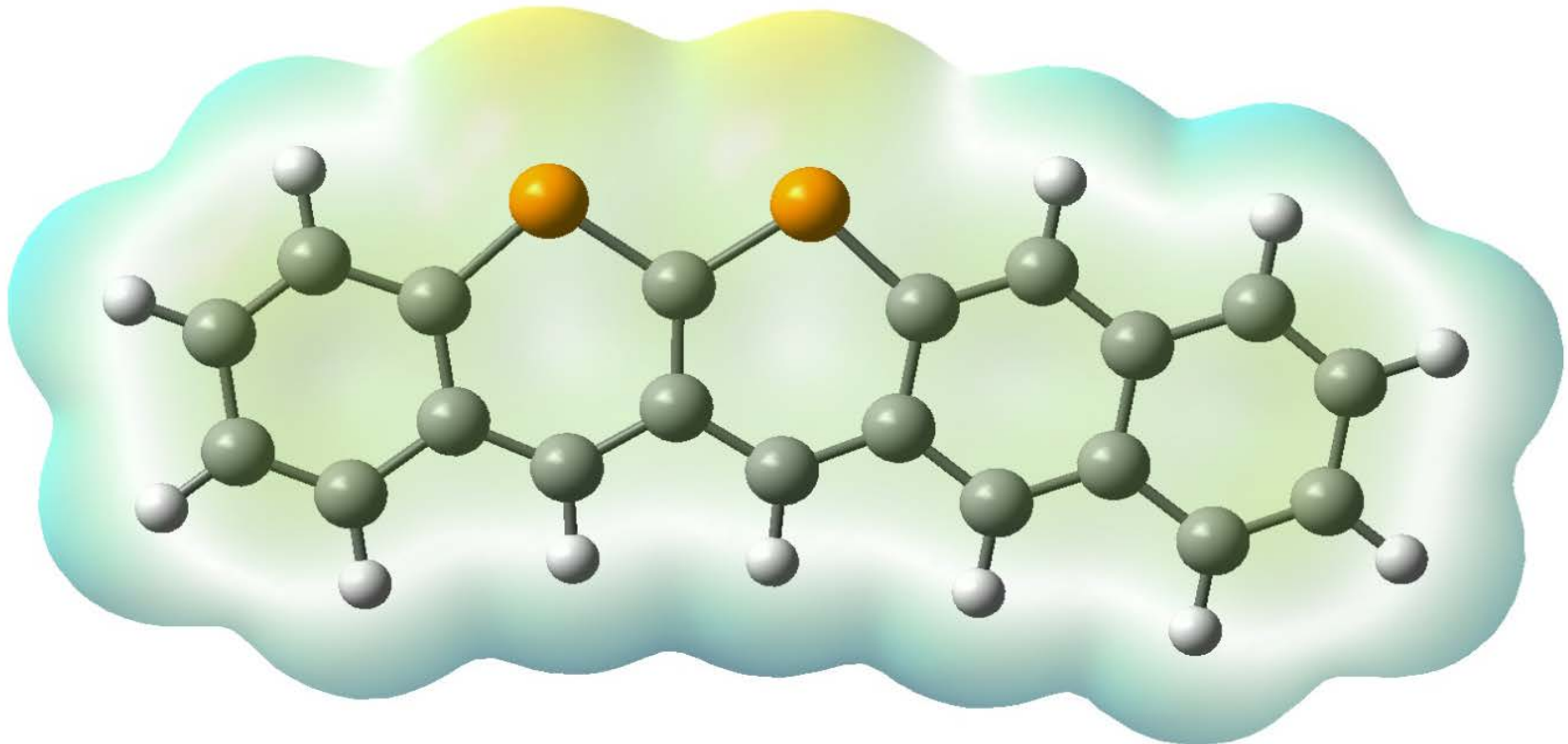
5,14-diphosphapentacene



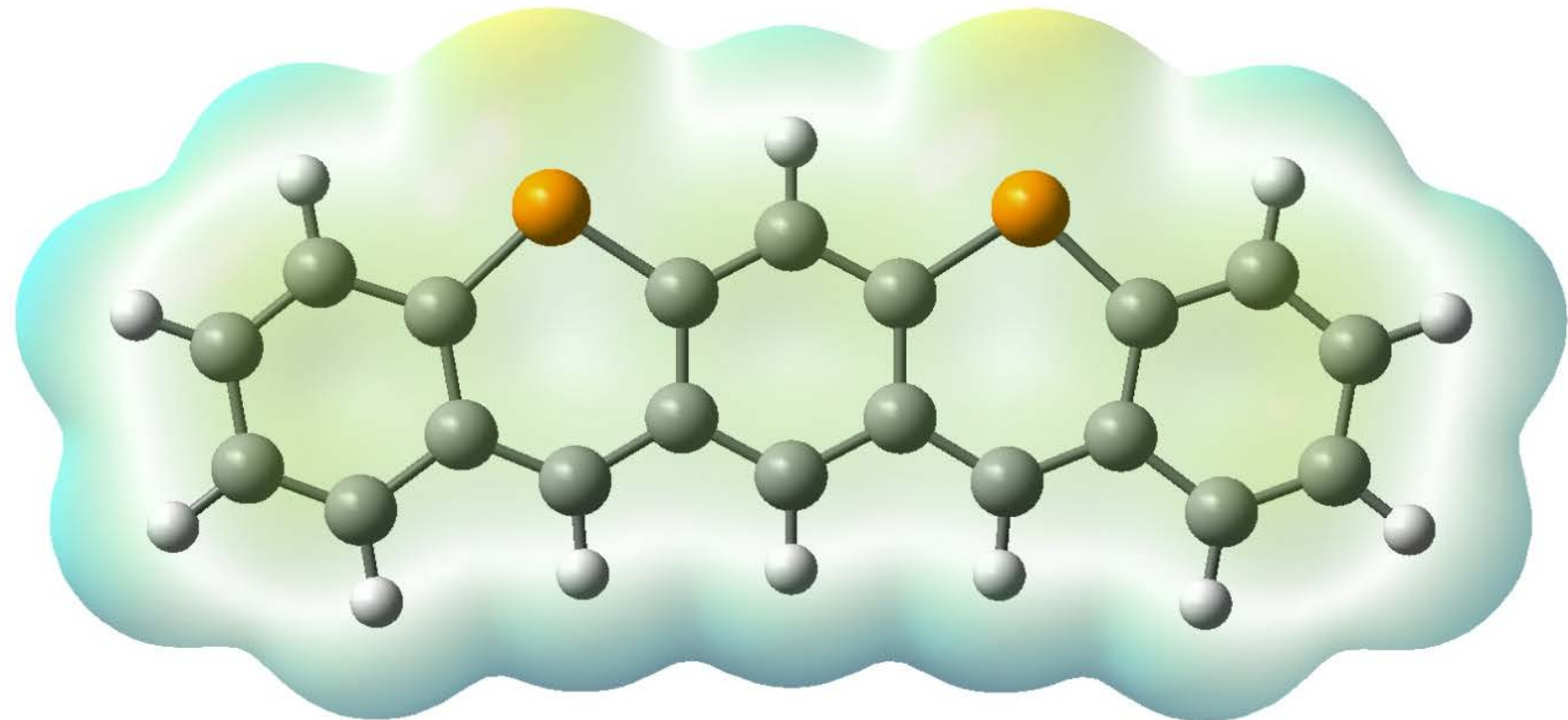
6,13-diphosphapentacene



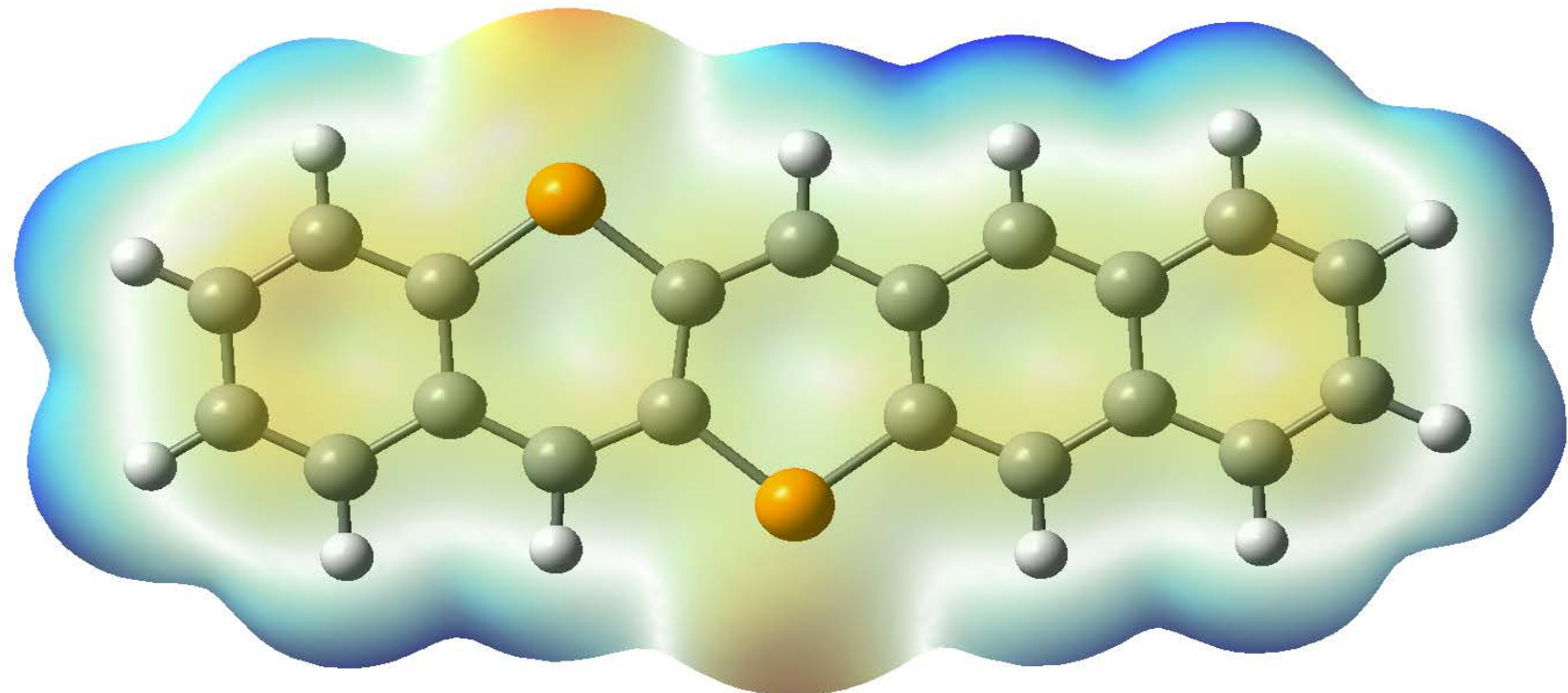
5,6-diphosphapentacene



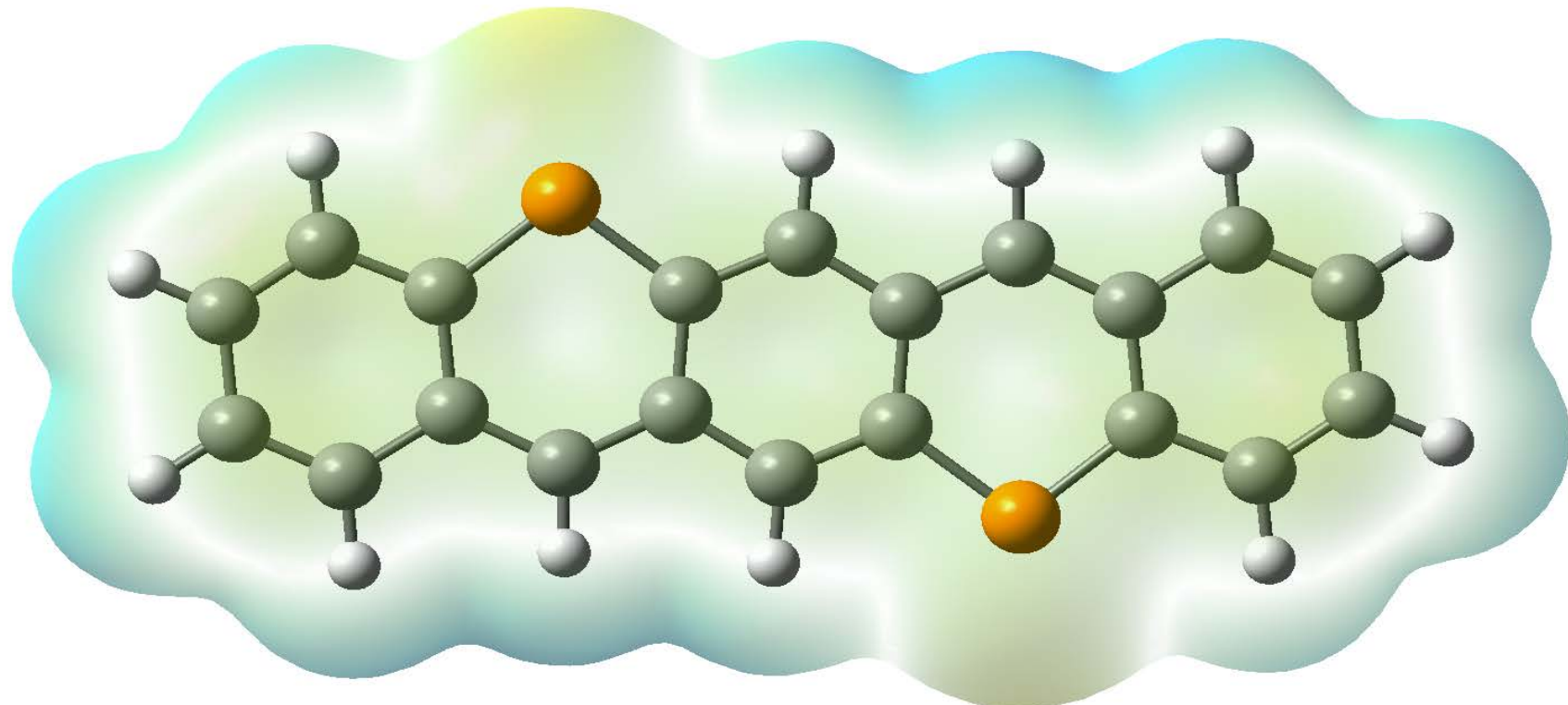
5,7-diphosphapentacene



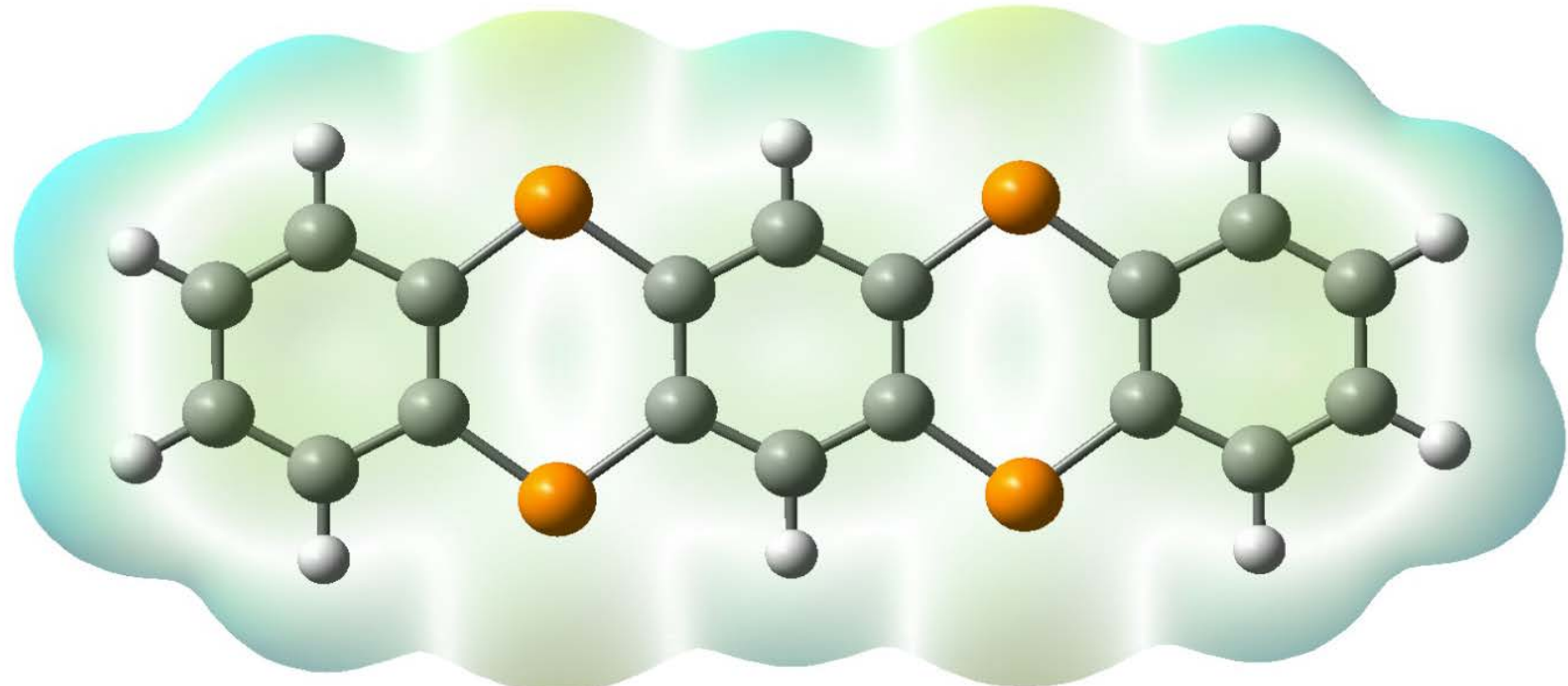
5,13-diphosphapentacene



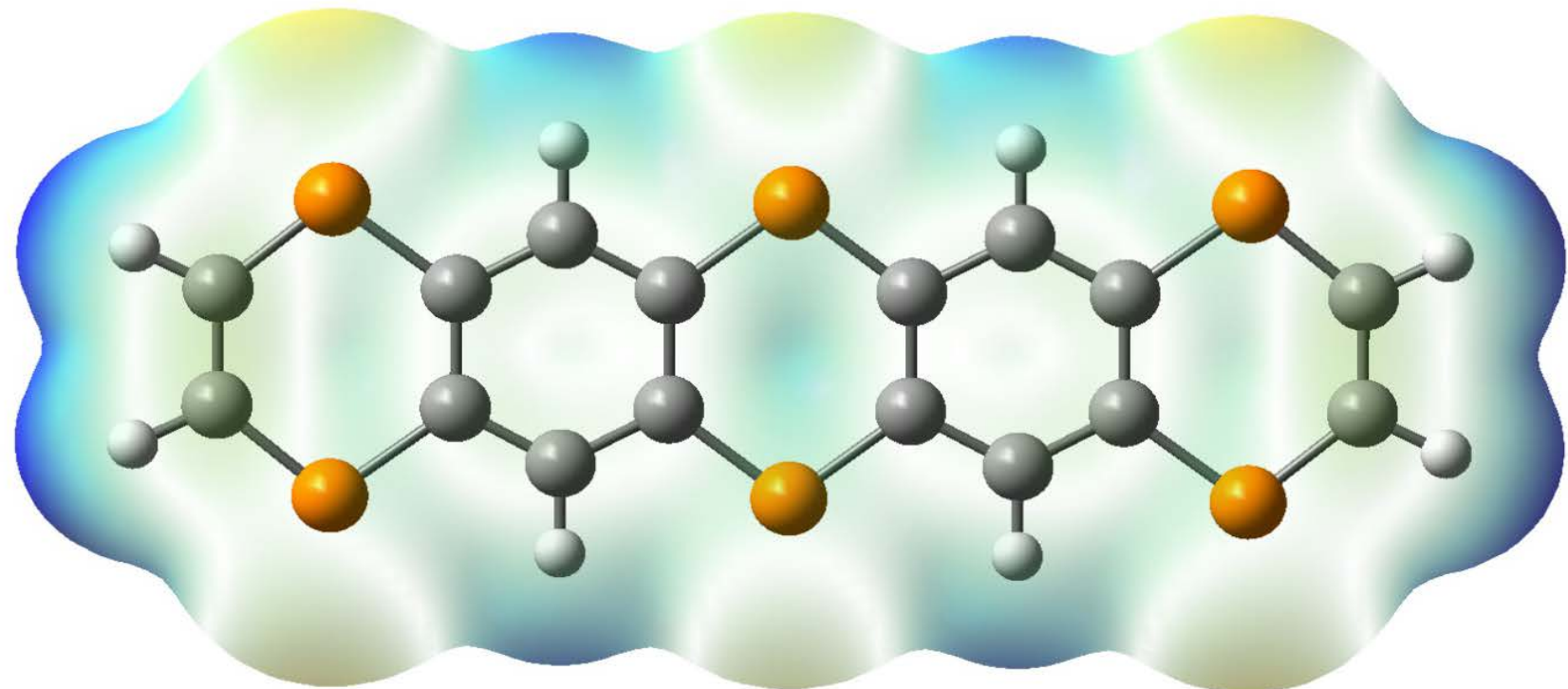
5,12-diphosphapentacene



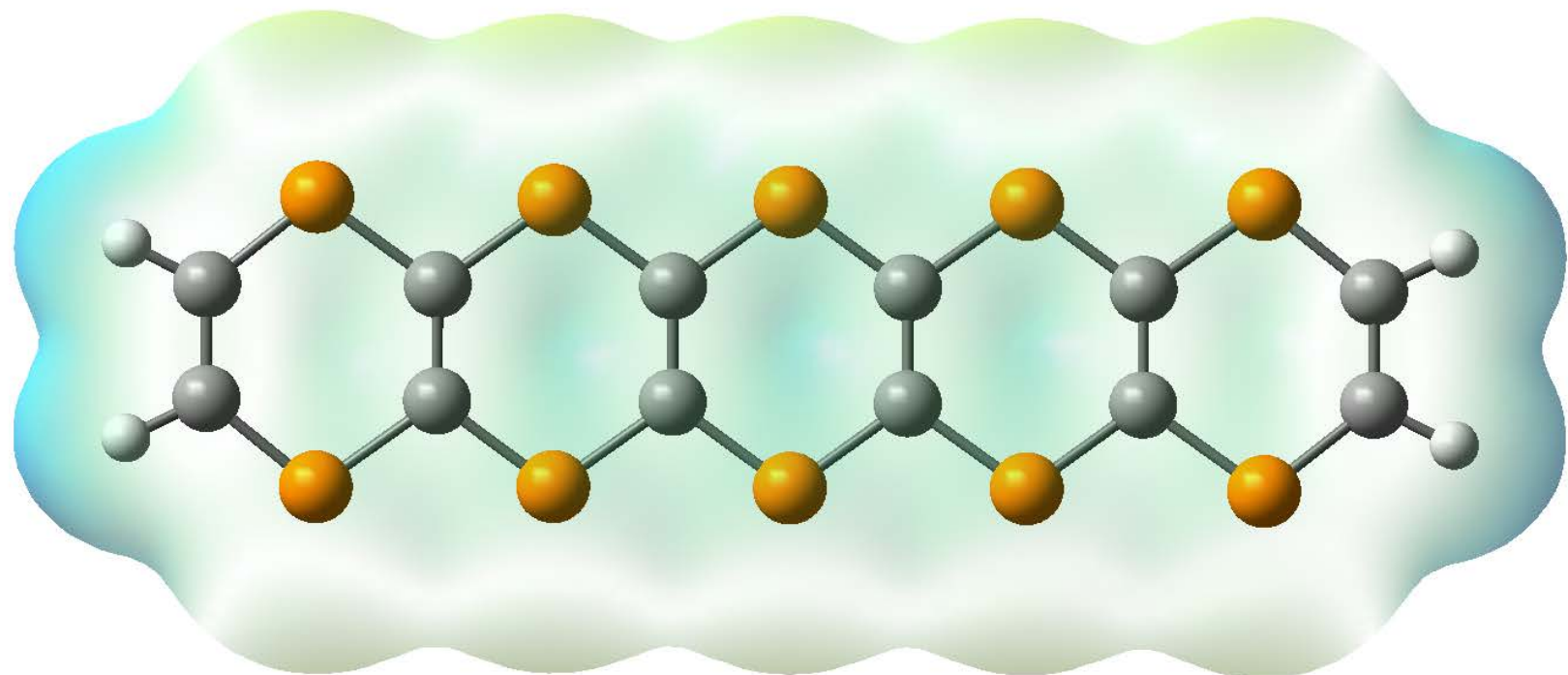
5,7,12,14-tetraphosphapentacene



1,4,6,8,11,13-hexaphosphapentacene



1,4,5,6,7,8,11,12,13,14-decaphosphapentacene



Reference List

- [1] A. Becke. *J. Chem. Phys.* **1993**, *98*, 5648.
- [2] C. Lee, W. Yang, R. G. Parr. *Phys. Rev. B* **1988**, *37*, 785-789.
- [3] Gaussian 09, Revision A.1, M. J. Frisch, G. W. Trucks, H. B. Schlegel, G. E. Scuseria, M. A. Robb, J. R. Cheeseman, G. Scalmani, V. Barone, B. Mennucci, G. A. Petersson, H. Nakatsuji, M. Caricato, X. Li, H. P. Hratchian, A. F. Izmaylov, J. Bloino, G. Zheng, J. L. Sonnenberg, M. Hada, M. Ehara, K. Toyota, R. Fukuda, J. Hasegawa, M. Ishida, T. Nakajima, Y. Honda, O. Kitao, H. Nakai, T. Vreven, J. A. Montgomery, Jr., J. E. Peralta, F. Ogliaro, M. Bearpark, J. J. Heyd, E. Brothers, K. N. Kudin, V. N. Staroverov, T. Keith, R. Kobayashi, J. Normand, K. Raghavachari, A. Rendell, J. C. Burant, S. S. Iyengar, J. Tomasi, M. Cossi, N. Rega, J. M. Millam, M. Klene, J. E. Knox, J. B. Cross, V. Bakken, C. Adamo, J. Jaramillo, R. Gomperts, R. E. Stratmann, O. Yazyev, A. J. Austin, R. Cammi, C. Pomelli, J. W. Ochterski, R. L. Martin, K. Morokuma, V. G. Zakrzewski, G. A. Voth, P. Salvador, J. J. Dannenberg, S. Dapprich, A. D. Daniels, O. Farkas, J. B. Foresman, J. V. Ortiz, J. Cioslowski, and D. J. Fox, Gaussian, Inc., Wallingford CT, 2009.
- [4] J. R. Reimers. *J. Chem. Phys.* **2001**, *115*, 9103-9109.
- [5] M. Bendikov, H. M. Duong, K. Starkey, K. N. Houk, E. A. Carter, F. Wudl. *J. Am. Chem. Soc.* **2004**, *126*, 7416-7417.